The Dissertation Committee for Natalie Nicole Gath Certifies that this is the approved version of the following Dissertation:

THE ROLES OF *MAB21L2* IN DEVELOPMENT OF THE EYE

Committee:

Steven Vokes, Supervisor

Jeffrey Gross, Co-Supervisor

Seema Agarwala

Andreas Matouschek

David Stein

THE ROLES OF *MAB21L2* IN DEVELOPMENT OF THE EYE

by

Natalie Nicole Gath

Dissertation

Presented to the Faculty of the Graduate School of

The University of Texas at Austin

in Partial Fulfillment

of the Requirements

for the Degree of

Doctor of Philosophy

The University of Texas at Austin

August 2019

Dedication

To my family, for endless support, encouragement and curiosity along this journey.

Acknowledgements

Firstly, I would like to thank my mentor, Dr. Jeffrey Gross, for his support, mentorship, and the opportunity to pursue a project that taught me so much. I also thank my thesis committee, Dr. Steven Vokes, Dr. Seema Agarwala, Dr. David Stein, and Dr. Andreas Matouschek for their support and valuable suggestions throughout my thesis work.

I also thank all the members of the Gross Lab, past and present, for their support, friendship, and guidance along the path from my first day in the lab to the writing of this document. In particular, Nicholas Hanovice, Krista Angileri, and Pawat Seritrakul deserve thanks for being good friends, science mentors and DOTA teammates.

Thanks also to my many mentors and teachers who set me on the path towards pursuing science as a career. From elementary school to college, I would never have begun without you. Special thanks to Andrew White, my high school biotechnology teacher, for giving me my first taste of life in the lab and encouraging me to go after it, and Drs. Julin Maloof and Amanda Schrager-Lavelle of UC Davis, for three wonderful years learning countless techniques and for giving me the push to decide on grad school.

Lastly, many thanks to my family. My parents have supported me all the way, pushing me to follow my dreams and being there in good times and bad. Without the curiosity and perseverance that they taught me, I would not be where I am. And to Matt, for patience with 2AM phone calls and moving halfway across the country, for support and a generous spirit and never letting me give up. Love you all.

Abstract

THE ROLES OF *MAB21L2* IN DEVELOPMENT OF THE EYE

Natalie Nicole Gath, PhD

The University of Texas at Austin, 2019

Supervisor: Steven Vokes

Co-Supervisor: Jeffrey Gross

Mutations in *MAB21L2* result in severe ocular defects including microphthalmia, anophthalmia, coloboma, microcornea, and cataracts. The molecular and cellular underpinnings of these defects are unknown, as is the normal cellular function of MAB21L2. Zebrafish *mab21l2*^{au10} mutants possess ocular defects resembling those in humans with *MAB21L2* mutations, providing an excellent model to characterize mab21l2 functions during eye development. *mab21l2* $^{-/-}$ mutants possessed a host of ocular defects including microphthalmia and colobomas as well as small, disorganized lenses and cornea dysgenesis. Decreased proliferation, increased cell death, and defects in marker gene expression were detected in the lens. Cell death in the optic stalk was elevated in *mab21l2* $^{-/-}$ mutants and the basement membrane between the edges of the choroid fissure failed to break down. Neuronal differentiation in the retina was normal, however. *mab21l2* $^{-/-}$ mutant corneas were disorganized, possessed an increased number of cells, some of which proliferated ectopically, and failed to differentiate the corneal stroma. Human mutant *MAB21L2*^{R51C} and *MAB21L2*^{R51H} mRNAs possessed dominant negative function, inducing colobomas in wild type fish. Yeast-2-hybrid assays provided potential binding partners for the function of mab21l2, including transcription factors and actin/myosin related proteins. mab21l2 function is required for morphogenesis and cell

survival in the lens and optic cup, and basement membrane breakdown in the choroid fissure. mab21l2 function also regulates proliferation in the lens and cornea; in its absence, the lens is small and mispatterned, and corneal morphogenesis and patterning are also disrupted. mab21l2 protein function may involve transcriptional regulation or control of cell shape and movement.

Table of Contents

List of Tables

List of Figures

Chapter 1: Introduction to development of the eye and the gene *mab21l2*

1.1 DEVELOPMENT OF THE OPTIC CUP AND THE NEURAL RETINA

1.1.1 Structure and development of the early optic cup

During embryonic development, the formation of the eye is a complex process involving many different morphogenetic, patterning, and differentiation events. Despite the relative differences in model organisms from mice to zebrafish, the process of eye formation is remarkably conserved. The first step is the evagination of two subfields of the forebrain, called the optic vesicles (Wall, 1942). These vesicles undergo complex morphogenic movements, elongating to form wing-like structures connected to the brain via the optic stalk (Fig. 1.1A) (Wall, 1942). The center of the optic vesicle will then begin to invaginate, as the surface ectoderm with which it is in contact begins to proliferate and undergo its own morphogenesis to produce the primordial lens (Fig 1.1B) (reviewed in Cavodeassi 2018; Fuhrmann 2010). These complementary processes will form the bilayered optic cup, comprised of the lateral and medial layers, and the lens vesicle which it surrounds (Fig. 1.1B). The medial and lateral layers of the optic cup will undergo a series of complex morphogenetic cell movements (Kwan *et al.*, 2012), eventually producing a presumptive neural retina at the lateral layer, and the immature retinal pigmented epithelium (RPE) from the medial layer (Fig. 1.1C) (Li et al. 2000; reviewed in Fuhrmann 2010). This process is controlled by intrinsic factors, like the transcription factors rx/RAX, vsx2, lhx2, pax6 and mitf, among many others, and extrinsic factors, including signaling from the BMP, and, particularly, FGF pathways (reviewed in Fuhrmann 2010).

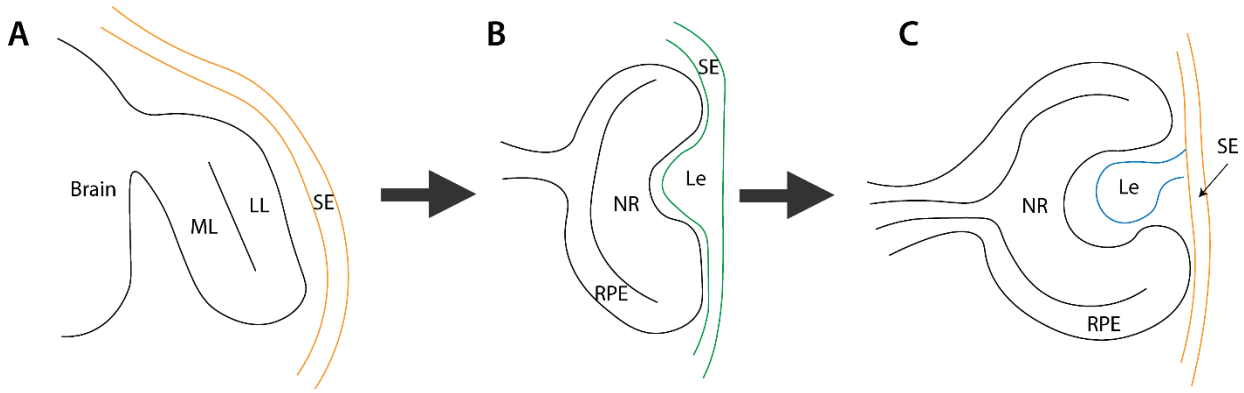

Figure 1.1: Optic cup morphogenesis during early development of the eye

A: Evagination of the early optic vesicle from the forebrain.
B: Formation of the eye cup, invagination of the optic cup and beginnings of lens morphogenesis from the surface ectoderm
C: Refinement of the optic cup, progression of lens separation from the surface ectoderm
ML = medial layer. LL = lateral layer. RPE = Retinal pigmented epithelium. NR = neural retina. Le = lens. SE = Surface Ectoderm.

1.1.2 Differentiation of retinal cell types and growth of the eye

In the early stages of retinal development, the retina is made up of largely indistinguishable progenitors called retinal progenitor cells. Over time, these progenitor cells will undergo stereotyped, sequential differentiation processes to produce the seven retinal cell types that make up the mature retina (reviewed in Bassett & Wallace 2012). These include 6 neural cell types: retinal ganglion cells, amacrine cells, horizontal cells, bipolar cells, cone photoreceptors, and rod photoreceptors; as well as the sole glial cell of the retina, the Müller glia. Together, these cells make up the mature retina, and allow for the transduction of light into neural signals.

In the zebrafish, the retina will continue to grow throughout the life of the animal. This is accomplished by the persistent production of retinal cells from a resident stem cell population at the distal edges of the retina, known as the ciliary marginal zone, or CMZ. The CMZ will remain proliferative and is the major source of new retinal cells after embryonic development in the zebrafish (Raymond *et al.*, 2006).

1.2 DEVELOPMENT AND DIFFERENTIATION OF THE LENS

1.2.1 Specification and morphogenesis of the early lens

The retina is not the only tissue undergoing movements, differentiation, and maturation. The lens is also a complex tissue, with its own developmental processes.

The lens is formed from the embryonic surface ectoderm that overlies the developing optic cup (Fig. 1.2A). This ectoderm will be induced to undergo morphogenesis and differentiation by signals from and interaction with the underlying retina, including BMP-related signals (Furuta and Hogan, 1998; Wawersik *et al.*, 1999; Morcillo *et al.*, 2006; Rajagopal *et al.*, 2008, 2009), retinoic acid signaling (reviewed in Cvekl & Wang 2009), and inhibition of WNT (Smith *et al.*, 2005; Kreslova *et al.*, 2007; Song *et al.*, 2007; Grocott *et al.*, 2011) and Shh activity (Kerr et al. 2012; reviewed in Gunhaga 2011, Cvekl & Zhang 2017) in the prospective placode. In addition, a pax6/six3 dependent gene regulatory cascade will induce the cells of the surface ectoderm to

become the lens placode. In response to these paracrine and autocrine signals, the surface ectoderm will begin to proliferate. In zebrafish, unlike in mammalian systems, the lens will not invaginate to form a lens pit, but the proliferative cells will pile up on one another, moving into the space left behind as the presumptive neural retina invaginates (Fig. 1.1B, Fig 1.2B) (Schmitt and Dowling, 1994; Easter, Jr. and Nicola, 1996). These cells will form a semi-spherical structure called the lens mass, made up of seemingly indistinguishable lens progenitor cells (Fig. 1.2C). As development and proliferation continues, these cells will take on different morphologies, corresponding with their later fates in the mature lens (Greiling and Clark, 2009). As the lens continues to round up, apoptosis and delamination events at the distal edge will separate the lens mass from the remaining surface ectoderm (Zhao *et al.*, 2006; Greiling *et al.*, 2010). By about 24hpf, the lens is completely detached from the surface ectoderm, and is wrapped at the distal edge by a single layer of cuboidal cells, which will become the lens epithelium (Fig. 1.2D). The core is made up of teardrop shaped cells, wrapped by rings of elongated cells which comprise the primary lens fibers (Greiling and Clark, 2009).

In the mature lens, epithelial cells form a single layer of cuboidal cells that wrap the anterior 2/3 of the lens. These cells retain their organelles, and remain proliferative throughout the life of the animal, continuing to add cells to the lens. At the approximate equator of the lens, newborn lens cells produced from the proliferation of lens epithelia pass through the transition zone, where they will elongate and differentiate into lens fibers (Fig 1.2E). These new fibers must undergo many drastic changes, including turning on lens-fiber-specific genes and factors, degrading their nuclei and other organelles, and becoming filled with crystallin proteins, in order to allow them to perform their primary function of refracting light onto the neural retina.

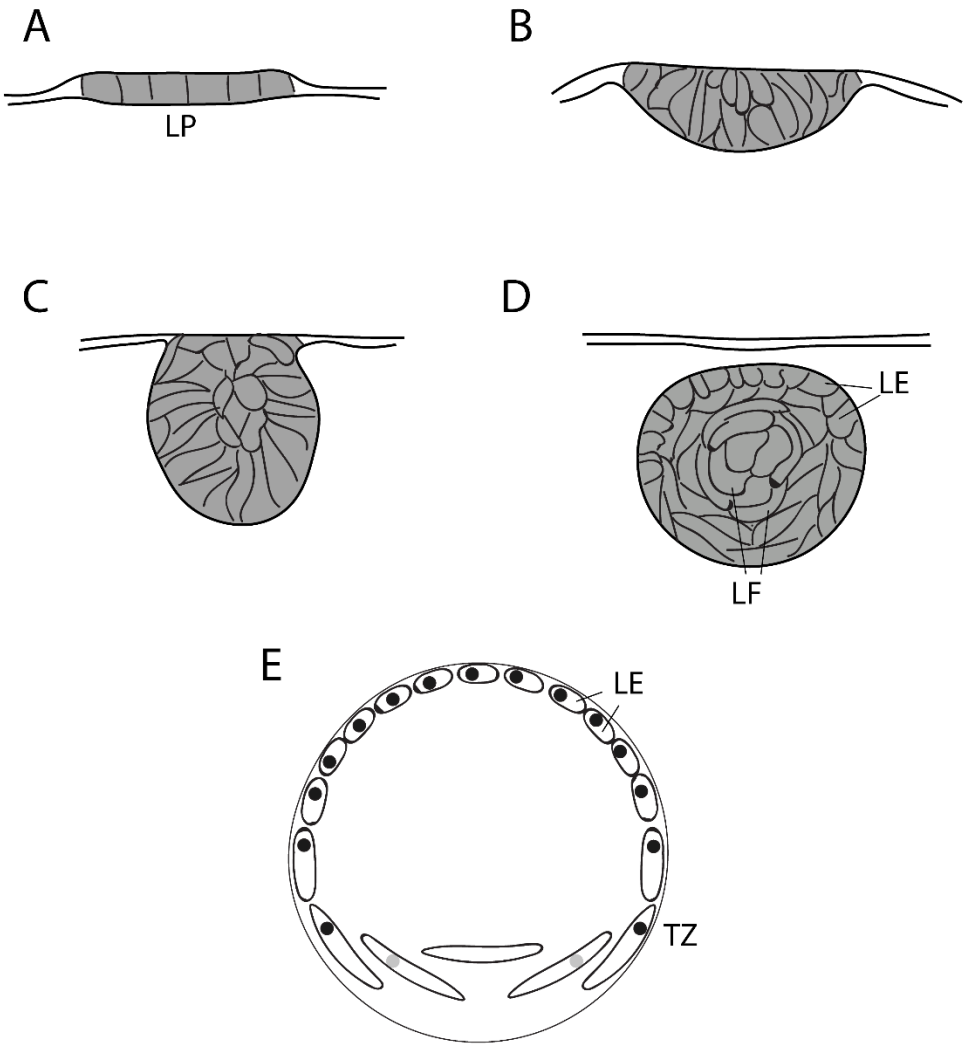

Figure 1.2: Development of the zebrafish lens

A: Lens placode (gray), approximately 16 hours post fertilization
B: Lens, approximately 18 hours post fertilization
C: Lens beginning to separate from overlying surface ectoderm, approximately 20 hpf
D: Lens at approximately 28hpf, showing fully separated, spherical lens with early lens epithelial and fiber cells. Remaining overlying surface ectoderm will become the corneal epithelium.
E: Schematic of lens epithelial cells proceeding through the transition zone to elongate, lose nuclei, and become fibers wrapped around the lens core
LP = lens placode. LE = lens epithelial. LF = lens fibers. TZ = transition zone. Black circles represent cell nuclei.

1.2.2 Differentiation and gene expression in the lens

During the differentiation process, lens epithelial and fiber cells express a host of genes that enable them to take on their lineage-specific characteristics (summarized in Cvekl & Zhang 2017). The lens epithelial cells express multiple factors, but one of the most vital is a gene belonging to the forkhead-box family of transcription factors, *foxe3*. This epithelial-expressed gene is critical for the separation of the lens from the surface ectoderm through controlled apoptosis of cells in the area of contact between these two tissues, and is required for epithelial cells to retain their proliferative state and continue contributing to the formation of new lens fibers (Blixt *et al.*, 2000; Cvekl and Zhang, 2017a). In the absence of *foxe3* expression, lenses remain adhered to the cornea, do not produce secondary lens fibers, and are dysplastic and cataractous (Blixt *et al.*, 2000).

At the transition zone, lens epithelial cells express prox1, a key FGF-responsive transcription factor that regulates the downstream expression of a host of genes that are critical to the maturation and function of newly born lens fiber cells. Most critically, prox1 is responsible for the activation of crystallin genes, including beta and gamma crystallins (Cui *et al.*, 2004), while alpha crystallins are activated in parallel in a pax6-dependent manner (Cvekl *et al.*, 1995; Ashery-Padan *et al.*, 2000; Yang and Cvekl, 2005).

Other factors involved in terminal differentiation of lens fibers include: gata3, responsible for upregulating expression of gamma-crystallins and required for nuclear degradation (Maeda *et al.*, 2009); celf1, a post-transcriptional regulator responsible for control of cell cycle exit and DNase activity in the new fiber cell (Siddam *et al.*, 2018); maf-family transcription factors, involved in upregulation of all four types of lens crystallins as well as differentiation of fibers (Reza and Yasuda, 2004); sox1, a direct regulator of gamma crystallin expression also involved in lens fiber elongation and shape changes (Nishiguchi *et al.*, 1998); and many more (reviewed in Cvekl & Zhang 2017).

1.3 DEVELOPMENT OF THE CORNEA

1.3.1 Specification, morphogenesis and structure of the cornea

The surface ectodermal cells that directly overlay the developing lens will become the cornea. These two tissues are separated during early development of the eye by programmed delamination and apoptotic events in the connecting cells (Zhao *et al.*, 2006; Greiling *et al.*, 2010). The mature human cornea is made up of 5 layers. From the distalmost in, these layers include the corneal epithelium, Bowman's layer, the stroma, Descemet's membrane, and the corneal endothelium. Most organisms, including zebrafish, share this overall organization, although in some lower mammals such as mice and rats, the presence of a distinct Bowman's layer (as opposed to an amorphous subregion of the stroma) is controversial (Haustein, 1983; Hayashi *et al.*, 2002; Song and Joo, 2004; Zhao *et al.*, 2006; Henriksson *et al.*, 2009). In zebrafish, by contrast, Bowman's layer is clearly present as a distinct layer separate from the stroma, similar to humans, suggesting that zebrafish may be a better model of the human cornea in that respect (Soules and Link, 2005; Zhao *et al.*, 2006).

During zebrafish corneal development, which is highly similar to that in other vertebrates, those surface ectodermal cells overlying the optic cup that do not become part of the lens will form a monolayer, the presumptive corneal epithelium, which is the first layer to be produced (Soules and Link, 2005). The corneal endothelium will then be produced from neural crest-derived periocular mesenchymal cells, which migrate into the eye, accumulating at the peripheral angles of the anterior chamber, and crawl over the lens to form the corneal endothelial monolayer (Soules and Link, 2005). Concurrently, the epithelium will assume cornea-like characteristics, proliferate to form additional cell layers, and begin to lay down components of the extracellular matrix that comprises the stroma, although the stroma will require the formation of the corneal endothelium before it acquires its proper organization (Zhao *et al.*, 2006). In zebrafish, the corneal epithelium will proliferate and become two cell layers thick, remaining at this thickness for four weeks of development, after which it will gradually increase to its final thickness of 4-5

cell layers (Zhao *et al.*, 2006). The stroma will gradually increase in thickness, comprising layers of collagenous fibers, but will remain acellular until between 14 and 28 days post fertilization (dpf), at which time the first keratocytes will begin to populate the stroma. These keratocytes will increase in number as the stroma continues to thicken, until it reaches its mature size of 36-40 collagen layers thick at approximately 60 dpf. Bowman's layer appears formed at approximately 5dpf, while Descemet's membrane is found to be fully mature by approximately 60dpf (Soules and Link, 2005; Zhao *et al.*, 2006).

1.3.2 The role of BMP signaling in cornea/lens fate choice

The fating of the surface ectodermal cells into lens and corneal compartments is controlled in part by BMP signaling. In chick and mouse, BMP signaling induces the lens fate (Furuta and Hogan, 1998; Wawersik *et al.*, 1999), while a lack of BMP signaling will lead the surface ectoderm to default into a corneal epithelial state; when BMP signaling is blocked in chick, the lens fails to form, but the cornea forms normally (Collomb *et al.*, 2013). Further evidence that these tissues are produced from a common pool of cells comes from the fact that when the lens is removed during early development, a replacement lens can be produced by the cell cycle re-entry and differentiation of partially-committed corneal cells into lens cells (Collomb *et al.*, 2013). However, this cross-differentiation is only possible before the committed corneal epithelium loses the capacity to rapidly downregulate pax6, which is ordinarily accomplished through several mechanisms, including an EGF-dependent transcriptional repressive response at the *pax6* promoter (Li and Lu, 2005; Collomb *et al.*, 2013). This suppression of *pax6* is required for the production of cells in the lens lineage, but cannot occur in the cornea once it has become fully committed to the corneal fate, therefore preventing future production of lens cells from the cornea (Li and Lu, 2005; Collomb *et al.*, 2013). The permanent stabilization of pax6 in the corneal epithelium and thus, commitment into the corneal fate, appears to be dependent on the formation of the corneal stroma (Collomb *et al.*, 2013). It has been shown that cells exposed to a corneal stromal environment undergo a

host of changes, including downregulation of microRNAs known to repress the expression of *pax6*, which could contribute to the stabilization of pax6 and the commitment of corneal fate once the stroma has begun to be laid down by early epithelial cells (Shalom-Feuerstein *et al.*, 2012).

1.4 CLOSURE OF THE CHOROID FISSURE

As the retina develops, it produces a transient opening at the ventral side of the eye called the choroid fissure (Fig. 1.3A-C). The choroid fissure is an opening between the two edges of the neural retina/RPE which is produced as a result of the complex morphogenetic movements that the eye undergoes during development (Fig. 1.3C). The choroid fissure is the entry site for the vasculature that nourishes the developing eye. The developing optic nerve also exits the eye through the choroid fissure and is routed toward the brain (Mann, 1921; Nickla and Wallman, 2010). However, for the eye to mature fully, the choroid fissure must close, creating a complete, spherical eye with no gaps in the retina.

The process of choroid fissure closure is relatively poorly understood, but it is proposed to proceed in three main phases (Fig. 1.3D-F). In the first phase, tissue growth and morphogenesis bring the two sides of the retina/RPE into the correct orientation at the correct time to allow fusion to proceed (Fig. 1.3D). In the second phase, the basement membrane, which surrounds the two lips of the fissure, must break down to allow the retina/RPE to contact one another and eventually fuse (Fig. 1.3E). In the third phase, the sides of the fissure come together and undergo cellular rearrangement and formation of junctions to create one complete, fused tissue (Fig 1.3F) (James *et al.*, 2016).

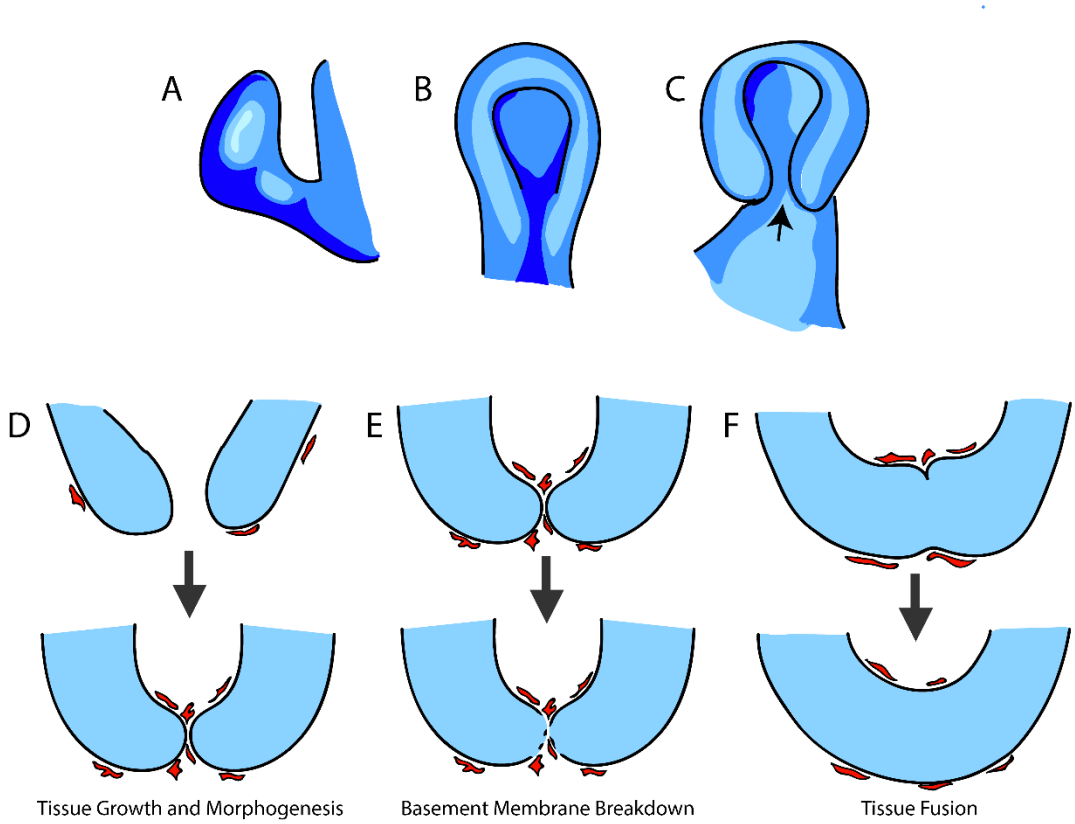

Figure 1.3: Formation and closure of the choroid fissure

A-C: Schematic of optic cup morphogenesis and formation of the choroid fissure (indicated by arrow in C)
D-F: Diagrams representing the three main stages of choroid fissure closure: tissue growth and morphogenesis (D), breakdown of the basement membrane (E), and tissue fusion (F). Black line represents basement membrane wrapping the retina/RPE. Blue = optic cup. Red = periocular mesenchyme.

1.4.1 Growth and morphogenesis of the eye and apposition of the choroid fissure

During morphogenesis, the eye undergoes rapid shape changes that contribute to the production of the choroid fissure. As the eye grows and the edges of the fissure approach one another, the fissure is not of uniform width throughout the proximal-distal axis; at the distal edge, the two sides of the optic cup are widely separated, while at the proximal-medial region, the edges are much more closely apposed (Bernstein *et al.*, 2018). In addition, the leading edges are initially oriented ventrally, only later pivoting to face one another (Bernstein *et al.*, 2018). During the growth and orientation phase of choroid fissure closure, the edges of the retina are dynamic, with the basement membrane extending processes to the opposite side of the fissure and the intervening periocular mesenchyme (POM), though the function of this activity is unknown (Williams, 2016; Bernstein *et al.*, 2018). It is proposed that this dynamic activity may act to assist alignment of the fissure edges (Bernstein *et al.*, 2018), but this is yet to be proven.

1.4.2 Basement membrane breakdown in the choroid fissure

The process of basement membrane breakdown is incompletely understood. It is thought that the retinal cells, at the sides of the choroid fissure, extend small cellular processes to contact the basement membrane (Geeraets, 1976; Hero, 1990), and that these processes help to degrade the basement membrane. It has been proposed that these retinal cell extensions may comprise podosomes, which are small, actin-rich cell adhesions known to facilitate basement membrane breakdown in other contexts (reviewed in Linder 2007) through the action of actin-linked complexes, including matrix metalloproteases (Gawden-Bone *et al.*, 2010; Xiao *et al.*, 2010) but attempts to confirm the involvement of podosomes in the closure of the choroid fissure have thus far been inconclusive (Williams, 2016; Gestri *et al.*, 2018). However, recent research has shown that actin-rich bridges and extensions of the basement membrane dynamically contact the opposing side of the fissure, which may contribute to membrane breakdown (Bernstein *et al.*, 2018). Research involving the POM, also found within the choroid fissure, suggests that these

cells may also play an important role in degradation of the basement membrane at the fissure (James *et al.*, 2016). POM cells are found tightly associated with the fissure during the fusion process, lining the choroid space as the fissure closes (Hero, 1990; Hero *et al.*, 1991). In particular, the POM- derived hyaloid vasculature is closely linked with the closing fissure (James *et al.*, 2016; Bernstein *et al.*, 2018; Gestri *et al.*, 2018). Hyaloid vasculature cells have been observed to accumulate F-actin in foci that contact the basement membrane at sites of breakdown, suggesting a possible role in assisting basement membrane breakdown (James *et al.*, 2016). In addition, *talin* mutants, which lack a key component of the actin cytoskeleton that allows integrins to be linked to actin fibers, had both a morphologically affected hyaloid vasculature, and displayed failure of basement membrane breakdown and choroid fissure closure (James *et al.*, 2016; Williams, 2016). Further supporting a role for the hyaloid vasculature in breakdown of the basement membrane at the fissure, *cloche* mutants, which lack all vasculature, displayed a delay in membrane breakdown and fissure closure, although the process was eventually completed (James *et al.*, 2016). This suggests an actin-dependent role for the POM-derived hyaloid vasculature in the process of basement membrane breakdown during closure of the choroid fissure.

1.4.3 Tissue fusion at the choroid fissure

The tissue fusion phase of choroid fissure closure is rather poorly understood. However, research indicates that the fusion process is not identical or simultaneous along the entire proximal-distal axis of the choroid fissure. Fusion in the zebrafish happens along a wave-like front, beginning in the central-proximal portion of the fissure and proceeding outward in both directions, first to the proximal edge of the fissure, and then to the distal edge (James *et al.*, 2016). However, a small section of the proximal fissure, near the optic disk, is not closed by tissue fusion, and is instead closed via intercalation of the optic nerve, hyaloid artery, and edges of the retina (Bernstein *et al.*, 2018). Additionally, it appears that the cells at areas of the choroid fissure where fusion occurs

must reorient their apico-basal axes and repolarize to form one coherent tissue, which may be dependent on contributions from the POM (Gestri *et al.*, 2018)

Little is known about the molecular regulation and control of the fusion process. Cadherin complexes and adherens junctions have a known role; zebrafish N-cadherin mutants display defects in choroid fissure closure called colobomas (Masai *et al.*, 2003) and the fusion site is marked by co-localization of beta-catenin and F-actin, which indicates the formation of adherens junctions, once tissue fusion has begun (Halbleib and Nelson, 2006; Hartsock and Nelson, 2008; James *et al.*, 2016). α-catenin performs a critical role in mediating adhesion and organization of the retinal cells during fissure closure (Chen *et al.*, 2012) In addition, during the process of choroid fissure closure, N-cadherin is downregulated in the fusing tissues, possibly allowing for the delamination of sox2+ retinal cells which move toward the fissure space and facilitate the fusion event (Bernstein *et al.*, 2018). Other molecular mechanisms are likely involved, but have yet to be investigated.

1.4.4 Signaling pathways in choroid fissure closure

Choroid fissure closure is known to involve signaling from many of the major developmental pathways, which when disrupted, often lead to closure failures. These include Wnt (Liu *et al.*, 2016), retinoic acid (Matt *et al.*, 2008; See and Clagett-Dame, 2009; Lupo *et al.*, 2011), FGF (Cai *et al.*, 2013; Chen *et al.*, 2013; Atkinson-Leadbeater *et al.*, 2014), Hedgehog (Schimmenti *et al.*, 2003; Koudijs *et al.*, 2008; Lee *et al.*, 2008), and BMP signaling pathways (Morcillo *et al.*, 2006; Patel and Sowden, 2017). BMP signaling has at least two roles in closure of the choroid fissure (reviewed in Patel & Sowden 2017). BMP4 signaling is antagonistic to SHH signaling at the choroid fissure, keeping SHH ventrally restricted while BMP4 remains primarily dorsal (Zhao *et al.*, 2010). BMP4 also maintains ventral restriction of key transcription factors such as vax2 by upregulating dorsal-specific antagonistic transcription factors in its expression domain (Behesti *et al.*, 2006). However, BMP7 is a ventrally localized molecule, being found at the ventral midline near the site of the choroid fissure, and is additionally associated with

the POM that forms the hyaloid vasculature (Dudley and Robertson, 1997), which as noted above, is involved in fissure closure (James *et al.*, 2016). Interestingly, evidence from BMP7 null mice suggests that BMP7 may also have a role in *formation* of the choroid fissure as well as its closure (Morcillo *et al.*, 2006).

1.4.5 Defects in choroid fissure closure: colobomas

When the process of choroid fissure closure goes wrong, a structural defect known as a coloboma is produced. Colobomas are persistent openings in the eye that can vary in severity, loosely correlated with their relative position along the proximal-distal axis (reviewed in Pagon, 1981). Distal colobomas are visible as a "keyhole" like opening below the pupil, where the distal retina has not properly fused. Distal-only colobomas have relatively mild effects on sight, mostly causing extra light sensitivity. However, colobomas can also occur in a more proximal location along the choroid fissure. In this case, a hole will be produced in the retina, and depending on the extent of the gap, can lead to loss of sight in large parts of the visual field, or complete blindness in the affected eye(s) (Nakamura *et al.*, 2011). Approximately 10% of childhood blindness is associated with colobomas (Onwochei *et al.*, 2000).

Colobomas often present in patients as part of syndromes or spectrum disorders (Onwochei *et al.*, 2000; Nakamura *et al.*, 2011). One of these spectrums is a disorder known as MAC (microphthalmia, anophthalmia, and coloboma) spectrum (Bardakjian *et al.*, 2015). This disorder is produced by many independent mutations within the genomes of affected patients (reviewed in Bardakjian et al. 2015), including mutations in the gene *MAB21L2* (Rainger *et al.*, 2014; Deml *et al.*, 2015; Horn *et al.*, 2015).

1.5 *MAB21L2* IN THE EYE

Human patients with five different point mutations in the *MAB21L2* gene have been identified. These mutations include E49K, R51C, R51H, R51G, and R247Q (Fig. 1.4) (Rainger *et al.*, 2014; Deml *et al.*, 2015; Horn *et al.*, 2015).

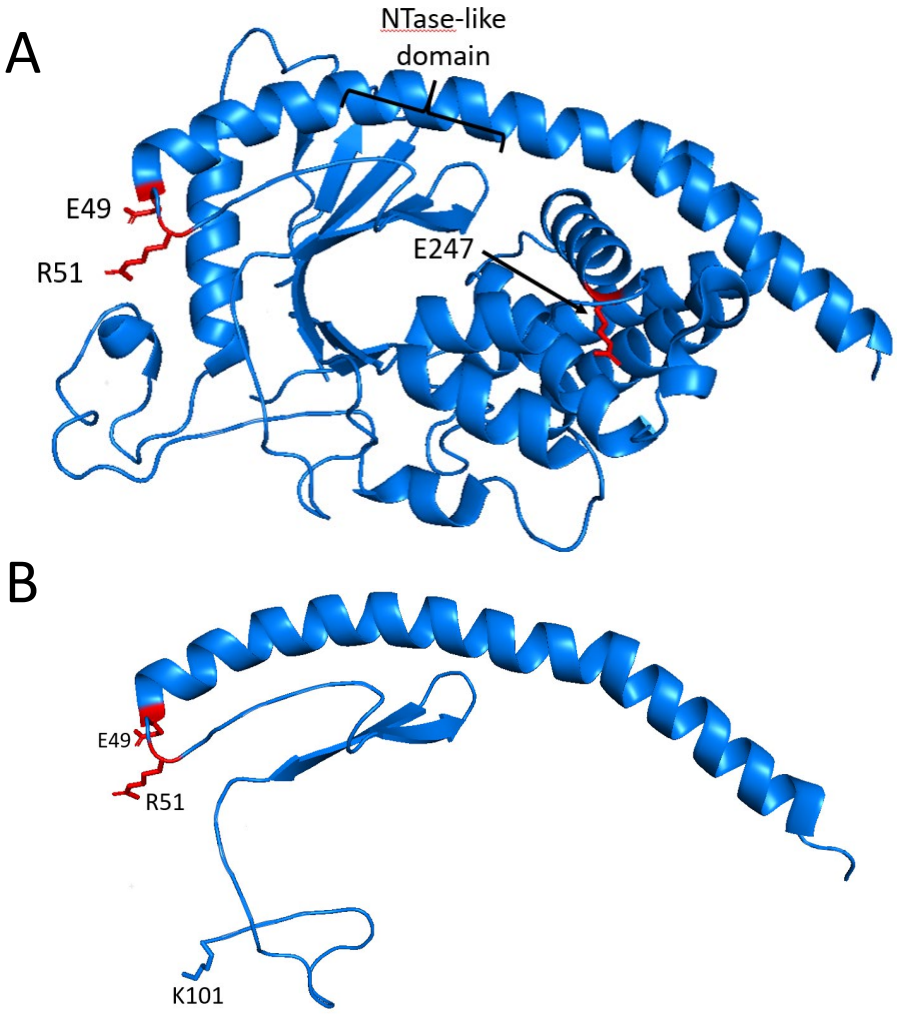

Figure 1.4: Crystal structure of mab21l1 overlaid with known mab21l2 mutations

A: Crystal structure of mab21l1 as crystallized by de Oliveira Mann et al (2016) showing amino acids mutated in MAB21L2 in human patients highlighted in red. Note positioning of these amino acids allowing formation of salt bridges with adjacent protein loops. Additionally note nucleotidyl transferase-like domain contained within the protein's core. B: Crystal structure of mab21l1 with all amino acids beyond K101 removed, showing the theoretical remaining portion of the protein expressed in *mab21l2*^{au10} fish. Amino acids mutated in full length MAB21L2 in human patients are shown in red.

All mutations are dominant, with the exception of R247Q (Rainger *et al.*, 2014; Deml *et al.*, 2015). The primary phenotypes noted in these patients include microphthalmia or anophthalmia, coloboma, and (in the case of R51G) microcornea (Rainger *et al.*, 2014; Deml *et al.*, 2015; Horn *et al.*, 2015). Additional clinical observations include intellectual disability and skeletal rhizomelic dysplasia, which comprises a shortening of the bones of the proximal limbs (Rainger *et al.*, 2014; Horn *et al.*, 2015).

While mutations in *MAB21L2* in human patients have been identified, the developmental and cell biological role for this protein is still largely unknown.

1.5.1 Expression and localization of *mab21l2*

MAB21L2, or mab-21 like 2, is one of two vertebrate paralogs of the *C. elegans* gene mab-21, short for "male-abnormal" due to its observed role in the proper formation of tail rays in the male *C. elegans* animal (Chow *et al.*, 1995; Ho *et al.*, 2001). It is a highly conserved gene, with >97% amino acid identity shared between humans, mice, and zebrafish (Rainger *et al.*, 2014). MAB21L2 was first discovered in 1999 as one of two murine and human homologs of mab-21 (Mariani *et al.*, 1999). However, due to the obvious differences between *C. elegans* and vertebrate models and the relatively lower protein identity between mab-21 and MAB21L2, it was unclear what role, if any, MAB21L2 served in vertebrates.

MAB21L2 is expressed in slightly different domains in mouse, chick, and zebrafish, but some similarities exist. In mouse, at E9.5, *Mab21l2* is found in the brain and throughout the retinal layer of the optic cup, as well as in the forelimb bud and brachial arches, with a lower expression level detected in the surface ectoderm that will become the lens (Wong *et al.*, 1999; Yamada *et al.*, 2004). Later, at E12, *Mab21l2* expression persists in the brain and throughout the entire retina, and is found in the somites, developing limbs, and jaw, though expression in the lens is no longer present (Wong *et al.*, 1999; Yamada *et al.*, 2004). By E14, *Mab21l2* expression is largely undetectable in most areas, except for the brain (Wong *et al.*, 1999).

In chick, *Mab21l2* is seen in the optic vesicle and surface ectoderm at HH9, and persists in both layers of the optic cup as well as the lens vesicle through HH13-14 (Sghari and Gunhaga, 2018). By HH18, *Mab21l2* remains in the RPE, but is restricted to the vitreal edge of the retina, and is largely absent from the developing lens (Sghari and Gunhaga, 2018). At E6, *Mab21l2* in the retina is found only in the ganglion cell layer, but by E8 it is detected in the ganglion cell layer (GCL), inner nuclear layer (INL), and outer nuclear layer (ONL), where expression is sustained (Sghari and Gunhaga, 2018).

In zebrafish, *mab21l2* is expressed in the entire presumptive optic field as early as bud stage, with a midbrain expression domain becoming apparent by 5 somite stage (Kudoh and Dawid, 2001). It persists in both the midbrain and throughout the developing optic cups through 24hpf, at which point it is additionally found in the lens, the pharyngeal arches, and the spinal cord (Deml *et al.*, 2015). Just after 24hpf, the retinal expression becomes restricted to the vitreal edge of the retina, adjacent to the lens (Cederlund *et al.*, 2011; Deml *et al.*, 2015). By 48hpf, *mab21l2* is found in the GCL and INL, with a region of higher expression in the ventral part of the eye, near the closing choroid fissure; *mab21l2* is also found in the CMZ, but is absent from the lens (Deml *et al.*, 2015). By 72hpf, most retinal expression of *mab21l2* is gone, except for expression in the CMZ and in a small ventral patch at the site of the closed choroid fissure (Deml *et al.*, 2015). By 5dpf, the CMZ expression has disappeared, but the ventral patch, now highly restricted to a line marking the previous site of choroid fissure fusion, persists (Cederlund *et al.*, 2011).

1.5.2 Developmental roles of *mab21l2* in knockout and knockdown models

Although the expression domains have been relatively well characterized, much less is known about the function of mab21l2 in these regions. Many previous studies seeking to elucidate the function of mab21l2 used knockout or knockdown approaches to determine its function in particular tissues and processes in the animal. Much like the expression patterns of the *mab21l2* gene, putative roles in each model organism are similar in some ways, and different in others.

In mouse, *Mab21l2* knockouts have severe retinal and lens developmental defects. The retina is produced in only a rudimentary fashion, arresting at the optic vesicle stage, and does not correctly remain in contact with the surface ectoderm nor differentiate into its mature, laminated form (Yamada *et al.*, 2004). The lens also never forms, and the surface ectoderm does not appear to undergo any of the proliferative or morphogenic changes required for lens formation (Yamada *et al.*, 2004). This suggests that in mouse, mab21l2 has a critical role in growth and differentiation of the retina, and in induction of the lens. In addition, in the optic vesicle of *Mab21l2* knockout mice, proliferation is significantly decreased, suggesting a possible role for *Mab21l2* in maintenance of proliferative cell populations; however, no increase in cell death is observed, suggesting no direct role in cell survival (Yamada *et al.*, 2004). *Mab21l2* knockout mice also display defects in the ventral body wall leading to extrusion of organs and death *in utero,* consistent with the mouse-specific expression of *Mab21l2* in the ventral body wall. *Mab21l2*$^{R51C/+}$ mice have also been produced, and have been shown to possess only rudimentary retinas, lack lenses, and display defects in skeletal structures including abnormal fusion of joints and growth plates (Tsang *et al.*, 2018).

In zebrafish, morphant knockdowns for *mab21l2* show microphthalmia and discontinuities in the inner plexiform layer (IPL) and outer plexiform layer (OPL) as well as "holes" in the periphery of the lens, but no other defects (Kennedy *et al.*, 2004). This evidence suggests a role for *mab21l2* in the production or maintenance of the retinal plexiform layers, and in the proper growth of the zebrafish eye. Further supporting this, CRISPR mutant lines mab21l2^{Q48Sfs*5} and mab21l2^{R51_F52del} also display defects in the plexiform layers, although they are confined only to the IPL, which displays foldings and discontinuities (Deml *et al.*, 2015). Interestingly, only the frameshift mab21l2^{Q48Sfs*5} line displays microphthalmia and lens defects (comprising a small, degenerate lens) (Deml *et al.*, 2015), suggesting that the amino acids R51 and F52 are dispensable for *mab21l2'*s apparent role in the lens, and in controlling the size of the eye. Unlike in mutant mice, there are no known defects in mutant or morphant zebrafish affecting parts of the

zebrafish body outside of the eye, consistent with the exclusive expression of zebrafish *mab21l2* in the eye and related neural tissues (Kennedy *et al.,* 2004; Deml *et al.*, 2015).

In both morphant and mutant zebrafish, cell death is elevated in the lens and retina at 24hpf, particularly in the ventral side of the eye, which is not observed in the mouse (Kennedy *et al.*, 2004; Yamada *et al.*, 2004; Deml *et al.*, 2015), suggesting *mab21l2* might have an additional role for lens and retinal cell survival in the zebrafish. Similar to the knockout mouse, mutant zebrafish show decreased proliferation in the eye, although this proliferative defect was only noted at 48hpf (Deml *et al.*, 2015), by which point the zebrafish eye is largely finished forming, and much later than the corresponding defect in knockout mice (Yamada *et al.*, 2004). Still, these data suggest that *mab21l2* has a role in maintenance of proliferation in both mice and zebrafish.

Both mutant zebrafish lines display severe colobomas (Deml *et al.*, 2015), much like the human patients with mutations in *MAB21L2* (Rainger *et al.*, 2014; Deml *et al.*, 2015; Horn *et al.*, 2015), which correlates with a wider expression domain of *pax2* at the ventral side of the mutant eye (Deml, Kariminejad, R. Borujerdi, *et al.*, 2015). This could suggest that mab21l2 plays a role in closure of the choroid fissure, or in proper ventral patterning of the eye.

In chicks electroporated with a dsDNA construct against *Mab21l2* at an early time point (HH8-10), the formation of the retina fails (Sghari and Gunhaga, 2018), much like in knockout mice (Yamada *et al.*, 2004), though interestingly, the lens seems largely unaffected (Sghari and Gunhaga, 2018). These differences may be organism specific, or have to do with the fact that the dsDNA knockdown primarily targets the developing optic vesicle, leaving expression of *Mab21l2* in the surface ectoderm relatively intact, while the mouse knockout removes *Mab21l2* from all tissues. In these knockdown chicks, the retina displays decreased proliferation at E2, but cell death is not increased (Sghari and Gunhaga, 2018), similar to the mouse data (Yamada *et al.*, 2004).

When *Mab21l2* is knocked down in chick at a later time point (HH11-12), microphthalmia and colobomas are produced, again with no lens involvement (Sghari and Gunhaga, 2018), suggesting a common role for mab21l2 in growth of the retina across

mouse, zebrafish, and chick, and a common role in closure of the choroid fissure in zebrafish and chick.

However, retinal defects in *Mab21l2* knockdown chick are markedly different from those in mutant zebrafish. Chick knockdowns display failure of the cells of the GCL and INL to separate and differentiate, as well as hypoplasia of the optic nerve, but the plexiform layers are unaffected (Sghari and Gunhaga, 2018) Therefore, it seems that in chick, *mab21l2* is involved in retinal differentiation but not in formation of the plexiform layers (Sghari and Gunhaga, 2018), while in zebrafish, mab21l2 may be required for proper formation of the plexiform layers, but retinal differentiation has never been investigated (Deml *et al.*, 2015). This apparent discrepancy could indicate organismal differences, or differences inherent in the knockdown versus mutation-based paradigms.

In summary, knockdown and knockout experiments across three animal models show possible roles for mab21l2 in closure of the choroid fissure, growth of the retina and lens, induction of the lens, and proper differentiation and patterning of the retina. In addition, mab21l2 appears to have a role in maintenance of cell proliferation and cell survival in the optic tissues, though the tissues affected and the timings of these roles varies and was incompletely studied (Kennedy *et al.*, 2004; Yamada *et al.*, 2004; Deml *et al.*, 2015; Sghari and Gunhaga, 2018).

1.5.3 Molecular and functional roles of mab21l2

The molecular role of mab21l2 has been of interest to the research community as well. This protein is extremely highly conserved, but its role and functional domains have been remarkably resistant to prediction. mab-21, the *C. elegans* ortholog to Mab21l2, has some association with the TGFβ pathway in *C. elegans*. Through epistasis, mab-21 appears to be downstream of and antagonistic to TGFβ signaling, and furthermore, to be post-transcriptionally regulated by this pathway (Morita *et al.*, 1999). Along similar lines, in *Xenopus laevis*, xmab21l2 was shown to be antagonistic to BMP signaling, able to rescue dorsalization of ventralized BMP4 overexpression embryos (Baldessari *et al.*, 2004). In addition, tagged xmab21l2 coimmunoprecipitates with BMP signaling effector

SMAD1, suggesting that xmab21l2 may be able to modulate BMP signaling through direct binding to and control of its downstream effectors (Baldessari *et al.*, 2004). Later work supports this, showing that the level of p-SMAD1/5/8 is not increased directly upon overexpression of MAB21L2, but downstream pERK signaling is increased (Rainger *et al.*, 2014). Furthermore, in an *in vitro* assay, GAL4-fused xmab21l2 strongly represses the activity of 5XUAS-luciferase constructs (Baldessari *et al.*, 2004), suggesting xmab21l2 might be able to act (alongside SMAD1) directly on expression of mRNAs as a repressive transcription factor.

Whether endogenous mab21l2 is a transcription factor, or if not, what function it might possess, is controversial. In concordance with the above evidence, MAB21L2 and its paralog MAB21L1 are both nuclear localized (Yamada *et al.*, 2003; Kennedy *et al.*, 2004; Deml *et al.*, 2015), which could allow for a transcriptional role, but experiments to prove this have not yet been published.

In fact, other roles have also been proposed for MAB21L2. The family of 12 human mab-21 paralogs, of which MAB21L2 is a member, are predicted to adopt a nucleotidyl transferase fold (Fig. 1.4A) (Rainger *et al.*, 2014). One member of this family, cyclic GMP-AMP synthase (cGAS) is known to bind cytoplasmic DNA and create cyclic GMP-AMP (Sun *et al.*, 2013). Overlay of MAB21L2 on the cGAS structure appears to indicate conservation of the DNA binding groove and active site, but *in vitro* assays of nucleotidyl transferase activity show no apparent ability of MAB21L2 to perform nucleotidyl transferase function (Rainger *et al.*, 2014). Crystal structures of closely-related paralog MAB21L1, which shares 94% amino acid identity with MAB21L2, show that compared to the cGAS NTase site, MAB21L1 lacks several key residues and the active site is conformationally inaccessible (Fig. 1.4A) (de Oliveira Mann *et al.*, 2016). These key residues are also absent in MAB21L2 (de Oliveira Mann *et al.*, 2016), which could explain the apparent lack of NTase function *in vitro.* In addition, MAB21L2 appears to be unable to bind to ssDNA *in vitro*, instead binding only to ssRNA (Rainger *et al.*, 2014). An ability to bind only to RNA would suggest that

endogenous MAB21L2 is not likely a direct transcription factor, although post transcriptional control of newly made mRNAs is still a possible function.

Without knowledge of the function of wild type MAB21L2, or a definitive structure, it is difficult to predict the mechanism by which mutations can destroy this function. However, attempts have been made to determine the effects of mutations on the protein stability and RNA binding activity of MAB21L2. Rainger et al. found that the MAB21L2 mutations E49K, R51C, and R51H (dominant mutations) are stabilizing, while R247Q (recessive mutation) has no effect on protein stability (Rainger *et al.*, 2014). This is inconsistent with evidence from the structure of MAB21L1, which suggests that all four mutations affect residues that would form salt bridges critical for the stabilization of MAB21L1 and L2 (Fig. 1.4A) (de Oliveira Mann *et al.*, 2016). It is unclear why stabilization is observed for 3 of 4 mutations in these *in vitro* assays, against structural predictions. Interestingly, almost the opposite is shown in another assay for protein stability of the mutated versions of MAB21L2. R51G, a mutation affecting the same arginine residue as two of the above assays, is shown by Deml et al. to destabilize MAB21L2, as does a deletion of amino acids 51 and 52 (Deml *et al.*, 2015), more consistent with predictions from structural evidence. All four mutations tested (E49K, R51C, R51H, R247Q) completely abolish the observed ssRNA binding activity of MAB21L2, consistent with their predicted locations along the DNA-binding groove of cGAS which likely becomes the RNA binding site of MAB21L2 (Rainger *et al.*, 2014).

The goals of my thesis work were to further characterize the role of mab21l2 in the development of the vertebrate eye using a mutant zebrafish, particularly focusing on the development of the lens and cornea, which have not previously been studied in detail. I used imaging and immunohistochemistry-based techniques to provide evidence for mab21l2's role in maintenance of cell survival in various tissues including the optic stalk, its role in growth and differentiation of the lens, and its involvement in controlling growth and patterning of the cornea. In addition, I used embryo microinjection of human

variants and yeast-2-hybrid assay to attempt to elucidate the role of this protein in the biology of the cell, and how mutations could affect its function.

Chapter 2: Zebrafish mab21l2 mutants possess severe defects in optic cup morphogenesis, lens and cornea development

This chapter is modified from the following publication, with permission from the authors:

Gath, N. and Gross, J. M. (2019) Zebrafish mab21l2 mutants possess severe defects in optic cup morphogenesis, lens and cornea development . *Dev. Dyn.*, 248(7), pp. 514-529.

NG and JMG conceived the experiments and concepts for the work, and interpreted data.

NG performed experiments, collected and analyzed data.

2.1 INTRODUCTION

MAB21L2 (male-abnormal 21-like-2) is a highly conserved, yet poorly understood protein that has been shown to be involved in lens and retina development in vertebrate models (Yamada *et al.*, 2004; Rainger *et al.*, 2014; Deml *et al.*, 2015; Sghari and Gunhaga, 2018). Mouse *Mab21l2* knockouts display major eye defects, including a complete failure of lens formation and severe defects in retinal development (Yamada *et al.*, 2004). Zebrafish *mab21l2* mutants also possess lens and retina defects, as well as colobomas (Hartsock *et al.*, 2014; Deml *et al.*, 2015), and *Mab21l2* knockdown in chick embryos results in defects in retinal neuron differentiation (Sghari and Gunhaga, 2018), suggesting diverse roles for the protein during eye development. Expression of *Mab21l2* in mice and chick is similar to that of zebrafish in that broad, eye-wide expression is common early on in development, and expression becomes restricted to a few tissues or domains later on. However, there are also organism-specific differences, such as the fact that, in chick, *Mab21l2* remains evenly expressed along the dorsoventral axis of the retina, though it is restricted to the ganglion cell and inner/outer nuclear layers, while in zebrafish, the expression of *mab21l2* becomes ventrally restricted, but is found throughout all retinal layers (Cederlund *et al.,* 2011; Deml *et al.*, 2015; Sghari and

Gunhaga, 2018). Which model organism's expression pattern most closely recapitulates that found in humans is unknown.

Highlighting the clinical importance of these studies and the utility of animal models, mutations in *MAB21L2* are associated with Microphthalmia, Anophthalmia, Coloboma (MAC) Syndrome in which affected patients display a range of severe ocular malformations (Rainger *et al.*, 2014; Deml *et al.*, 2015; Horn *et al.*, 2015). The function(s) of the Mab21l2 protein are largely unknown, making it difficult to understand the molecular and cellular underpinnings of ocular defects in these patients. Results from several studies have proposed possible functions as a transcriptional repressor (Baldessari *et al.*, 2004), the ability to bind single-stranded RNA *in vitro* (Rainger *et al.*, 2014), and structural similarity to nucleotidyl transferases (Kuchta *et al.*, 2009; de Oliveira Mann *et al.*, 2016). Despite these studies, however, definitive roles for mab21l2 are currently unclear.

Eye development is a complex process involving intrinsic and extrinsic factors and precise interactions between a number of ocular and non-ocular tissues. Defects in any of these processes during development can lead to severe congenital ocular disorders, and animal model systems have been critical in providing mechanistic insight into the nature of these disorders (Bibliowicz *et al.*, 2011; Gestri *et al.*, 2012). Amongst these models, zebrafish have emerged as a highly useful system given the ability to perform forward and reverse genetic screens to generate disease alleles, and combine these with state of the art molecular, behavioral and imaging assays (Dooley and Zon, 2000; Adamson *et al.*, 2018). While numerous specification and tissue segregation events precede overt eye development in zebrafish, the prospective optic cup emerges from the diencephalon at approximately the 5 somite stage (SS), and eye development proceeds rapidly thereafter. Lens development begins at approximately the 16-18SS, when cells of the surface ectoderm begin to columnarize, divide and thicken to form the lens placode (Schmitt and Dowling, 1994; Greiling and Clark, 2009). Unlike in other vertebrates, where the developing lens pinches off from the surface ectoderm to form a hollow lens vesicle, the zebrafish lens develops as a mass of cells which remains attached to the

surface ectoderm through much of its early development, until approximately 24 hours post fertilization (hpf) when it separates from the overlying surface ectoderm (Schmitt and Dowling, 1994; Greiling and Clark, 2009). This mass forms a solid spherical structure composed of cells which are becoming specified to either lens epithelial or lens fiber fates via the combined action of several signaling pathways (reviewed in Cvekl & Zhang 2017).

Between 28 and 36hpf, the lens epithelium and lens fiber cells are organized in their mature locations: the epithelium wraps the front, outermost layer of the lens, while differentiating and elongating fibers proceed from the transition zone at the lens equator to wrap the lens core (Greiling and Clark, 2009). At ~30hpf, the surface ectoderm that did not become part of the lens begins to adopt corneal epithelial identity, and will soon begin to lay down an acellular corneal stroma (Zhao *et al.*, 2006). At ~36hpf, corneal endothelial cells, derived from the neural crest (Johnston *et al.*, 1979), migrate into the eye and move between the lens and corneal epithelium to form the corneal endothelial monolayer (Hay, 1980; Zhao *et al.*, 2006). Between 30hpf and 14dpf, the corneal stroma will thicken and mature, and between 14 and 28dpf, resident stromal cells known as keratocytes will invade the stromal layer (Zhao *et al.*, 2006). Between 36hpf and 5dpf, markers of corneal epithelial, endothelial, and stromal identity will be expressed and laid down in the corresponding tissue (Zhao *et al.*, 2006).

Concomitant with lens and cornea development, the optic cup is also undergoing specification into retina and RPE domains and significant morphogenesis to form the three-dimensional architecture of the mature eye. As a consequence of the invagination and morphogenesis of the early eye field into a bilayered optic cup, a transient opening known as the choroid fissure forms in the ventral optic cup (Schmitt and Dowling, 1994) which enables the hyaloid vasculature to enter the eye (Hartsock *et al.*, 2014), and the optic nerve to exit (Schmitt and Dowling, 1994). The choroid fissure must close such that retina and RPE tissue are properly contained within the eye, and failure of this process results in colobomas (reviewed in Gregory-Evans et al. 2004; Williamson & FitzPatrick 2014; Patel & Sowden 2017).

As mentioned above, previous studies have identified or generated *mab21l2* mutant zebrafish (Hartsock *et al.*, 2014; Deml *et al.*, 2015) which display ocular phenotypes. However, these ocular defects have not been fully documented and characterized, which is necessary for these zebrafish models to be useful in providing mechanistic insight into ocular defects in human patients with *MAB21L2* mutations, as well as to begin to unravel the functions of the mab21l2 protein during ocular development. Here, we characterize the zebrafish *mab21l2*^{au10} allele, which was identified in a forward genetic screen (Lee *et al.*, 2012) and shown to possess a nonsense mutation (K101Stop) that truncates the mab21l2 protein to ~1/3 of its total size (Fig. 1.4B) (Hartsock *et al.*, 2014). Our results demonstrate that *mab21l2* $^{-/-}$ mutants possess defects in lens morphogenesis, lens epithelial cell proliferation and survival, and lens patterning. *mab21l2* $^{-/-}$ embryos display variable colobomas which are associated with elevated cell death in the early optic stalk and a failure to break down the basement membrane separating the two sides of the choroid fissure. Finally, we identify corneal defects in *mab21l2* $^{-/-}$ mutants which manifest as a cornea that contains multiple extra layers of cells, is swollen, and lacks differentiation of the corneal stroma.

2.2 RESULTS:

2.2.1 *mab21l2* $^{-/-}$ mutants possess severe malformations of multiple ocular tissues.

mab21l2 $^{-/-}$ mutants were identified in a previous forward genetic screen conducted in our laboratory (Lee *et al.*, 2012), and were identified based on defects that included either small lenses or a complete lack of lenses, as well as a misshapen optic cup (Hartsock *et al.*, 2014). In working further with *mab21l2* $^{-/-}$ mutants, we noted additional and complex ocular defects and sought to characterize them in detail. We first examined *mab21l2* $^{-/-}$ ocular phenotypes in whole mount embryos throughout the first five days of development (Fig. 2.1). Prior to 24 hours post fertilization (hpf), ocular development appears largely normal in *mab21l2* $^{-/-}$ mutants when compared to wild type siblings, with ocular defects becoming apparent at approximately 24hpf (Fig. 2.1A, F). At 24hpf,

mutant eyes are microphthalmic, lenses appear smaller, eyecups are misshapen, and pigmentation is delayed (Fig. 2.1A, F). These differences persist through 36hpf (Fig. 2.1B, C, G, H).

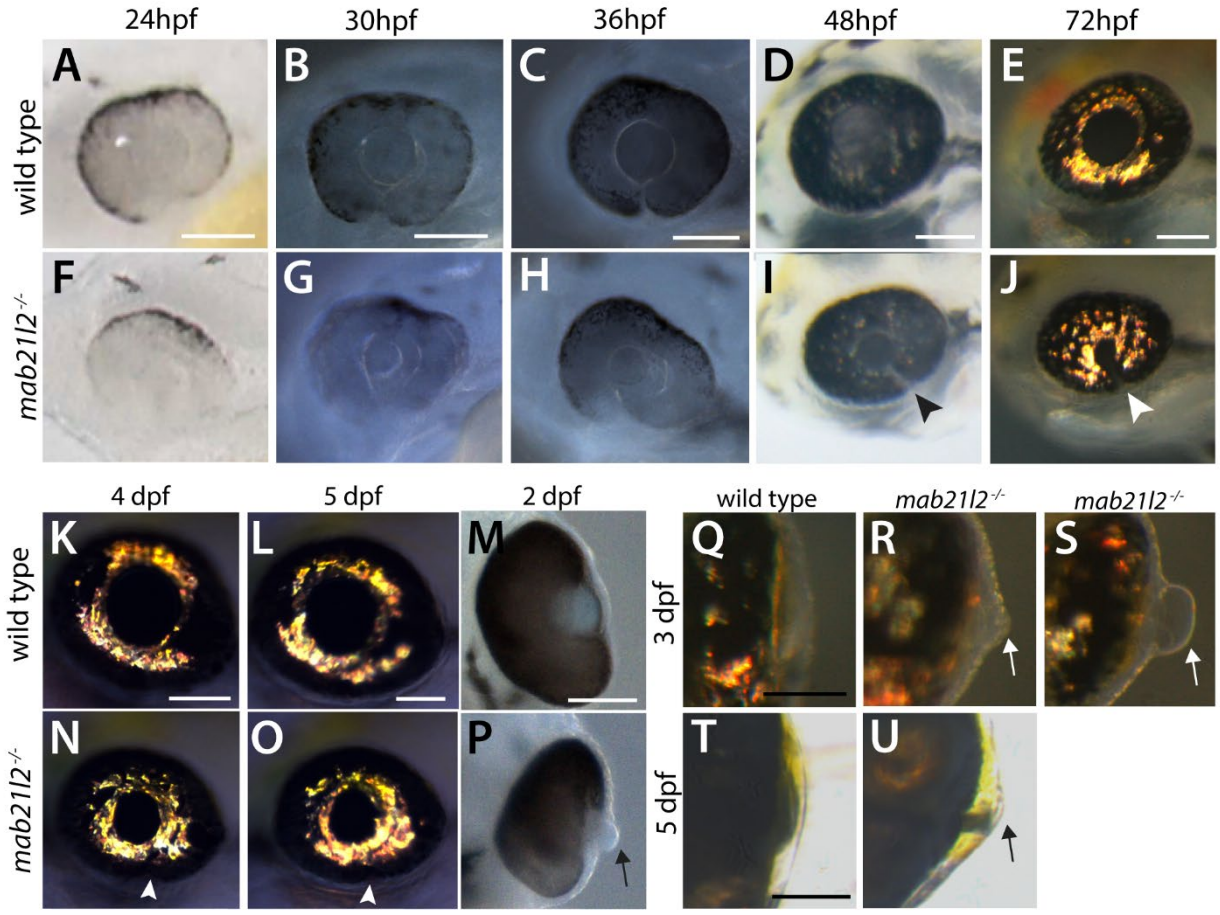

Figure 2.1: *mab21l2* mutants possess complex eye defects that include small lenses, microphthalmia, coloboma, and corneal malformations.

A-L, N, O: Whole mount images of wild type (A-E, K, L) and *mab21l2* $^{-/-}$ (F-J, N, O) mutant embryos. Compared to wild type embryos, *mab21l2* $^{-/-}$mutants display lens defects, microphthalmia and misshapen eyes beginning at 24hpf (compare A-E, K,L to F-J, N, O). Arrowheads in I, J indicate colobomas present in *mab21l2* $^{-/-}$ mutants.
M, P, Q-U: Ventral whole mount images of wild type (G, J) and *mab21l2* $^{-/-}$ (H, I, K) embryos at time points indicated. Note corneal malformations and lens displacement in *mab21l2* $^{-/-}$ mutants (arrows in P, R, S, U).
Scale bars = 100µm.

In addition to abnormalities in the shape of the optic cup, the choroid fissure remains open in *mab21l2* $^{-/-}$ mutants at 48hpf and they display prominent colobomas (Fig. 2.1D, I, arrowhead). At 72hpf, mutants remain microphthalmic and colobomas persist. Differences in lens size are also obvious at this time (Fig. 2.1E, J). Interestingly, subsequent to our initial identification of the *mab21l2* $^{-/-}$ line and after several generations of outcrosses, we rarely identify homozygous mutants that completely lack a lens, although the penetrance of the small lens phenotype remains close to 100% in homozygous embryos (data not shown). By 4 and 5dpf, the severity of colobomas varies in *mab21l2* $^{-/-}$ mutants, with some showing severe retinal blowout in which the proximal retina and RPE are extruded into the brain, while others (Fig. 2.1K, L, N, O) have subtle colobomas largely visible only through histology.

mab21l2 $^{-/-}$ mutants also possess corneal defects. During early development, the lens and cornea are specified from a common population of surface ectodermal cells (Collomb *et al.*, 2013). Many mutations that disrupt development of the lens also disrupt formation of the cornea, and vice versa (Lwigale and Bronner-Fraser, 2009; Choi *et al.*, 2014; Silla *et al.*, 2014). As we had noted lens defects in *mab21l2* $^{-/-}$ mutants, we were curious whether corneal defects were also present in these mutants, which may suggest defects in a common pathway involved in development of both structures. *mab21l2* $^{-/-}$ corneas appear overtly normal until 48hpf, when obvious morphological defects emerge. In ventral views of 48hpf *mab21l2* $^{-/-}$ mutants, corneal thickening and bulging are obvious, and in many mutant embryos there is an outward displacement of the lens (Fig. 2.1M, P, arrow). Corneal defects become more pronounced at 3dpf (Fig. 2.1 Q-S, arrows). At this time, *mab21l2* $^{-/-}$ mutant corneas remain thickened and many bulge outwards over a displaced lens (Fig. 2.1R). In rare cases (≈ 5-10% of mutants), the cornea appears to be fluid filled and the lens is dysplastic, floating within an enclosed corneal "pouch" (Fig. 2.1S). Corneal thickening and bulging with displaced lenses persists through 5dpf (Fig. 2.1T, U).

Collectively, these data indicate that *mab21l2* $^{-/-}$ mutants display complex, multi-tissue ocular defects that include small lenses, microphthalmia, colobomas, and corneal

malformations. Several of these phenotypes overlap with those observed in human patients with *MAB21L2* mutations (Rainger *et al.*, 2014; Deml *et al.*, 2015; Horn *et al.*, 2015); however, the etiology of these defects is unknown. Thus, we next focused on each phenotype/tissue malformation to begin to determine its ontogeny during development and potential molecular underpinnings.

2.2.2 *mab21l2* $^{-/-}$ mutants possess defects at several stages of lens development.

To assess defects in lens formation in *mab21l2* $^{-/-}$ mutants, we first examined early lens morphogenesis to determine when lens malformations manifest. Sections of 18SS embryos revealed that the initiation of lens morphogenesis was impaired in *mab21l2* $^{-/-}$ mutants (Fig. 2.2H) when compared to wild type siblings (Fig. 2.2A). Lens defects manifest at these early stages as a lack of columnar cells that invaginate inward from the lens placode toward the retina to generate the primary lens. The delay is transient, however, as *mab21l2* $^{-/-}$ embryos reach an equivalent level of invagination approximately two hours later, at about 22SS (Fig. 2.2I). Defects in lens formation in *mab21l2* $^{-/-}$ mutants continue to worsen at 26SS (compare Fig. 2.2C, J), a time at which pyknotic nuclei appear in the mutant lens (Fig. 2.2J). By 28hpf, phenotypically wild type sibling lenses have separated from the surface ectoderm and become spherical, while many *mab21l2* $^{-/-}$ mutant lenses appear to remain attached to the overlying surface ectoderm (Fig. 2.2D, K), and mutant lenses contain a number of pyknotic nuclei (Fig. 2.2K, arrowhead) compared to wild type. At 36hpf, wild type sibling lenses are well organized, with distinct lens epithelium and early lens fibers present (Fig. 2.2E). However, the lens epithelium and primary fibers are not distinguishable in *mab21l2* $^{-/-}$ lenses; mutant lenses remain as a mass of cells that appear to still be connected to the surface ectoderm/developing cornea (Fig. 2.2L). At 48hpf, *mab21l2* $^{-/-}$ mutant lenses are smaller, and lens fibers are not as well organized into concentric rings (Fig. 2.2M) when compared to wild type siblings (Fig. 2.2F). Lens defects persist through 5dpf (Fig. 2.2G, N).

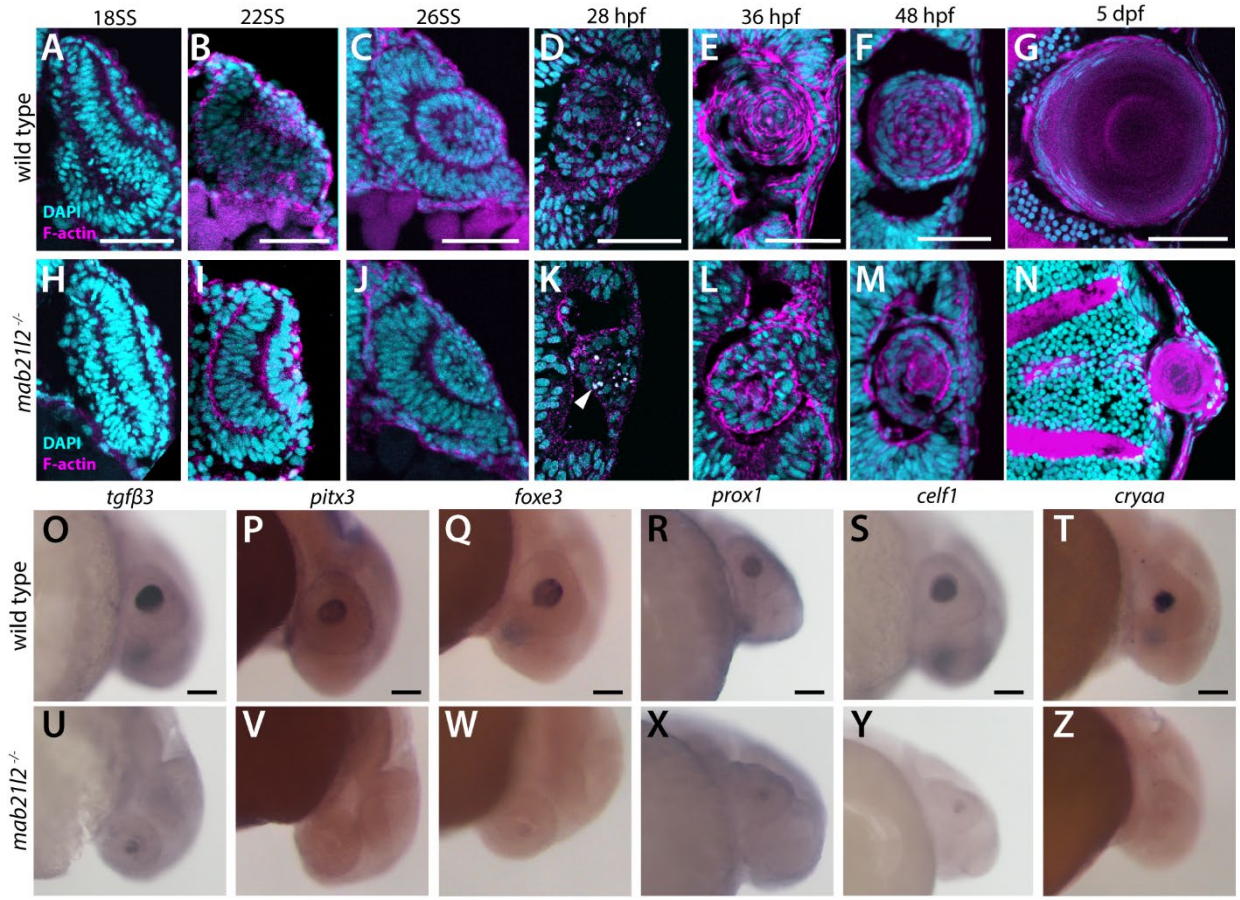

Figure 2.2: *mab21l2* $^{-/-}$ mutants possess delays in lens morphogenesis and lens growth, and do not properly express markers of mature lens cell types

A-G: Transverse sections of wild type (A-G) and *mab21l2* $^{-/-}$ mutant (H-N) embryos showing lens development over time. Compared to wild type, *mab21l2* $^{-/-}$ mutants do not show induction of lens morphogenesis at 18SS (H); instead, comparable development isn't detected until 22SS (I). Lenses remain smaller at 28hpf (K), 36hpf (L), 48hpf (M), and 5dpf (N). Note pyknotic nuclei in 28hpf mutant (K, arrowhead).
O-Z: Whole mount in situ hybridizations of 48hpf wild type (O-T) and *mab21l2* $^{-/-}$ (U-Z) embryos. Note apparently reduced *tgfβ3* (U), *prox1* (X), and *celf1* (Y) in *mab21l2* $^{-/-}$ mutants, compared to wild type (O, R, S respectively). Note also that *mab21l2* $^{-/-}$ mutants lack detectable *pitx3* (V), *foxe3* (w), and *cryaa* (Z) expression.
Dorsal is up in all panels. Scale bars = 50μm.

Given the apparent disorganization of the lens in *mab21l2* $^{-/-}$ mutants, we next determined whether the mutant lens expressed markers of lens epithelial cells and fiber cells, or if lens patterning and differentiation were also disrupted. To assess lens epithelial and fiber specification, we performed *in situ* hybridizations for several well-established markers of lens epithelial fates: *tgfb3* (Gordon-Thomson *et al.*, 1998; Cheah *et al.*, 2005), *pitx3* (Semina *et al.*, 1997), and *foxe3* (Blixt *et al.*, 2000), and of lens fiber fates: *prox1* (Wigle *et al.*, 1999), *celf1* (Blech-Hermoni *et al.*, 2013), and *cryaa* (Robinson and Overbeek, 1996) (Fig. 2.2O-Z). At 48hpf, *mab21l2* $^{-/-}$ embryos display an apparent reduction in lens epithelial marker *tgfb3* (Fig. 2.2O, U), while the expression of other lens epithelial markers *pitx3* and *foxe3* was not detected in *mab21l2* $^{-/-}$ mutants (Fig. 2.2V and W respectively) when compared to wild type controls (Fig. 2.2P, Q respectively). *prox1*, a marker of the lens epithelium to fiber transition zone, also appeared to be reduced in mutants (Fig. 2.2X) when compared to wild type siblings (Fig. 2.2R). Of the markers of lens fiber cell identity, *celf1* also appeared to be reduced in *mab21l2* $^{-/-}$ mutants (Fig. 2.2Y) compared to wild type controls (Fig. 2.2S), and *mab21l2* $^{-/-}$ mutants showed no visible *cryaa* expression (Fig. 2.2T, Z). Collectively, these data support a model in which lens morphogenesis is delayed in *mab21l2* $^{-/-}$ mutants, and their lenses are smaller and not properly patterned.

2.2.3 Lens cells require mab21l2 function to maintain proliferation and survival.

Having established that there may be both developmental and patterning defects in *mab21l2* $^{-/-}$ lenses, we sought to determine the cellular underpinnings of the reduced lens size *mab21l2* $^{-/-}$ mutants. Previous studies of *Mab21l2* knockout mice showed that proliferation in the developing optic vesicle and overlying surface ectoderm was decreased upon loss of Mab21l2, and that these defects correlated with microphthalmia and absence of lenses (Yamada *et al.*, 2004). We therefore hypothesized that increased cell death and/or reduced cellular proliferation could explain the relatively fewer cells found in the lens of *mab21l2* $^{-/-}$ mutants. To test this hypothesis, we performed TUNEL assays to quantify cell death in the developing lens, and we performed BrdU

incorporation assays and quantification of the proportion of proliferative cells within the lens at several times points in early lens development when the wild type lens epithelium is actively proliferating (Fig. 2.3). At 22SS, *mab21l2* $^{-/-}$ mutants have a significantly increased proportion of TUNEL^{+} cells in their lenses when compared to their wild type siblings, with a mean of 6.0% of lens cells TUNEL^{+} in mutants, compared to 2.1% in wild type siblings (Fig. 2.3A, F, K; $p = 0.027$). Similarly, at 26SS, there is a significant increase in the number of TUNEL^{+} cells per total cell number in the *mab21l2* $^{-/-}$ lens, with a mean of 8.9% of lens cells being TUNEL^{+} in mutants, compared to 1.7% in wild type siblings (Fig. 2.3B, G, L; $p = 0.0010$). Interestingly, this increase in cell death appears to be transient, as by 48hpf, there is no longer a significant increase in TUNEL^{+} lens cells in *mab21l2* $^{-/-}$ mutants when compared to wild type siblings (Fig. 2.3C, H, M; $p = 0.63$). Together, the TUNEL assays suggest increased cell death during the early stages of lens development in *mab21l2* $^{-/-}$ mutants likely contributes to the decreased lens size observed at 5dpf.

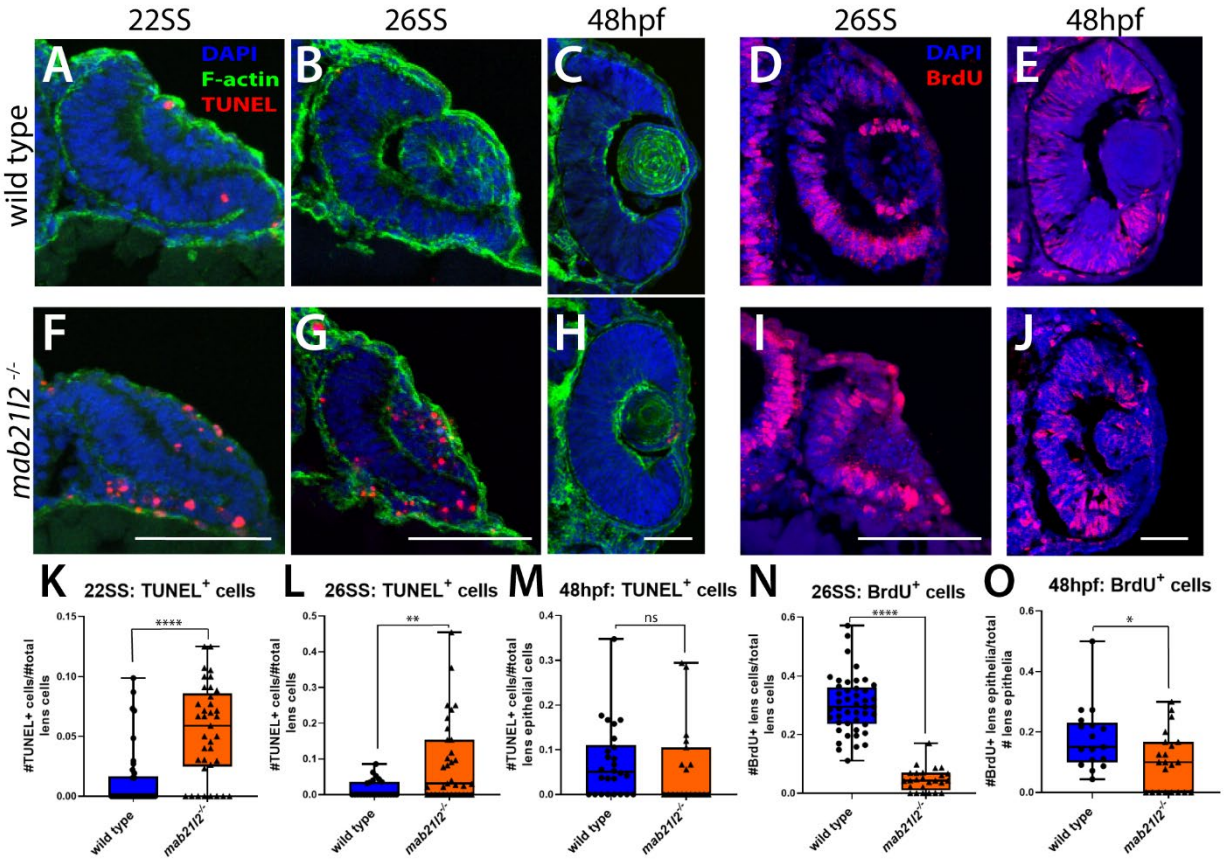

Figure 2.3: *mab21l2* $^{-/-}$ embryos display transient increase in cell death, decreased proliferation in the developing lens

A-C, F-H: TUNEL stain of wild type (A-C) and *mab21l2* $^{-/-}$ mutant (F-H) embryos. Compared to wild type, *mab21l2* $^{-/-}$ mutants possess a transient increase in cell death at 22SS (F) and 26SS (G) while 48hpf (H) embryos have equivalent proportions of dying cells to their wild type siblings (B, A and C respectively).
K-M: Quantification of TUNEL^{+} cells in images A-C, F-H. Note significant differences in proportion of TUNEL^{+} cells in 22SS (K, $p < 0.0001$) and 26SS (L, $p = 0.001$) but not 48hpf (M, $p = 0.63$) samples.
D,E,I,J: BrdU incorporation assay in wild type (D,E) and *mab21l2* $^{-/-}$ mutant (I,J) embryos. Compared to wild type (D), *mab21l2* $^{-/-}$ (I) mutants possess a decrease in proliferative cells in the lens at 26SS.
N,O: Quantification of BrdU^{+} cells in images D,E,I,J. Note significant differences in the proportion of BrdU^{+} lens cells in 26SS (N) samples.
Dorsal is up in all panels. Scale bars = 50µm.

To assess the contribution of altered cell proliferation to the small lens phenotype observed in *mab21l2* $^{-/-}$ mutants, we next performed BrdU incorporation assays. Analyses at 26SS revealed a significantly reduced proportion of BrdU^{+} cells in the lens of *mab21l2* $^{-/-}$ embryos when compared to wild type siblings; only 4.6% of *mab21l2* $^{-/-}$ lens cells were BrdU^{+}, compared to 30.0% of wild type lens cells (Fig. 2.3D, I, N; $p < 0.0001$). This reduction in the proportion of proliferating cells in *mab21l2* $^{-/-}$ embryos persists through 48hpf, at which time 10.1% of the anterior outermost layer of lens cells (presumptive lens epithelial cells) are BrdU^{+} in *mab21l2*$^{-/-}$ embryos compared to 18.0% in wild type siblings (Fig. 2.3E, J, O; $p = 0.024$). These data support decreased proliferation within the *mab21l2* $^{-/-}$ lens as also likely contributing to the small lens phenotype detected in these embryos.

2.2.4 Colobomas in *mab21l2* $^{-/-}$ mutants are associated with failure of basement membrane breakdown in the choroid fissure.

As discussed above, *mab21l2* $^{-/-}$ mutants possess colobomas of varying severity, with some mutant embryos possessing severe closure defects along the proximal-distal axis of the fissure and retinal blowout (Fig. 2.4A, D), while others display relatively normal closure of the fissure proximally, with colobomas only detected at more distal regions. To more directly assess choroid fissure closure and colobomas, we sectioned severe and mild *mab21l2* $^{-/-}$ mutants and wild type siblings at 5dpf. *mab21l2* $^{-/-}$ mutants with severe colobomas showed extrusion of retinal and RPE tissue out of the eye (Fig. 2.4E, arrow). In milder *mab21l2* $^{-/-}$ mutants, sagittal sections revealed modest colobomas, detected by the misalignment of the retinal layers in the ventral portion of the eyecup where the two sides of the fissure have not fused (Fig. 2.4F, arrowhead).

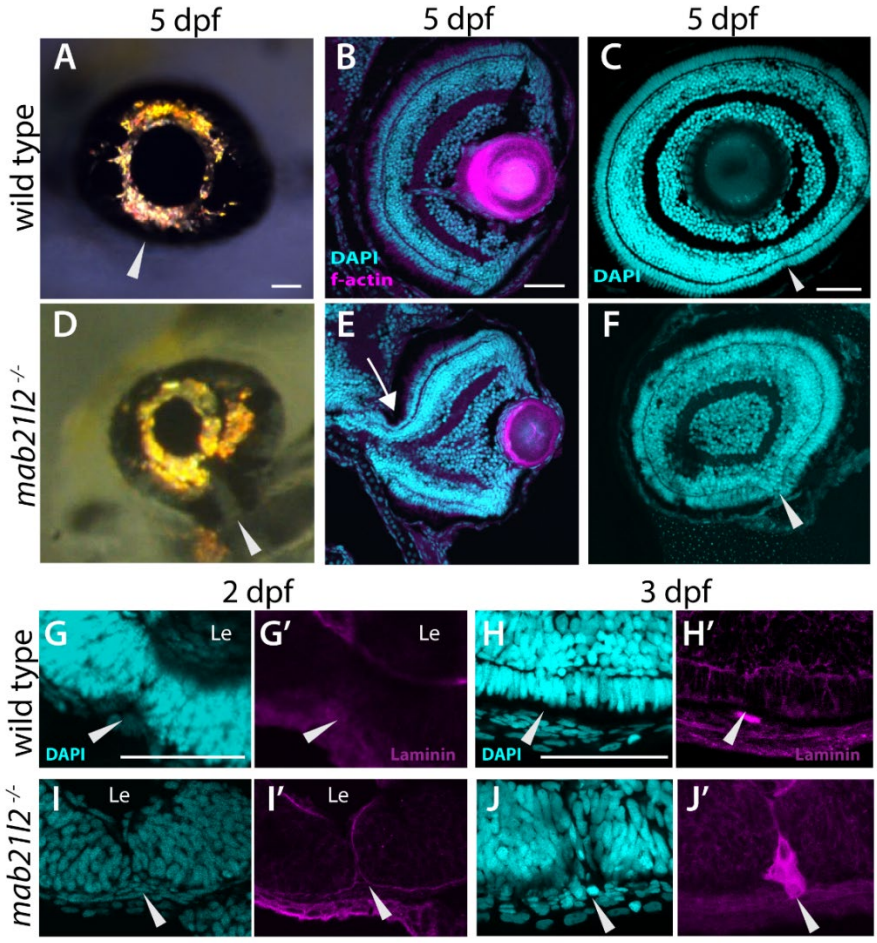

Figure 2.4: *mab21l2* $^{-/-}$ mutants possess colobomas of varying severity, and retain basement membrane markers in the choroid fissure

A,D: Whole mount images of wild type (A) and *mab21l2* $^{-/-}$ mutant (D) embryos highlighting colobomas. Compared to wild type, *mab21l2* $^{-/-}$ embryos show colobomas of varying severities at 5dpf (D).
B,C,E,F: Transverse (B,E) and sagittal (C,F) sections of wild type (B,C) and *mab21l2* $^{-/-}$ mutant (E,F) embryos at 5dpf. Note the severe coloboma in proximal eye cup of the *mab21l2* $^{-/-}$ mutant (E, arrow) compared to wild type (B). In sagittal section view, (C,F), the *mab21l2* $^{-/-}$ retina (F) displays discontinuity of retinal lamina and failure of choroid fissure fusion (arrowhead) when compared to wild type (C).
G-J': Laminin α1 localization in wild type (G-H') and *mab21l2* $^{-/-}$ (I-J') eyes. Magenta=laminin, cyan=DAPI. Le= lens. Arrowhead marks the site of the choroid fissure. Note that wild type embryos (G, G', H, H') do not display laminin α1 at the site of the closed choroid fissure, while *mab21l2* $^{-/-}$ mutants (I, I', J, J') retain laminin α1 localization at the open choroid fissure (arrowheads).
Scale bars = 50μm.

It is known that breakdown of the basement membrane that lines the two edges of the retina/RPE within the choroid fissure correlates with choroid fissure closure, and that failure of this process can lead to colobomas (Torres *et al.*, 1996; Barbieri *et al.*, 2002; See and Clagett-Dame, 2009; Tsuji *et al.*, 2012; James *et al.*, 2016). We investigated whether basement membrane breakdown proceeded correctly in *mab21l2* $^{-/-}$ mutants via immunohistochemical staining for laminin α1, a component of laminin-111, which is a constituent of the basement membrane lining the edges of the choroid fissure (Smyth *et al.*, 1999; Lee and Gross, 2007), comparing wild type to mutant eyes at 2dpf, when most wild type fish have completed choroid fissure closure. In wild type embryos, the laminin α1 distribution around the outside of the fused eyecup is continuous, which indicates successful closure and fusion of the choroid fissure (Bernstein *et al.*, 2018) and no laminin α1 is detected at the site of the now fused choroid fissure (Fig. 2.4G and 2.4G', arrowheads). In 2dpf *mab21l2* $^{-/-}$ mutants, however, laminin α1 persists between the two edges of the retina/RPE, and the fissure is not fused (Fig. 2.4I and 2.4I', arrowheads). At 3dpf, this laminin α1 layer persists in the fissure of mutant eyes (Fig. 2.4J and 2.4J', arrowheads), while it remains undetectable at the site of the former choroid fissure in wild type siblings (Fig. 2.4H and 2.4H', arrowheads). These results suggest that *mab21l2* $^{-/-}$ mutants possess defects in basement membrane breakdown and that this could contribute to colobomas in the mutant eye.

2.2.5 Cell death in the optic stalk is increased in *mab21l2* $^{-/-}$ mutants.

In addition to defects in basement membrane breakdown, defects in patterning and growth of the optic stalk can also lead to colobomas (Schwarz *et al.*, 2000; Mui *et al.*, 2005; Morcillo *et al.*, 2006; Lee *et al.*, 2008, 2012). We hypothesized that optic stalk defects could contribute to colobomas in *mab21l2* $^{-/-}$ mutants, given that the mutant eye cup is misshapen at early developmental stages (see Fig. 2.1, Fig. 2.2A-B, H-I). To assess this possibility, we examined the segregation of the early optic vesicle into proximal (stalk) and distal (retina/RPE) domains using *pax2* and *pax6* as markers. At 18SS, a time at which changes in the distribution of these markers correlates with colobomas in several

models (Schwarz *et al.*, 2000; Lee *et al.*, 2008), no differences in the distribution of these markers was detected between *mab21l2* $^{-/-}$ mutants and siblings, indicating that segregation of the early optic vesicle is not disrupted in *mab21l2* $^{-/-}$ mutants (data not shown).

Elevated cell death in the optic stalk is also known to contribute to colobomas (Viringipurampeer *et al.*, 2012; Lee *et al.*, 2013). Thus, we next used TUNEL staining to assess the presence of dying cells in the optic stalk of *mab21l2* $^{-/-}$ mutants at 22SS and 26SS (Fig. 2.5). In wild type siblings, few to no TUNEL^{+} cells are present in the optic stalk at either time point (Fig. 2.5A-C). However, in *mab21l2* $^{-/-}$ embryos, an increase in TUNEL^{+} cells in the optic stalk was detected at both 22SS and 26SS (Fig. 2.5E-G). To verify that dying cells were localized to optic stalk tissue, we performed an immunohistochemical stain for pax2, a marker of the optic stalk (Nornes *et al.*, 1990; Torres *et al.*, 1996), in conjunction with TUNEL staining at 26SS (Fig. 2.5D, H). In wild type siblings, few pax2^{+} cells were also TUNEL^{+} (Fig. 2.5D). In contrast, in *mab21l2* $^{-/-}$ mutants, significantly more pax2^{+}/TUNEL^{+} cells were detected (Fig. 2.5H, I; $p = 0.014$), suggesting that loss of mab21l2 function affects cell survival within the optic stalk.

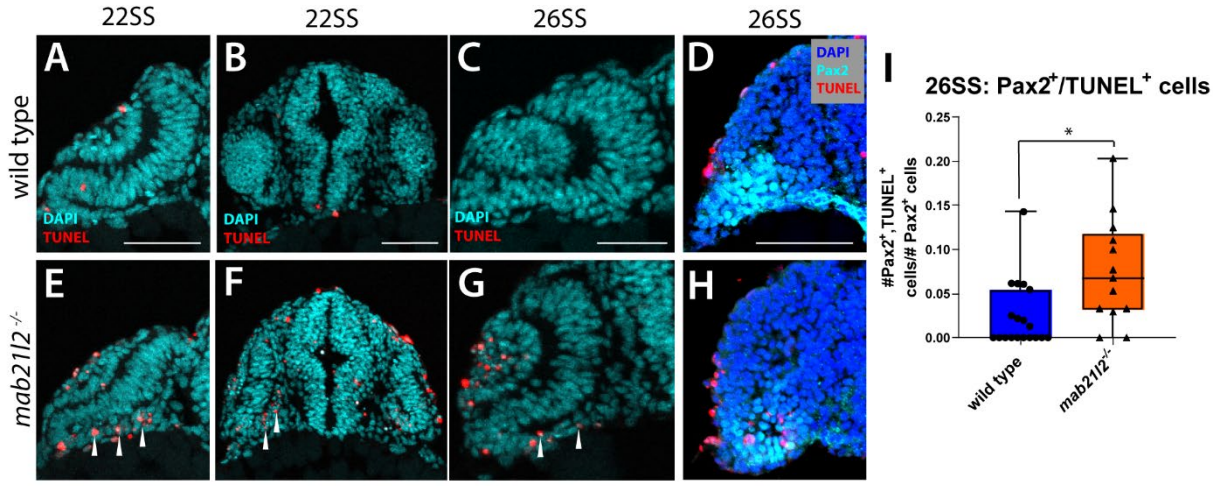

Figure 2.5: *mab21l2* $^{-/-}$ possess elevated cell death in their optic stalk

A-C, E-G: TUNEL stain of wild type (A-C) and *mab21l2* $^{-/-}$ mutant (E-G) embryos. Compared to wild type, 22SS mutant embryos (E,F) possess an increase in cell death in the optic stalk region of the eye. This difference persists through 26SS (G).
D and H: Pax2 and TUNEL co-stain of 26SS wild type (D) and *mab21l2* $^{-/-}$(H) embryos. Compared to wild type (D), *mab21l2* $^{-/-}$embryos possess increased dying cells in the pax2^{+} optic stalk region.
I: Quantification of the proportion of pax2^{+} and TUNEL^{+} cells in D and H. Note a significantly higher ($p = 0.014$) proportion of pax2^{+} cells are TUNEL^{+} in *mab21l2* $^{-/-}$ mutants when compared to wild type embryos.
Dorsal is up in all panels. Scale bars = 50µm.

2.2.6 Neuronal differentiation in the retina of *mab21l2* $^{-/-}$ mutants is normal

Although the gross anatomy of the retina appeared normal in *mab21l2* $^{-/-}$ mutants, previous studies showed a range of defects in retinas where mab21l2 was disrupted. In *Mab21l2* mouse knockouts, the retina was severely malformed, becoming arrested at the optic vesicle stage (Yamada *et al.*, 2004). In chick, while retinal anatomy was not obviously disrupted, *Mab21l2* knockdowns showed failure of horizontal and amacrine cell differentiation, and defects in separation of amacrine and ganglion cells into the inner nuclear layer and ganglion cell layer respectively (Sghari and Gunhaga, 2018). In zebrafish *mab21l2*^{Q48Sfs*5} and *mab21l2*$^{R51\_F52del}$ mutants, the retina was disorganized with folding and bulging of the inner plexiform layer, but whether specific cell types were affected is unknown (Deml *et al.*, 2015). We therefore sought to determine if our *mab21l2* $^{-/-}$ mutants possessed any defects in retinal neuron differentiation. Using immunohistochemical markers for amacrine and retinal ganglion cells (HuC/D), red/green cones (zpr-1), and retinal ganglion cells and their axons (zn-8), we examined the patterning of the *mab21l2* $^{-/-}$ mutant retina (Fig. 2.6). In wild type siblings, HuC/D is expressed throughout the inner nuclear and ganglion cell layers (Fig. 2.6B). *mab21l2* $^{-/-}$ mutants also expressed HuC/D in this region (Fig. 2.6H), in a pattern indistinguishable from wild type siblings. Along the same lines, the retinal ganglion cell marker zn-8 is expressed in the axons of ganglion cells in the ganglion cell layer in both wild type (Fig. 2.6D) and *mab21l2* $^{-/-}$ mutant embryos (Fig. 2.6J). Both wild type (Fig. 2.6F) and *mab21l2* $^{-/-}$ mutants (Fig. 2.6L) show normal zpr-1 staining in the photoreceptor layer. Taken together, these data indicate that *mab21l2* $^{-/-}$ mutant zebrafish do not have defects in retinal patterning or differentiation.

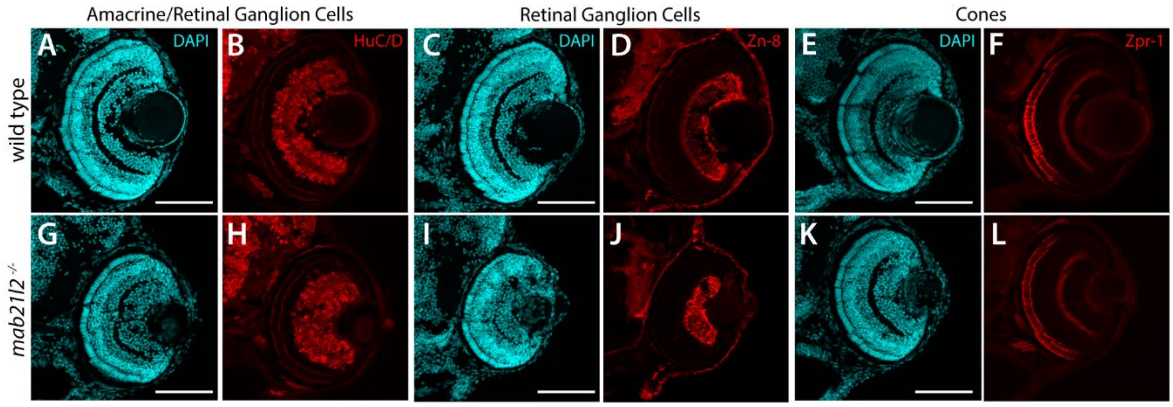

Figure 2.6: *mab21l2* $^{-/-}$ mutants do not possess defects in retinal neuron differentiation

A-L: Wild type (A-F) and *mab21l2* $^{-/-}$ mutant (G-L) 3dpf sections stained for markers of various retinal cell types. Amacrine cell/retinal ganglion cell marker HuC/D staining is similar in wild type (B) and *mab21l2* $^{-/-}$ mutant (H). Retinal ganglion cell marker zn-8 staining is similar in wild type (D) and *mab21l2* $^{-/-}$ mutant (J). Cone marker zpr-1 staining is similar in wild type (F) and *mab21l2* $^{-/-}$ mutant (L).
Dorsal is up in all panels. Scale bars = 100µm.

2.2.7 *mab21l2* $^{-/-}$ mutants possess disorganized corneas.

We next sought to analyze the corneal phenotype in *mab21l2* $^{-/-}$ embryos. Corneal defects were not detected in mouse *Mab21l2* knockouts (Yamada *et al.*, 2004), but abnormalities were noted from histology of *mab21l2*^{Q48Sfs*5} and *mab21l2*$^{R51\_F52del}$ zebrafish mutants, but not characterized in detail (Deml *et al.*, 2015). *mab21l2* is expressed in the early surface ectoderm that will give rise to the cornea in zebrafish (Deml *et al.*, 2015) and mouse (Yamada *et al.*, 2004), and is expressed in the maturing cornea in chicken (Sghari and Gunhaga, 2018). We investigated the progression of corneal defects between 30 and 48hpf, a time window during which the cornea is undergoing substantial morphogenesis and maturation (Fig. 2.7; Zhao et al. 2006). At 30hpf, wild type embryos possess a well-organized single epithelial layer overlying the lens (Fig. 2.7A). In contrast, *mab21l2* $^{-/-}$ mutants possess a dysmorphic anterior segment region consisting of multiple layers of cells overlying the lens, and an unclear delineation between lens and cornea (Fig. 2.7G). At 36hpf, wild type siblings possess a single corneal epithelial layer overlying the lens, with corneal endothelial cells beginning to migrate into the eye near the area where the ciliary margin meets the lens (Fig. 2.7B, C, arrows). In *mab21l2* $^{-/-}$ mutants, a mass of cells is detected over the lens, with aggregations present between the lens and the peripheral retina (Fig. 2.7H, I). These cells displayed disorganized F-actin when compared those in the cornea of wild type siblings. At 48hpf, the cornea in wild type siblings was well organized, consisting of two layers of evenly spaced cells overlying the lens (Fig. 2.7D). In *mab21l2* $^{-/-}$ mutants, by contrast, multiple cell layers were present, and the cells were not evenly spaced (Fig. 2.7J).

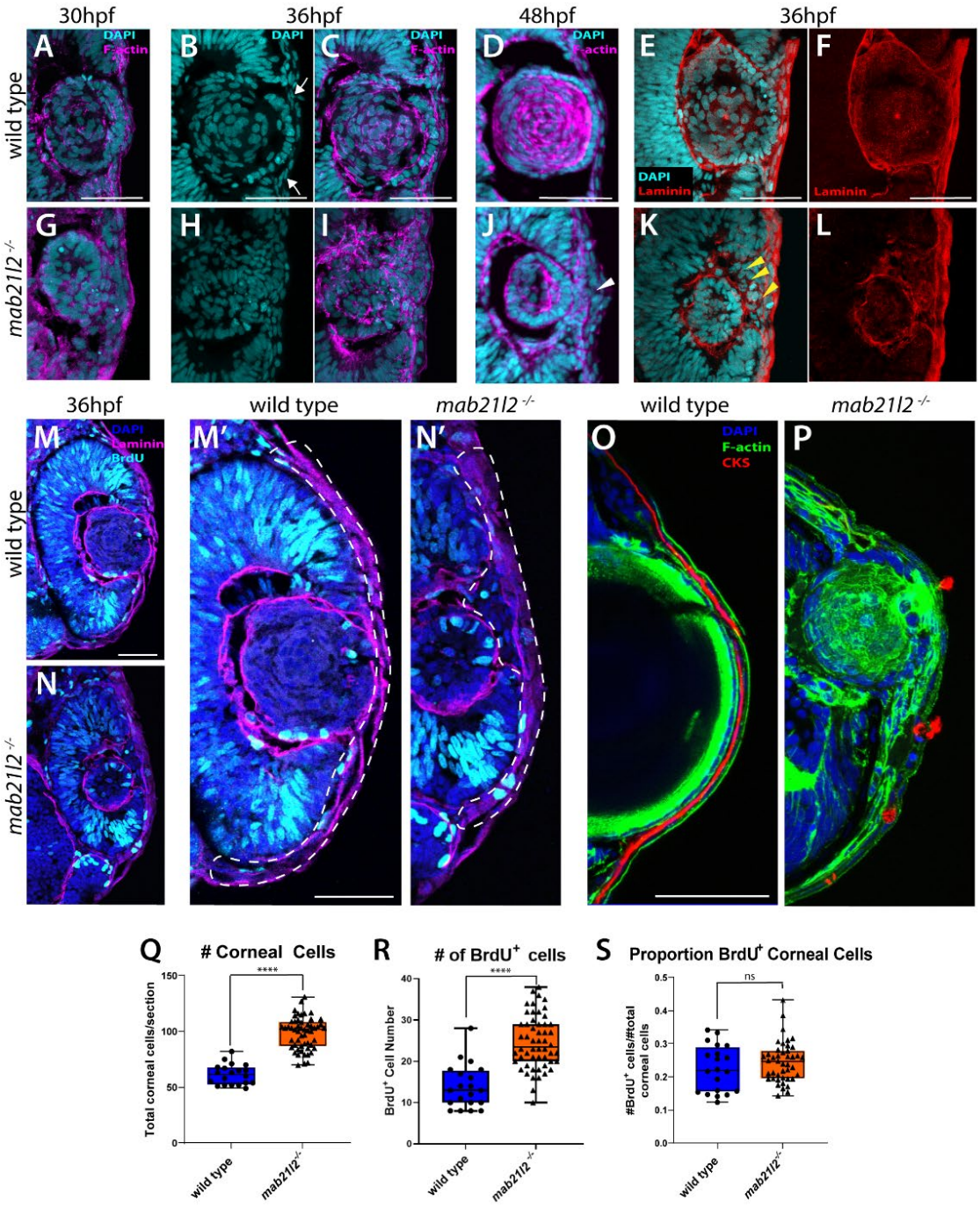

Figure 2.7: *mab21l2* $^{-/-}$ mutants display corneal dysgenesis and failure of stromal patterning

(Figure 2.7 continued)
A-D, G-J: Wild type (A-D) and *mab21l2* $^{-/-}$ mutant (G-J) sections demonstrating corneal phenotypes. At 30 and 36hpf, when compared to wild type eyes (A-C), *mab21l2* $^{-/-}$ lenses (G-I) appear continuous with the overlying surface ectoderm. At 48hpf, *mab21l2* $^{-/-}$ mutants (J) possess a multilayered mass of cells (arrowhead) at the ocular surface when compared to wild type (D).
E,F,K,L: Laminin α1 distribution in 36hpf wild type (E,F) and *mab21l2* $^{-/-}$ mutant (K,L) embryos demonstrating the presence of ectopic, non-lens, non-retinal cells in *mab21l2* $^{-/-}$ mutants (K, arrowheads).
M-N': BrdU incorporation assays of 36hpf wild type (M) and *mab21l2* $^{-/-}$ mutant (N) embryos. At 36hpf, *mab21l2* $^{-/-}$ mutants (N) possess more corneal cells, but these cells are not ectopically proliferative relative to wild type (M). Zooms in M' and N'; dotted lines show area counted for quantification.
O-Q: Quantification of total and $BrdU^{+}$ corneal cells in M and N. ($p < 0.0001$, $p < 0.0001$, $p = 0.27$ respectively)
R,S: Corneal keratan sulfate (CKS) stain of 5dpf wild type (R) and *mab21l2* $^{-/-}$ mutant (S) embryos. Mutants do not properly express CKS in the stroma.
Scale bars = 50μm.

We hypothesized that the extra cells present in the anterior segment could be part of a disorganized lens or a lens that had not separated properly from the surface ectoderm, or that they could be corneal in origin. To distinguish between these two possibilities, we stained for laminin α1, a known marker of the lens capsule (Parmigiani and McAvoy, 1984), to demarcate lens vs non-lens cells (Fig. 2.7E-F, K-L). At 36hpf, in wild type siblings, the lens capsule is clearly visible and separates the lens from the cornea (Fig. 2.7E, F). In *mab21l2* $^{-/-}$ mutants, the lens capsule also encloses the lens normally. Interestingly, the extra cells lie outside of this compartment as well as outside the laminin α1 distribution that defines the retina/RPE (arrowheads), suggesting that these cells have neither lens nor retinal/RPE identity and are likely corneal in origin.

2.2.8 Cell proliferation is normal in the *mab21l2* $^{-/-}$ cornea.

We hypothesized that the cells outside of the lens and retina/RPE in *mab21l2* $^{-/-}$ embryos may have been produced as a result of increased proliferation of corneal cells. To investigate this possibility, we performed a BrdU incorporation assay and compared the proportion of $BrdU^+$ corneal cells in *mab21l2* $^{-/-}$ and wild type embryos, using a co-stain with laminin α1 to define the presumptive corneal cells as the cells that are not part of either the lens or retina/RPE compartments (Fig. 2.7M-N). BrdU incorporation assays revealed that there were significantly more total corneal cells in *mab21l2* $^{-/-}$ mutants as compared to siblings (Fig. 2.7O, $p < 0.0001$), but the proportion of these cells that were $BrdU^+$ was not significantly different between the two populations of embryos (Fig. 2.7P, $p = 0.27$). However, the overall total number of $BrdU^+$ cells was in fact increased in *mab21l2* $^{-/-}$ embryos, from an average of 13.8 $BrdU^+$ cells per section in wild type to an average of 24.7 $BrdU^+$ cells per section in *mab21l2* $^{-/-}$ (Fig. 2.7Q, $p < 0.0001$). This difference in total $BrdU^+$ cell number raises the possibility that while the proportion of proliferating cells is not increased upon loss of *mab21l2,* the total proliferative population may be larger, commensurate with the larger overall corneal population.

2.2.9 *mab21l2* is required for patterning of the corneal stroma

Since corneal morphology was severely disrupted in *mab21l2* $^{-/-}$ mutants, we hypothesized that the cornea may not be patterned correctly. To assess this possibility, we performed immunohistochemical stains for markers of various layers of the cornea at 5dpf (Fig. 2.7R-S), a time point at which the cornea is maturing and beginning to express markers differentiated cell identities (Zhao *et al.*, 2006). Experiments to test for the presence of markers of the corneal endothelium and corneal epithelium were inconclusive due to lack of antibody cross-reactivity in zebrafish. However, we were able to investigate differentiation of the corneal stroma, which is at this time point an acellular layer between the epithelium and endothelium that is marked by high levels of the glycosaminoglycan corneal keratan sulfate (CKS) (Zhao *et al.*, 2006). In wild type siblings, CKS staining was highly specific and localized as a discrete layer in the area between the corneal endothelium and corneal epithelium (Fig. 2.7R). However, in *mab21l2* $^{-/-}$ embryos, CKS staining was detected in only a few, amorphous, bleb-like deposits both within and outside the corneal region (Fig. 2.7S, arrowhead). These bleb-like structures did not appear to contain nuclei, but their cellular origin is unclear.

2.3 DISCUSSION:

MAB21l2 is a gene of growing interest in the ophthalmic community. Its association with human disease (Rainger *et al.*, 2014; Deml *et al.*, 2015; Horn *et al.*, 2015) as well as its high degree of genetic (Tsang *et al.*, 2009) and functional conservation across animal species (Mariani *et al.*, 1999; Hartsock *et al.*, 2014; Deml *et al.*, 2015) and enigmatic function have made it the focus of a number of recent studies. Here we present a detailed characterization of ocular defects in zebrafish *mab21l2* mutants, identifying functional requirements during a variety of developmental processes including optic fissure closure and lens and cornea development.

mab21l2 $^{-/-}$ mutant zebrafish possess ocular defects that are similar to those in human patients with point mutations in the *MAB21L2* gene; these include

microphthalmia, coloboma, and microcornea (Rainger *et al.*, 2014; Deml *et al.*, 2015; Horn *et al.*, 2015). Interestingly, unlike in human patients, *mab21l2* $^{-/-}$ zebrafish mutants also displayed lens defects: the mutant lens was substantially smaller than that in wild type siblings, and often, the lens was dysplastic and eventually extruded from the eye. Lens defects are also noted in chick Mab21l2 knockdown (Sghari and Gunhaga, 2018) and mouse knockout models (Yamada *et al.*, 2004). Zebrafish *mab21l2* $^{-/-}$ mutants also possessed severe corneal defects in which the mutant cornea was thickened and bulged from the eye. In contrast, some of the human mutations result in anopthalmia (Rainger *et al.*, 2014; Horn *et al.*, 2015), which was not detected in our zebrafish *mab21l2* $^{-/-}$ mutants. The differences between the human patients and animal models could reflect that the human patients all carry point mutations that result in single amino acid replacements and are heterozygous, while the animal models either truncate the proteins (Hartsock *et al.*, 2014; Deml *et al.*, 2015), decrease overall transcript levels (Sghari and Gunhaga, 2018), or remove large regions of the coding sequence (Yamada *et al.*, 2004). Indeed, our *mab21l2*^{au10} mutant line is a nonsense allele (K101Stop) that truncates the protein to ≈1/3 of its normal length. While the molecular function of mab21l2 is unknown, it is possible that a functional domain remains intact in the human patients which is absent or non-functional in our zebrafish model, and that this manifests as more severe defects in the anterior segment. Further studies to identify the molecular and cellular function of the protein, as well as structure-function relationships, are required to test this possibility.

The reduction or absence of expression of markers associated with lens epithelial and lens fiber cell types, as well as the apparent disorganization of the lens in *mab21l2* $^{-/-}$ mutants, could indicate that the lens is failing to progress from its earliest developmental stage, remaining as an immature lens nucleus/mass of primary fibers. The maturation of the lens and generation of distinct epithelial and secondary fiber zones is controlled by a host of signals from the surrounding ocular tissues. These signals include members of the BMP, Wnt, and FGF pathways (Boswell et al. 2008; reviewed in Cvekl & Zhang 2017). In this model, *mab21l2* $^{-/-}$ lens cells may not properly initiate patterning, remaining in an undifferentiated, disorganized state and therefore failing to express markers like *celf1,*

cryaa, or *foxe3,* which are characteristic of mature lens cell types. It is also possible that *mab21l2* $^{-/-}$ lenses do have lens epithelial-like and fiber-like cells, which have begun to differentiate, but that these cells' ability to turn on their key markers such as *cryaa* or *foxe3* is disrupted by loss of mab21l2 function, resulting in aberrant lens development. Indeed, given that nuclei in the center of *mab21l2* $^{-/-}$ lenses appear to have been degraded, it is likely that lens epithelial and fiber cells are present, but not patterned properly.

mab21l2 $^{-/-}$ mutants possessed colobomas of varying severity, ranging from very severe retinal blowouts, where retinal and RPE tissue extruded out the back of the eye, to mild discontinuities of the retinal lamina visible only in sectioned tissue. Choroid fissure closure is a precisely orchestrated process, and critical events include specification of the optic stalk/optic cup boundary, tissue growth and morphogenesis, and basement membrane breakdown (Hero, 1989; Hero *et al.*, 1991; Schwarz *et al.*, 2000; Mui *et al.*, 2005; Morcillo *et al.*, 2006; Lee *et al.*, 2008; Tsuji *et al.*, 2012; James *et al.*, 2016; Bernstein *et al.*, 2018). The optic stalk/optic cup markers *pax6* and *pax2* were correctly distributed in *mab21l2* $^{-/-}$ embryos, leading us to conclude that early tissue patterning defects are unlikely to be responsible for colobomas. However, we did detect significantly elevated levels of cell death in the *mab21l2* $^{-/-}$ optic stalk. Cell death in this region of the developing eye is well known to be associated with colobomas (Viringipurampeer *et al.*, 2012; Lee *et al.*, 2013). Elevated cell death in the optic stalk could prevent the opposing sides of the choroid fissure from coming into correct orientation and/or contact and thereby prevent closure. Moreover, cell death in the optic stalk in conjunction with microphthalmia and abnormalities in eye shape in *mab21l2* $^{-/-}$ embryos could also collectively lead to colobomas.

Alternatively, it is known that choroid fissure closure requires contributions from the hyaloid vasculature (James *et al.*, 2016), neural-crest derived periocular mesenchyme (McMahon *et al.*, 2009; Gestri *et al.*, 2018), and the retina itself (Barbieri *et al.*, 2002; Morcillo *et al.*, 2006). Of these tissues, *mab21l2* is known to be highly expressed in the retina, in a domain that gradually restricts to a small region of cells that comprise the lateral edges of the choroid fissure (Cederlund *et al.*, 2011; Deml *et al.*, 2015). Thus, it is

also possible that mab21l2 functions directly in mediating the closure process within these cells; for example, it could facilitate the formation of junctional processes or cellular rearrangements necessary for fusion in the fissure. It is also possible that mab21l2 function is associated with cell non-autonomous signals that modulate the activities of other cells types at or near the choroid fissure that are required for proper closure. With respect to cell non-autonomous functions, it is interesting that the laminin α1-containing basement membrane was not properly degraded in the *mab21l2* $^{-/-}$ choroid fissure, given that previous studies have shown that the hyaloid vasculature contributes to the breakdown process, but is not the sole requirement (James *et al.*, 2016). Indeed, retinal cells themselves extend protrusions into the site of membrane breakdown (Hero, 1990), although it is not known whether these are functionally relevant. That *mab21l2* is expressed in cells at the choroid fissure, and expression has not been reported in the periocular mesenchyme, again suggests two possible models for mab21l2 in this process: a direct role within the fissure in mediating basement membrane breakdown, or a cell non-autonomous role in recruiting cells that migrate into the fissure to degrade the membrane. Targeted experiments are needed to test these possibilities.

Interestingly, despite previous reports of retinal defects in other mab21l2 knockdown and knockout models (Yamada *et al.*, 2004; Deml *et al.*, 2015; Sghari and Gunhaga, 2018), we do not observe any effects on retinal differentiation or lamination in our *mab21l2* $^{-/-}$ embryos. This difference could be partially attributed to differences between the model organisms and methods of knockdown/knockout used in each study. While some human patients with MAB21L2 mutations are anophthalmic, is not known whether retinal development or function are affected in the subset of patients that possess eyes (Rainger *et al.*, 2014; Deml *et al.*, 2015; Horn *et al.*, 2015). These phenotypic differences highlight the need for diverse animal models to investigate mutations which are of interest in human disease, and also the strength in examining phenotypes resulting from different mutant alleles or loss of function approaches.

We identified corneal defects in *mab21l2* $^{-/-}$ mutants, which have not been described previously in mouse knockouts, other zebrafish *mab21l2* mutant alleles, or

knockdown assays in chick embryos (Yamada *et al.*, 2004; Deml *et al.*, 2015; Sghari and Gunhaga, 2018). We observed an increase in presumptive corneal cells at 30hpf in *mab21l2* $^{-/-}$ mutants; however, this increase was not correlated with an increase in the proportion of proliferative cells in the cornea. Rather, the total number of proliferative cells was increased in the *mab21l2* $^{-/-}$ cornea, suggesting that altered cell proliferation likely contributes to the defects, but not simply from normally non-proliferative cells ectopically proliferating. It is possible that at an earlier developmental stage, more cells could be fated to the cornea, where they then proliferate normally and the resultant increase in total cell number disrupts overall morphogenesis of the tissue. It is also possible that the proliferative population proceeds more rapidly through the cell cycle, leading to increased production of new cells. Defects in optic cup morphogenesis could create a smaller overall space within the anterior segment, leading these cells to accumulate and not differentiate properly. Importantly, corneal defects in *mab21l2* $^{-/-}$ mutants were not limited to the presence of extra corneal cells. Corneal cell layers were not properly organized, actin and laminin α1 deposits appeared improperly localized, and the cornea was thickened and bulged distally in conjunction with retinal collapse and lens dysplasia. The mutant cornea also did not properly deposit keratan sulfate in the corneal stroma, indicating additional patterning defects. Unfortunately, due to the absence of cross-reactive antibodies in zebrafish, we were unable to determine whether differentiated endothelial and epithelial cells were present in *mab21l2* $^{-/-}$ mutants.

Corneal malformations in *mab21l2* $^{-/-}$ mutants are interesting given the microcornea phenotype reported in human patients with *MAB21L2* mutations (Deml *et al.*, 2015; Horn *et al.*, 2015). Microcornea is thought to result from either an early arrest in corneal growth after differentiation is complete (Kenyon *et al.*, 2008), or from an overgrowth of the anterior edges of the optic cup (Sugar, 1978), although the specific developmental origins of the defect are still unknown. Lens and corneal cells come from a common pool of surface ectodermal precursors, and *mab21l2* is expressed in this region in chick and zebrafish (Cederlund *et al.*, 2011; Deml *et al.*, 2015; Sghari and Gunhaga, 2018). Specification of these cells as lens or cornea is determined in part by BMP

signaling, and it is known that manipulations of BMP signaling can affect corneal and lens development (Furuta and Hogan, 1998; Wawersik *et al.*, 1999; Collomb *et al.*, 2013; Huang *et al.*, 2015). mab-21, the *C. elegans mab21l2* ortholog and founding member of this gene family, has been shown to act antagonistically with members of the TGFβ signaling cascade in regulation of male tail morphology (Morita *et al.*, 1999). In addition, the *Xenopus* ortholog, xmab21l2, antagonizes overexpression of BMP4, and coimmunoprecipitates with SMAD1 (Baldessari *et al.*, 2004), providing some support for a model in which mab21l2 is involved in the regulation of BMP signaling. Disruption of BMP signaling can lead to lens and choroid fissure closure defects (Morcillo *et al.*, 2006; Huang *et al.*, 2015), like those observed in *mab21l2* $^{-/-}$ mutants, suggesting a potential unifying theme underlying each of these ocular defects. Combined with the observation that *mab21l2* $^{-/-}$ mutants have smaller lenses, it is possible that the cornea and lens phenotypes are linked via abnormal BMP signaling; in this model, more surface ectodermal cells would be specified to a corneal fate over a lens fate, and these cells are also space-limited by concomitant defects in optic cup morphology and size, which together result in the severe anterior segment defects detected in *mab21l2* $^{-/-}$ mutants.

Taken together, we present a thorough characterization of ocular defects in *mab21l2* $^{-/-}$ mutants, thereby providing a tractable model system through which the molecular underpinnings of these defects can be determined, and a platform through which one can determine how the human mutations lead to ocular malformations. mab21l2 is quite an enigmatic protein, as to date, its function within the cell is unknown. Our preliminary data show that mab21l2 is chromatin associated and almost completely contained within the cell nucleus (*unpublished observations*). In mouse, Mab21l1 is also largely nuclear localized (Yamada *et al.*, 2003). Published data indicate that MAB21L2 binds ssRNA (Rainger *et al.*, 2014), that it could have transcriptional repressive functions (Baldessari *et al.*, 2004), and that members of the mab21l2 protein family may have structural similarities with the nucleotidyl transferase c-GAS (Kuchta *et al.*, 2009; de Oliveira Mann *et al.*, 2016), collectively supporting a model in which mab21l2 might possess transcriptional or nuclear regulatory functions. Experimental data confirming

these proposed functions have been largely inconclusive, however. In the age of numerous -omic technologies, it is surprising that the function of mab21l2 has not yet been identified, and future studies will undoubtedly shed light on this protein and in doing so, elucidate how it contributes to normal eye development, function, and congenital ocular pathologies.

Chapter 3: Molecular roles of mab21l2 and the effects of mutations from human patients

3.1 INTRODUCTION:

The molecular and cell biological roles of mab21l2 have been elusive. The pathways with which mab21l2 is associated and the processes that are disrupted upon loss of mab21l2 have not been determined. The mab21l2 protein has been proposed to be able to bind DNA, ssRNA, and perform nucleotidyl transferase activities, but only the ssRNA binding has been validated, and the function of this ability is unknown (Rainger *et al.*, 2014; de Oliveira Mann *et al.*, 2016). The only proposed binding partner for mab21l2 is SMAD1, though this binding has only been investigated in a single paper (Baldessari *et al.*, 2004). Apart from this connection, circumstantial evidence, such as the similarity of BMP mutant phenotypes to those seen in mab21l2 mutants (Furuta and Hogan, 1998; Wawersik *et al.*, 1999; Morcillo *et al.*, 2006; Huang *et al.*, 2015), offers a weak connection of mab21l2 to the BMP signaling pathway.

Due to the number of diverse pathways involved in development, and the crosstalk between them, it is likely that the BMP signaling pathway is not the only pathway perturbed upon mutation of mab21l2, but little evidence exists to suggest what other defects may arise on a gene expression or cell biological level. Thus, we took a hypothesis-generating approach to determine pathways that may be involved in the functional role of mab21l2 and performed yeast-2-hybrid assays to identify possible binding partners for mab21l2.

Despite robust protein structure and domain prediction tools, the activity of the mab21l2 protein is unknown. However, 5 different human mutations in three locations along the protein length are known (Rainger *et al.*, 2014; Deml *et al.*, 2015; Horn *et al.*, 2015) and closely related protein mab21l1 has been crystallized (Fig. 1.4A) (de Oliveira Mann *et al.*, 2016). Therefore, it is possible to investigate the consequences of these mutations and the function of these locations on the mab21l2 protein. We used

microinjection of human mutation versions of MAB21L2 into zebrafish embryos to investigate the consequences of each mutation.

3.2 RESULTS:

3.2.1 mab21l2 may bind to transport proteins and regulators of the cytoskeleton, transcriptional regulators, and proteins related to ribosomal function

As noted above, while mab21l2 has been previously noted to bind to smad1 *in vitro*, no other binding partners have been identified. In addition, the biological relevance of the binding to smad1 in an *in vivo* system has never been tested.

Two parallel yeast-2-hybrid assays using zebrafish-derived mab21l2 as bait were performed. These assays were performed against a 20hpf zebrafish protein library consisting of protein fragments representing the entire proteome. The first assay used a traditional GAL4 based approach, while the second used a LexA base. Together, 132.6 million potential interactions were screened. 320 positive interactions were identified, representing 84 different preys. Seven of these were identified as highly likely to be experimental artifacts, leaving 77 preys suspected to bind to mab21l2.

Of the 77 preys pulled from this screen, 15 were at the highest confidence levels, and considered most likely to represent real, biologically relevant interactions. The other 62 preys were identified by only one or two protein fragments binding to mab21l2 in the screen, which could indicate weak binding not likely to be real in a living cell context, or represent a rare protein not well represented in the prey library. As such, these results could be relevant, or could be artifacts of the technique used. Of these likely preys, only 11 were identified proteins, while 4 were derived from recently mapped but unnamed and uncharacterized genes, often known to exist only from gene prediction. As such, only the 11 known proteins were carried forward in this study, and are listed in order of their confidence levels in Table 3.1.

Rank	Protein	Gene Name
1	tnpo2	transportin 2
2	klc2	kinesin light chain 2
3	klhl31	kelch-like 31
4	tnpo1	transportin 1
5	nop56	nucleolar protein 56
6	hnf4a	hepatocyte nuclear factor 4 alpha
7	ldb2a	LIM domain binding 2a
8	kdm3b	lysine demethylase 3b
9	etf1	eukaryotic translation termination factor 1
10	filip1	filamin a interacting protein 1
11	si:dkey-28e7.3	(orthologous to) huntingtin associated protein

Table 3.1 Candidate mab21l2 interacting proteins from yeast-2-hybrid screen

Preys pulled from the yeast-2-hybrid screen as possible binding partners for mab21l2 are listed in order of confidence level.

In order to validate the interaction of mab21l2 with these top 11 preys, the full-length sequence of *mab21l2* was cloned into 6xHIS-tagged mammalian cell culture expression vectors from a human gene library purchased from the Harvard gene repository. These genes were then co-transfected into HEK-293 cells alongside a GFP-tagged version of human mab21l2. The intention was to reciprocally co-immunoprecipitate both bait and prey using anti-HIS and anti-GFP antibodies, respectively, which would, if successful, indicate true binding of bait and prey in a cell culture context.

Unfortunately, due to difficulties getting HEK-293 cells to express the 6xHIS-tagged preys at a sufficiently high level, we were unable to co-immunoprecipitate any of the preys with mab21l2, and as such, were unable to validate any of these potential bindings. Without validation, these bindings could be yeast-specific, technical artifacts, or otherwise not biologically relevant. In addition, many candidates are not expressed in the eye, or are localized to parts of the cell other than the nucleus, which is where mab21l2 is found, making true binding unlikely. Still, the potential preys identified in our screen can lend some support to future experiments seeking to place the role of mab21l2 in the developmental and regulatory networks in the eye.

The candidates identified in the yeast-2-hybrid screens can be broadly separated into several categories: actin/myosin binders, kinesin associated proteins, transcriptional regulators, and proteins related to ribosomal function.

Actin/myosin binders found in the screen include klhl31 (kelch-like 31) and filip1 (filamin a interacting protein 1). Kelch family proteins are known in several contexts; some members of the family are known to act as post-translational regulators, via acting as substrate-ligase complex adaptors of E3 ubiquitin ligase complexes (Boyden *et al.*, 2012; Canning *et al.*, 2013; Shibata *et al.*, 2013). However, not all kelch-like proteins perform this role. Other kelch family members, including klhl31, are involved in the regulation of actin distribution in the cell, particularly in a skeletal muscle context (Papizan *et al.*, 2017). It is thought that klhl31 may act through filamin C to regulate the

formation of actin networks such as that at the muscle cell z-disc (Papizan *et al.*, 2017). Filip1a interacts with filamin A in the formation of actin branches (Nagano *et al.*, 2002; Popowicz *et al.*, 2006). It is also known to be involved in cellular migration; particularly, in migration of cells in the neocortex (Nagano *et al.*, 2002), and is highly expressed in neural and brain tissues (Nagase *et al.*, 1999).

Kinesin associated proteins identified in the yeast-2-hybrid screen include si:dkey-28e7.3 and klc2 (kinesin light chain 2). Si:dkey-28e7.3 is a relatively recently discovered protein from the zebrafish genome sequencing and annotation project; as such, very little is known about it. However, it is orthologous to the human protein HAP1 (huntingtin associated protein) and its family, the Milton protein family. HAP1 is involved in scaffolding cargo to microtubules during intracellular transport, binding to dynein subunit $p150^{glued}$ as well as to kinesin light chains (Wu and Zhou, 2009). Other Milton proteins are also associated with kinesin binding, and are involved in transport of mitochondria to nerve terminals in drosophila (van Spronsen *et al.*, 2013). klc2 is a component of the kinesin motor; knockdowns in zebrafish have shown defects in the tail and in swimming behavior, but no defects in the eye were detected (Melo *et al.*, 2015).

Transcription regulator candidate preys included hnf4a (hepatocyte nuclear factor 4a), ldb2a (lim domain binding factor 2a), and kdm3b (lysine demethylase 3b). hnf4a is most well known in the liver and kidney, where it regulates gene expression through direct binding to hormone response elements (Sladek *et al.*, 1990). hnf4a expression is restricted to the gut, liver, kidney, and pancreas, and it is not known to be expressed in the eye (Costa *et al.*, 1990; Sladek *et al.*, 1990; Bertrand *et al.*, 2007). ldb2a is a transcription factor known to be expressed in the central nervous system and vasculature (Toyama *et al.*, 1998; Gomez *et al.*, 2009). It is involved in fine control of TGFβ signaling through modulation of I-SMAD and R-SMAD activity, colocalizing with other transcription factors at transcriptional regulatory sites including the promoter of SMAD7 (Gu *et al.*, 2015). kdm3b is a histone modifying protein that preferentially demethylates the H3K9 repressive histone mark, allowing for activation of chromatin (Kim *et al.*, 2012). It is ubiquitously expressed, particularly in the brain and head (Thisse and Thisse,

2004) and is involved in maintenance of proliferative states while antagonizing differentiation (Kim *et al.*, 2012).

Candidates from the yeast-2-hybrid screen which are related to ribosomal function include etf1 (eukaryotic transcription termination factor 1) and nop56 (nucleolar protein 56). etf1 is a ubiquitously expressed (Thisse and Thisse, 2004) polypeptide release factor, involved in removal of new polypeptide chains from their associated ribosomes to allow for ribosomal recycling (reviewed in Inge-Vechtomov, Zhouravleva and Philippe, 2003). It is known that efficient termination of translation is associated with higher rates of cell proliferation- mutant yeast strains lacking the ability to properly terminate polypeptide chains display slower growth and division rates (Beznosková *et al.*, 2013). nop56 is a nucleolar protein that helps produce the 60s ribosomal subunit by complexing with and forming a bridge between pre-rRNA and the enzyme fibrillarin, which allows fibrillarin to methylate the rRNA, required for ribosomal assembly and function (Tollervey *et al.*, 1993; Gagnon *et al.*, 2012). High levels of nop56 are found in proliferative cells in the zebrafish midbrain, and nop56 is also highly expressed in the developing eye (Recher *et al.*, 2013). In addition, nop56 is a known marker of proliferative cell populations in the developing Xenopus eye (Parain *et al.*, 2012).

The last pair of yeast-2-hybrid candidates are the nuclear transportins tnpo1 and tnpo2, of which tnpo2 was the top hit in the screen. tnpo1 and 2 are two of the approximately 20 importins involved in the recognition of nuclear localization signals and transportation of newly synthesized proteins to the nucleus (Twyffels *et al.*, 2014). Proteins known to be imported into the nucleus via tnpo1 and 2 are involved in many pathways in the cell, including the cell cycle pathway, Hedgehog signaling, and many more; some are exclusively transported via tnpo1 and 2, while others can use many importins in their route to the nucleus (reviewed in Twyffels, Gueydan and Kruys, 2014).

3.2.2 Human mutant versions of mab21l2 have dominant negative or gain of function properties

Because some of the human variants of mab21l2 associated with disease appeared to be dominant in human families, while others were recessive (Rainger *et al.*, 2014; Deml *et al.*, 2015; Horn *et al.*, 2015), we sought to determine if the dominant variants could be explained via a gain of function mechanism. mRNA corresponding to the human mutant versions found in human patients was transcribed and injected into 1-cell wild type zebrafish embryos, and these embryos were assessed for any eye phenotypes (Fig. 3.1).

Injection of human wild type mRNA had no effect on the wild type fish, indicating that any effect caused by injection of mutant versions is specifically related to the mutations, and not an interaction between human mRNA and zebrafish, or a consequence of overexpression (Fig. 3.1 A). Human dominant variants *mab21l2*^{R51C} and *mab21l2*^{R51H}, when injected into wild type zebrafish, produced colobomas (Fig. 3.1 D,E). These colobomas were of varying severities, but approximately 80% of all injected fish displayed this phenotype. Unlike in the *mab21l2*^{au10} mutant, there was no apparent effect on lens or eye size. In section, colobomas appeared to be of the retinal blowout type, with retinal cells encroaching into the space behind the eye (Fig. 3.1 G) through a large gap in the retinal pigmented epithelium (Fig. 3.1 I) compared to wild type (Fig. 3.1 F and H). However, human dominant variant E49K, when injected into wild type zebrafish, had no effect - the fish did not display colobomas (Fig. 3.1 B). Human recessive mutation R247Q also had no phenotypic effect when injected into wild type fish (Fig. 3.1 C), as expected. Thus, it appears that a dominant negative/gain of function explanation for the dominant segregation in human families may apply to only mutations at amino acid 51 (R51C and R51H), while the human dominant E49K does not appear to act through a gain of function mechanism.

Because mab21l2 is well known to be localized to the nucleus (Mariani *et al.*, 1999; Deml *et al.*, 2015), it seemed possible that the defects observed in human patients with mutated versions could be due to the inability of the mutant versions of mab21l2 to

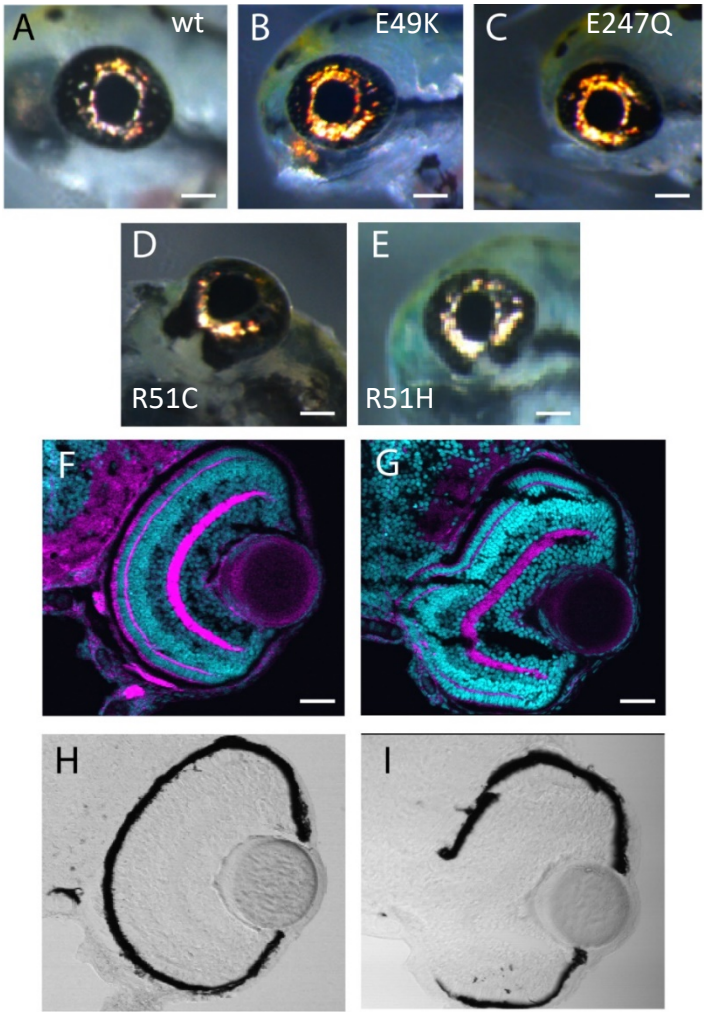

Figure 3.1 Embryos injected with human *mab21l2*^{R51C} and *mab21l2*^{R51H} display colobomas

A-E: Whole mount images of 5dpf wild type embryos injected with mRNA carrying various mutations derived from human patients. Wild type *mab21l2* injected (A), *mab21l2*^{E49K} injected (B), and *mab21l2*^{R247Q} injected (C) embryos show normal eyes, while *mab21l2*^{R51C} and *mab21l2*^{R51H} injected embryos display colobomas (D, E respectively). Scale bars = 100µm

F-H: Transverse sections of 5dpf embryos injected with human mutant mRNA and wild type mRNA, showing representative wild type/*mab21l2*^{E49K}/*mab21l2*^{R247Q} sections (F, H) versus representative *mab21l2*^{R51C}/*mab21l2*^{R51H} sections (G, I). Note retinal blowout type colobomas in G and I, with a large gap in the retinal pigmented epithelium visible in I. Cyan=DAPI, magenta=F-actin. Scale bars = 50µm

properly localize to the nucleus. Using GFP-tagged wild type and mutant versions of mab21l2, mRNA was injected into one-cell zebrafish embryos and subcellular localization was assessed at the beginning of epiboly (Fig. 3.2). All mutated versions of mab21l2 (Fig. 3.2 B-E) correctly localized to the nucleus, and were indistinguishable from wild type localization (Fig. 3.2 A). This evidence suggests that the mechanism by which mutations in mab21l2 cause defects is not simply through disruption of the ability of mab21l2 to enter the nucleus.

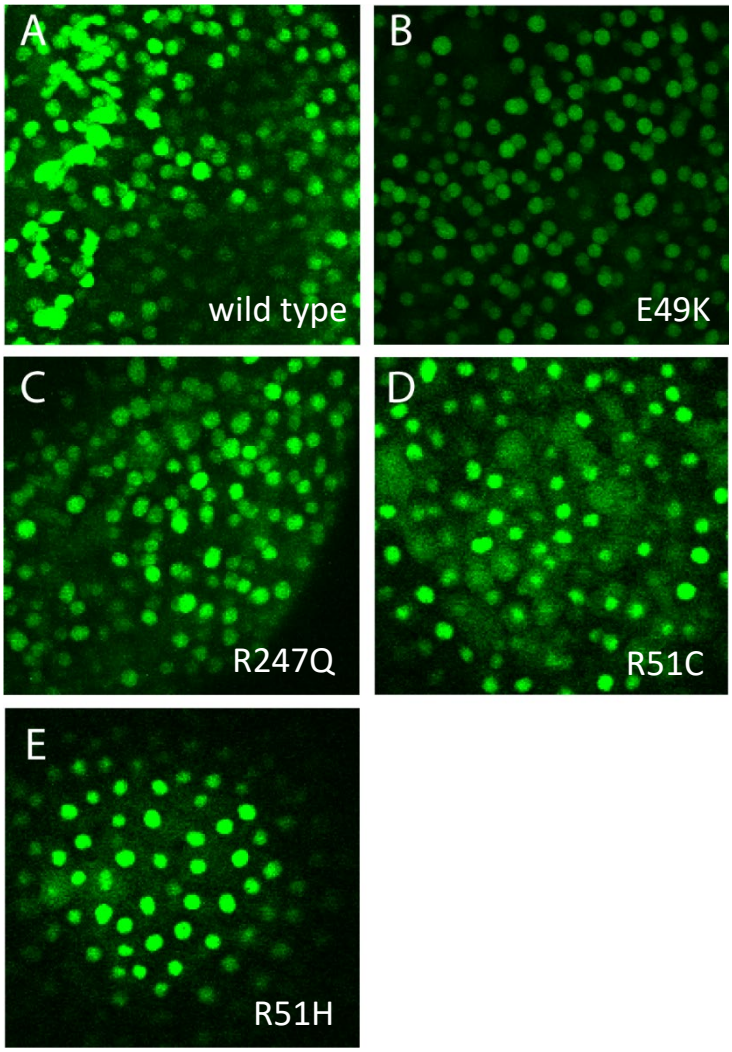

Figure 3.2 Human mutant versions of *mab21l2* still localize properly to the nucleus

A-E: Confocal images of approximately 5hpf embryos injected with GFP-tagged human mutant and wild type *mab21l2* mRNA. Note nuclear localization in the cells of *mab21l2* injected (A), *mab21l2*^{E49K} injected (B), *mab21l2*^{R247Q} injected (C), *mab21l2*^{R51C} injected (D), and *mab21l2*^{R51H} injected (E) embryos.

3.3 DISCUSSION:

3.3.1 Potential binding partners for mab21l2

While mab21l2 is a critical and highly conserved gene, the cell biological role it plays is not known. Some evidence suggests a possible role in regulation of BMP signaling; *C. elegans* ortholog mab-21 is known to antagonize members of the TGFβ signaling cascade in regulation of male tail morphology (Morita *et al.*, 1999), and *Xenopus* ortholog *xmab21l2* antagonizes overexpression of BMP4 while coimmunoprecipitating with BMP effector SMAD1 (Baldessari *et al.*, 2004). However, the role of mab21l2 in any other developmental pathways or in the regulation of other genes that could contribute to the phenotypes seen in mab21l2 mutants is still unknown. In addition, the mechanisms by which specific mutations in mab21l2 produce these phenotypes is unclear. Here we present the results of a yeast-2-hybrid screen to identify possible candidate interactors for mab21l2, and thus possible cell biological roles for this protein. We additionally present evidence that a subset of known mab21l2 human mutations confer gain of function activity on this protein, possibly explaining some of the known defects in human patients.

In the yeast-2-hybrid screen, mab21l2 was shown to interact with 2 proteins, klhl31 and filip1, known to be involved with the cytoskeleton and regulation thereof. klhl31 is unlike other members of the kelch family in that it does not appear to function in a E3 ubiquitin ligase context as do proteins like klhl3 and klhl7 (Ohta *et al.*, 2013; Shibata *et al.*, 2013). Instead, klhl31 is shown to be able to bind to actin regulatory protein filamin C, and to be critical to proper formation of skeletal muscles, particularly the formation of z-discs (Papizan *et al.*, 2017). Any function for klhl31 in actin regulation in other contexts has yet to be investigated, nor is klhl31 expressed outside of the skeletal and cardiac muscles (Wu and Gong, 2004), so this is likely not the direct mechanistic cause of eye defects in mab21l2 mutants.

filip1 binds to and promotes degradation of critical actin organizational protein filamin a (Nagano *et al.*, 2002). Filamin A is known to be involved in crosslinking of

actin filaments into branched networks that promote cell stability and allow for cell migration (reviewed in Stossel *et al.*, 2001); when filamin A is excessively degraded upon overexpression of filip1, cell migration fails (Nagano *et al.*, 2002). Some of the processes that fail upon mutation of mab21l2, such as choroid fissure closure (Bernstein *et al.*, 2018; Gestri *et al.*, 2018) and proper formation of the cornea (Johnston *et al.*, 1979; Hay, 1980; Zhao *et al.*, 2006), are known or suspected to be dependent on migratory cells and migratory behavior. Thus, it is possible that loss of mab21l2 could lead to upregulation of filip1, through loss of a repressive effect, followed by defective migratory cells in and around the eye that could contribute to the observed phenotypes.

As noted above, both klc2, one of the kinesin light chains, and si:dkey-28e7.3, orthologous to a human kinesin light chain binding protein, HAP1, were also identified as possible mab21l2 interacting proteins. These proteins are critical to microtubule-related transport of cargo across the cell. HAP1 is known to be involved in recycling of membrane receptors and maintaining consistent transduction of extracellular signals from the environment, particularly in the context of neurotransmitters (reviewed in Wu and Zhou, 2009). HAP1 is also known to have some limited ability to interact with and enhance the activity of certain transcription factors, such as NeuroD (Marcora *et al.*, 2003) and TATA-box binding protein (Prigge and Schmidt, 2007). It is possible, and even likely, that extracellular signaling and defects therein are involved in the production of the large-scale eye defects seen in mab21l2 mutants. It is well known that myriad extracellular signaling pathways are involved in development of the eye, so an inability to properly transduce these signals due to mab21l2-related defects in HAP1 function could explain some of the phenotypes seen in mab21l2 mutants, but further work to confirm the role of extracellular signals in mab21l2, and specifically, the role of HAP1-related transduction, would be required.

klc2 has vital roles not only in general microtubule-related transport, but also in maintenance of the optic nerve; human patients with mutations in KLC2 display optic atrophy (Macedo-Souza *et al.*, 2005). However, the relation of this protein to the function of mab21l2 and the phenotypic defects seen in *mab21l2* mutants is unclear. No *mab21l2*

mutants to date, in humans (Rainger *et al.*, 2014; Horn *et al.*, 2015), zebrafish (Deml *et al.*, 2015; this study), mice (Yamada *et al.*, 2004), or other organisms (Sghari and Gunhaga, 2018), have ever been noted to display defects of the optic nerve or optic atrophy. Therefore, no clear evidence for the involvement of klc2 in the production of defects observed in mab21l2 mutants has yet been presented. Further research into the eye-specific roles of klc2 or the importance of microtubule-related transport in the development of the eye would be needed to draw a clear connection between mab21l2 and klc2 function.

Of the transcriptional regulators identified from the yeast-2-hybrid screen, hnf4a would seem most promising. hnf4a is known to bind to smad proteins and act as an adaptor for the recruitment of these proteins to DNA, where they can upregulate gene expression required for differentiation of hepatocytes and other cell types (J. Li *et al.*, 2000; Kardassis *et al.*, 2000; Chou *et al.*, 2003). Furthermore, mab21l2 is also suspected to bind to smad1 (Baldessari *et al.*, 2004) and have some effects on differentiation of retinal and lens cell types (Sghari and Gunhaga, 2018, this work). In addition, hnf4a may be regulated by the action of prox1, a key regulator of some elements of eye development (Seth *et al.*, 2014; Armour *et al.*, 2017). However, due to the fact that it is not expressed anywhere near the eye (Bertrand *et al.*, 2007), nor are there known gut, kidney, or liver defects in mab21l2 mutants, it seems that hnf4a is likely not involved in the functions disrupted in mab21l2 mutants.

kdm3b, a histone modifying protein, could in principle be responsible for the kinds of wide-ranging changes in gene expression that would be likely to produce such diverse eye defects as seen in mab21l2 mutants. However, there is no known evidence linking mab21l2 to chromatin structure-level changes, as most current thought suggests mab21l2 acts either at the transcriptional or post transcriptional level (Baldessari *et al.*, 2004; Rainger *et al.*, 2014; de Oliveira Mann *et al.*, 2016), so further investigation of any connection would be required.

ldb2 is the sole transcription factor pulled from the yeast-2-hybrid screen which can be tangentially connected to what little is already known about mab21l2. It is

expressed in the eye and other neural tissues, allowing for colocalization *in vivo* with mab21l2. As mentioned above, ldb2 is associated with control of TGFβ signaling, and additionally, ldb2 assembles with a complex that includes smad1 and is known to occupy BMP response elements in the genome (Gu *et al.*, 2015). The suspected association of mab21l2 with smad1 could provide a link between these two proteins at a common BMP-responsive regulatory complex, where perhaps mab21l2 could act in its hypothesized transcriptional repressive manner, or bind nascent mRNAs using its ssRNA binding activity. As such, ldb2 is one of the most promising candidates pulled from this screen for future investigation.

Ribosomal function related genes nop56 and etf1 seem less likely to be relevant to the cell biological role of mab21l2, as mab21l2 is not known to be related in any way to translation or ribosomes. Although these two candidates are known to be related to maintenance of proliferation in the cell, and mab21l2 mutants do show disruptions of proliferation in the lens epithelium and CMZ (Deml *et al.*, 2015, this work), there is no other evidence linking them to mab21l2. Further, no eye related phenotypes have been reported in mutants for nop56 or etf, making them unlikely candidates for future investigation.

It is likely that the tnpo1 and tnpo2 binding reported in this screen is indicative of the use of these importins by mab21l2 for its entry into the nucleus. tnpo1 and 2 were some of the strongest binders found in the screen, but mab21l2 is known to be localized to the interior of the nucleus and chromatin rather than the nuclear envelope (unpublished observations, NG). In addition, mab21l2 is not predicted to have domains consistent with membrane association or channel protein function (de Oliveira Mann *et al.*, 2016). Therefore, it is unlikely that mab21l2 is directly acting in complex with tnpo1 and 2 for its cell biological function.

It is important to note that none of the above described potential binding partners have been validated. As such, these results may be real, biologically relevant bindings important for the function of mab21l2, or they may be false positives due to technical problems with the screen or yeast-specific binding. As mentioned above, some candidates

identified in the yeast-2-hybrid screen are very likely to fall into these categories, due to localization to tissues where mab21l2 is not expressed, localization to cellular compartments other than the nucleus, and more. However, it is still possible that one or more of the potential binding partners may be biologically relevant. Future work would be required to confirm this.

3.3.2 The effects of human mutations in mab21l2

The observation that some human mutations in mab21l2 are dominant and others are recessive has proven an interesting topic of study. The fact that mutations R51C and R51H cause colobomas even when injected into wild type fish (who therefore have two normal copies of non-mutated mab21l2), while mutation E49K, only two amino acids away, does not, is intriguing. This is especially interesting given that all three mutations are dominant and cause disease in human patients (Rainger *et al.*, 2014), suggests that there is something unique about amino acid 51 (or the domain which contains this amino acid) that, when mutated, confers gain of function or dominant negative effects. This is especially unexpected given the fact that, from the crystal structure of paralog MAB21L1, both amino acid 51 and 49 act to form a salt bridge with acid 115, and are located on the same loop of the MAB21L2 protein (Fig. 1.4A) (de Oliveira Mann *et al.*, 2016). The reason for gain of function in amino acid 51 mutations and not in amino acid 49 mutations is therefore unclear, and an interesting open question which would require further information on the specific differences in function between the two amino acids.

In addition, the fact that mutation R247Q, recessive in human patients (Rainger *et al.*, 2014), appears to perform much the same function at a structural level- stabilizing a loop via formation of a salt bridge with another amino acid – yet does not display gain of function effects either, is quite interesting. All four mutations were predicted to destabilize the protein due to destruction of salt bridges (de Oliveira Mann *et al.*, 2016), but the fact that the bridge disruption caused by mutation in amino acid 247 is recessive and the disruptions of amino acids 51 and 49 are dominant indicates that not all salt bridges in the protein structure may have the same consequences when disrupted.

However, the meaning of this observation is unclear, without further information on the role and domain functions of the MAB21L2 protein.

These data together provide a starting point for future investigation into the role of the mab21l2 protein. We have provided a list of candidate proteins which may interact with mab21l2 to allow it to perform its function, some of which are more likely involved in an *in vitro* context and some of which may either be experimental artifacts, or clues toward novel roles of mab21l2 that could not otherwise be predicted from current experimental evidence. In addition, we provide the first evidence that human mutations R51C and R51H may cause dominant phenotypic defects in human patients through a gain of function or dominant negative mechanism, while mutation E49K does not likely have the same effect, despite its closely related predicted role in the structure of MAB21L2.

Chapter 4: Future directions:

4.1 INVESTIGATION OF ORIGIN FOR CORNEAL DEFECTS:

4.1.1 Contribution of the neural crest-derived periocular mesenchyme to the *mab21l2* $^{-/-}$ cornea

Although work presented here shows that there is an increase in the number of corneal cells in *mab21l2* $^{-/-}$ embryos, it remains unclear where these cells originate. Future work to examine the corneal phenotype should investigate the origin of the extra cells, as well as their identity. Corneal endothelial cells are normally produced from mesenchymal cells derived from the neural crest, which migrate in around the eye and over the lens to form the endothelial layer. This normally takes place between 30 and 36hpf. It is possible that the extra cells seen in the *mab21l2*$^{-/-}$ cornea could be produced from extra migratory neural crest cells that enter the eye. Neural crest cells that enter the eye can be visualized with a sox9 (Spokony *et al.*, 2002) or sox10 (Dutton *et al.*, 2001; Kwak *et al.*, 2013) transgenic line. By crossing the *mab21l2* $^{-/-}$ line into a *sox10*:GFP transgenic, we can track the entry of neural-crest derived cells and count the number of these cells localizing to the cornea in *mab21l2* $^{-/-}$ mutant versus wild type embryos at the 36 hour timepoint.

4.1.2 Determining the contribution of failure of programmed cell death to corneal cell number increase in *mab21l2* $^{-/-}$

In addition, a second possible origin for the extra cells could be a deficiency in the programmed cell death at the lens/corneal connection. In the course of zebrafish lens development, the spherical lens is separated from the overlying surface ectoderm by apoptosis events in the cells located at the interface between these tissues, occurring at 24 and 25hpf (Dahm *et al.*, 2007). The lens never appears to separate from the ectoderm in *mab21l2* $^{-/-}$ embryos, and the cornea and lens cells seem indistinguishable even at 28 hpf, long after the lens should be a freestanding sphere (Dahm *et al.*, 2007; Greiling and

Clark, 2009). Therefore, it is possible that some of the extra cells in the corneal area in *mab21l2* $^{-/-}$ embryos could be leftover cells which were part of the lens-cornea connection, and failed to undergo apoptosis. Using TUNEL assays at the specific 24hpf and 25hpf time points, when this very transient cell death occurs in zebrafish, could allow us to determine if failure of extra cells to die off contributes to the increased cell number seen in the cornea of *mab21l2* $^{-/-}$ fish.

4.1.3 Elucidating the identity of additional cells found in the *mab21l2* $^{-/-}$ cornea

Corneal keratan sulfate stains showed that the corneal stroma is not properly patterned in *mab21l2* $^{-/-}$ embryos (Fig. 2.7 R,S). However, there is still investigation to be done to determine whether or not the other layers of the cornea are patterned correctly, and the identity of the extra cells, if any. The corneal stroma is, at the time points tested, an acellular tissue; keratocytes do not occupy the corneal stroma before 14-28dpf in zebrafish (Zhao *et al.*, 2006). Therefore, if the extra cells have taken on a differentiated corneal identity, they must be part of either the corneal endothelium or corneal epithelium. Antibody stains for these cell types in Chapter 2 of this dissertation failed due to lack of antibody cross-reactivity with the single antibody tested for each cell type (data not shown). However, there are multiple other markers for the corneal endothelium and corneal epithelium which can be tested and may show reactivity in zebrafish. For endothelium, these include clrn1, grip1, or zp4, among others (Yamaguchi *et al.*, 2015; Yoshihara *et al.*, 2015). For epithelium, many corneal keratins such as ck3, ck12, and others can be used as markers (Chen *et al.*, 1994; Auw-Haedrich *et al.*, 2011). In addition, if no antibodies currently available that have cross reactivity with zebrafish may be found, we could perform an *in situ* hybridization for the transcripts of these markers to determine if the corneal epithelium and endothelium are expressing genes consistent with their differentiated identities. Antibody stains or *in situ* hybridizations would also provide evidence for the identity of the extra cells at the cornea - the cells may express markers of endothelial or epithelial identity, or neither. Counting the cells expressing markers of

each identity would allow us to determine which cell type, if any, shows an increase in cell count or proportion.

4.1.4 Investigating possible defects in the anterior chamber and aqueous humor dynamics in *mab21l2* $^{-/-}$ mutants

An additional observation not further addressed in this work was that *mab21l2*$^{-/-}$ embryos appeared to have swelling or an excess of fluid trapped underneath the cornea surrounding the lens (Fig. 2.1 Q-S). It is possible that this fluid is an abnormally increased volume of aqueous humor, normally a small amount of fluid overlying the lens underneath the cornea. The mutant fish may accumulate an abnormally large amount of fluid in their anterior chamber, causing the observed "blister like" phenotype.

The dynamics and production of aqueous humor in zebrafish are somewhat different from those in mammals. In zebrafish, the aqueous humor is produced from a structure called the dorsal ciliary epithelium (Gray *et al.*, 2009). It then flows through the anterior chamber to the ventral canalicular network, where it is filtered into the choroid (Gray *et al.*, 2009). This is in contrast to the flow path in mammals, where the humor is produced at both the dorsal and ventral ciliary bodies, then flows out through Schlemm's canal and the trabecular meshwork into the choroid (reviewed in Goel *et al.*, 2010).

In zebrafish, the dorsal ciliary epithelium and the ventral canalicular network, and therefore the prerequisites for flow of the aqueous humor, are formed by 3dpf (Soules and Link, 2005). This is around the time that I first observe the apparent abnormal accumulation of fluid in the area of the anterior chamber of mab21l2 mutants. Due to observed defects in other tissues in the anterior chamber, such as the lens and the cornea, I hypothesize that there could also be defects in the formation of the structures required for aqueous humor flow. Therefore, it would be informative to investigate these structures and their morphology and differentiation. Sectioning both mutant and wild type fish at key points of formation for the dorsal ciliary epithelium and ventral canalicular network, such as 2.5, 3 and 5dpf, with both histology and TEM, would allow us to determine if there are any defects in these structures upon loss of mab21l2.

Ideally, measurement of intraocular pressure and outflow of the aqueous humor directly would be performed to identify any defects in the flow of aqueous humor in *mab21l2* $^{-/-}$ fish. Unfortunately, due to the aquatic nature of zebrafish, directly measuring intraocular pressure is possible, but difficult and requires highly specialized equipment compared to mammals (Link *et al.*, 2004). Thus far, methods of directly measuring rate of outflow have not been developed in zebrafish at all. Still, if there is reason to believe that there might be defects in humor flow, such as anatomical differences or developmental delays in formation or function of the ciliary epithelium or ventral canalicular network, measurements of intraocular pressure would theoretically be informative in determining if there truly is an abnormal accumulation of fluid in the eye.

4.2 INVESTIGATION OF EYE MORPHOGENESIS AND CHOROID FISSURE CLOSURE

4.2.1 Using *in vivo* time-lapse imaging to identify defects in early *mab21l2*$^{-/-}$ eye morphogenesis

The formation of the eye is a complex process, entailing three-dimensional tissue and cellular movements that bring each component into the proper orientation for the production of a mature eye. It is clear from the data and observations presented in this work that the loss of mab21l2 has dramatic effects on the overall shape of the eye, and the proper formation of a round eye of normal size. *mab21l2*$^{-/-}$ mutants show a "bean shaped" eye as early as 24hpf, with defects or delays in invagination and formation of the bilayered optic cup visible even earlier, at 18SS. The *mab21l2* $^{-/-}$ mutant eye remains abnormally oval in shape through 5dpf. In addition, the mutant eye appears to "collapse" around the lens, pushing it outwards by 3-5dpf, and in some *mab21l2* mutants, particularly those with the most severe colobomas, the ventral portion of the eye is shallower, with a shorter proximal-distal axis than the dorsal portion of the eye, while in wild type these axes are almost identical.

Due to the early onset and severe presentation of eye defects, it would be logical that early morphogenetic processes may be disrupted upon loss of mab21l2. The cell and tissue movements which take place from approximately 12-24hpf are precisely ordered, and controlled by the interplay of multiple signaling pathways in multiple tissues (Fuhrmann, 2010; Kwan *et al.*, 2012; Cavodeassi, 2018; Gordon *et al.*, 2018); therefore, the loss of mab21l2 could conceivably disrupt one or more of these functions and lead to morphogenetic defects. Zebrafish are highly amenable to *in vivo* time-lapse imaging of developmental processes (Meyers, 2018). *In vivo* time-lapse imaging has been used to great effect to explore the early morphogenesis of the eye and how it may be disrupted (Kwan *et al.*, 2012; Gordon *et al.*, 2018). Time-lapse imaging of *mab21l2* $^{-/-}$ and wild type embryos injected with a membrane and nuclear tag can allow for visualization of the tissue movements involved in events from evagination of the eye stalks to formation of the bilayered optic cup around 24hpf. Any differences in large-scale movements involved in the formation of the eye in *mab21l2* $^{-/-}$ should be visible. If smaller-scale changes in cell movements are suspected, cell tracking of individual or small groups of cells in the fashion of Kwan *et al.* could be performed (Kwan *et al.*, 2012) to determine if there are differences upon loss of mab21l2.

4.2.2 Examination of tissue dynamics during choroid fissure closure in *mab21l2* $^{-/-}$

The critical role of mab21l2 for morphogenetic events in the eye is evident from the colobomas present when mab21l2 function is lost. Evidence presented in this work shows that failure of basement membrane breakdown and abnormal cell death in the ventral optic stalk may contribute to the production of colobomas, but the process of choroid fissure closure is much more complex than that. Although not much is specifically known about the genes, mechanisms, and pathways that contribute to choroid fissure closure, closure is known to involve a series of tightly controlled tissue movements which are required to allow for fusion at the fissure (Bernstein *et al.*, 2018). The edges of the retina must orient themselves properly, move into close proximity with

the proper timing, and undergo tissue movements and cellular changes to allow for fusion (James *et al.*, 2016; Bernstein *et al.*, 2018; Gestri *et al.*, 2018).

Data presented in this work show that closure of the choroid fissure is disrupted in *mab21l2* $^{-/-}$ embryos, but the morphogenetic movements that lead to the formation of the fissure, and the tissue dynamics that occur during closure, were not investigated. Due to the importance of these events, and the fact that disruptions can lead to colobomas, it would be informative to perform a more thorough examination of the eye at time points corresponding to formation of the choroid fissure and events such as the change in orientation of the leading edges of the retina. Since *mab21l2* $^{-/-}$ embryos have smaller eyes, it is possible that, for example, fissure apposition may not occur at the correct time point, when conditions in the eye are conducive to the onset of choroid fissure closure, and as a result, fissure closure may then become impossible, even if apposition is achieved later on. *mab21l2* $^{-/-}$ embryos could be sectioned at time points such as 31hpf, when the sides of the fissure become apposed, or at 34-36hpf, when the basement membrane is being broken down and there are dynamic changes at the site of contact between the two sides (Bernstein *et al.*, 2018), and any differences between *mab21l2* $^{-/-}$ mutant and wild type embryos could be determined.

In addition, it is known that smaller-scale, more transient changes in the morphology and behavior of the cells and basement membrane at the choroid fissure site occur during the process of closure (James *et al.*, 2016; Williams, 2016; Bernstein *et al.*, 2018; Gestri *et al.*, 2018). As such, it may be informative to take advantage of the ability to perform *in vivo* time-lapse imaging of the choroid fissure process in zebrafish to observe *in vivo* the dynamics at the fissure site in wild type and *mab21l2* $^{-/-}$ embryos. This experiment would allow us to observe any differences in cell morphology, in the contacts extended by the basement membrane across the fissure, and in the localization and behavior of periocular mesenchymal cells at the fissure site in wild type versus mutant embryos, all of which could contribute to the colobomas observed in *mab21l2* $^{-/-}$ embryos.

4.3 INVESTIGATION OF FUNCTIONAL DOMAINS OF MAB21L2

Due to the relatively less severe phenotype in *mab21l2*^{au10} compared to full gene knockouts produced in mice (Yamada *et al.*, 2004), and the fact that the *au10* allele is a truncation of the protein that leaves approximately 1/3 of the protein's length intact (Fig. 1.4B), it is possible that this fragment is able to partially perform some of the functions of mab21l2 if it is not removed via nonsense mediated decay. Therefore, it is important to determine if the *au10* allele acts as a null allele, or if the first 1/3 of the mab21l2 protein still produced in *au10* fish is retained. Determining if *au10* undergoes nonsense-mediated decay would provide one piece of evidence to answer this question. This could be accomplished by examining *mab21l2*^{au10} zebrafish for the amount of *mab21l2* mRNA and protein that are present when the gene is mutated. In addition, production of a true null *mab21l2* knockout zebrafish line, for example by complete excision of the gene via dual Crisprs targeted to both ends of the gene, would be useful in investigating this question. Comparing the phenotypes of the *au10* allele and gene excision lines would allow us to determine if *au10* is likely a null allele. We could additionally inject mRNA corresponding to the *au10* allele into the gene excision line and determine if there is partial rescue of the observed phenotypes, which would suggest that *mab21l2*^{au10} is likely to retain some function.

In addition, once a complete knockout of the *mab21l2* gene has been produced, structure-function experiments could be performed to determine what domains of the mab21l2 protein are likely vital to its biological function. Microinjection of mRNA representing the *mab21l2* gene with various segments deleted can be used to determine which sections of the protein are critical for its function. If the *mab21l2* knockout zebrafish are rescued and no longer display phenotypes consistent with the loss of mab21l2 function, then the segment deleted from the gene is dispensable for the role of mab21l2. If the zebrafish still display phenotypes consistent with *mab21l2* knockout, then the deleted segment is required for full function of mab21l2. Some preliminary segments of the mab21l2 protein which may be informative to delete would be the RNA binding segment, the putative nucleotidyl transferase domain or parts thereof, and the potential

CTP binding domain as determined in closely related protein mab21l1 (de Oliveira Mann *et al.*, 2016). This could allow for determination of the functional relevance of these segments and proposed activities of the mab21l2 protein, which thus far may or may not be related to the observed phenotypes upon loss of mab21l2 function.

4.4 CREATION OF HUMAN MUTANT MAB21L2 ALLELES IN ZEBRAFISH

While zebrafish are a good model for defects and diseases of the eye, and have been useful in modeling the effects of mutations in mab21l2, the zebrafish mutant alleles in this study and in that performed by Deml *et al*. do not directly recapitulate the mutations found in human patients (Rainger *et al.*, 2014; Deml *et al.*, 2015; Horn *et al.*, 2015). In this study, the allele used is a truncation of the mab21l2 protein to 1/3 of its normal length, with the N-terminus remaining intact (Fig. 1.4B). Deml *et al.* used two TALEN lines, a deletion of amino acids 51 and 52, and a frameshift mutant leading to early truncation of the protein (Deml *et al.*, 2015). However, all human mutations described have been point mutations that alter only one amino acid (Rainger *et al.*, 2014; Deml *et al.*, 2015; Horn *et al.*, 2015). Therefore, the best model for these mutations would be to create zebrafish lines that contain the same amino acid substitutions, and characterize the effects on cell biology, gene expression, and more in these lines.

Due to the recent explosion in genome editing technology, it is possible to create point-specific and other targeted mutations in the genome using a combination of Crispr-Cas9 technology and directed genome repair. In mice, a commonly used technique is homologous recombination-based repair from a coinjected DNA template that contains the mutations or other genomic changes desired. This technique has also been used for precise genome editing in zebrafish. Future work could use homologous recombination-based repair with a template containing the human point mutations to create zebrafish lines that carry these precise mutations.

However, due to the fact that homologous recombination based repair occurs at a very low rate compared to repair via other mechanisms such as non-homologous end joining (Auer *et al.*, 2014; Horii and Hatada, 2016), with approximate success rates in zebrafish being reported in the 1-2% range (Zu *et al.*, 2013), it may be worthwhile to consider other methods of knock-in of the point mutations of interest. One such technique, recently applied to zebrafish, is the use of a cytidine deaminase fused to a Cas9 nickase to create non-double strand break-dependent conversions of cytidines to thymines (Komor *et al.*, 2016; Zhang *et al.*, 2017). Through targeting of this construct to the reverse strand, conversion of guanines to adenines in the gene of interest can also be achieved (Komor *et al.*, 2016). Conveniently, one of the human mutations in MAB21L2 described in the literature entails a C to T point mutation, while the other three are produced by the mutation of a G to an A (Rainger *et al.*, 2014). Therefore, it is possible to replicate all four currently identified human mutations in the zebrafish model using cytidine deaminase dependent base editing.

Through establishment of lines carrying the published human mutations, whether through homologous repair or cytidine deaminase base editing, we can use zebrafish as a more precise model for the eye defects observed in human patients. Many interesting observations could be tested - for example, zebrafish mutants display lens defects (Deml *et al.*, 2015; Gath and Gross, 2019 (Chapter 2 of this dissertation)), while human patients apparently do not (Rainger *et al.*, 2014; Deml *et al.*, 2015; Horn *et al.*, 2015), but it is unclear if this is due to organismal differences, or the different natures of the mutation in each system. By using knock-in zebrafish containing the exact mutations found in human patients, we could determine the precise effect of each mutation, and therefore extrapolate some information about the function of each amino acid that is mutated. For example, perhaps the mutation of amino acid 51 causes lens defects, but the mutation of acid 247 does not, which would provide evidence for which areas of the protein are required for the various functions of mab21l2 identified in previous research.

4.5 RNA-SEQUENCING EXPERIMENTS TO DETERMINE PATHWAYS AFFECTED BY LOSS OF MAB21L2

One of the most interesting facts about mab21l2 is that, despite its extremely high protein conservation and critical function in eye development, its exact role at the molecular and cellular level is almost completely unknown. DNA binding was predicted but could not be proven in an *in vitro* setting, while ssRNA binding appears to occur *in vitro* but has never been tested *in vivo.* Some evidence has suggested mab21l2 could have a transcriptional regulatory function, perhaps acting as a repressor of gene expression (Baldessari *et al.*, 2004). A few experiments suggest that mab21l2 might bind to SMAD1 and be involved in regulation of TGFβ/BMP signaling pathways. Otherwise, however, the pathways and genes that may be misregulated upon loss of mab21l2 are completely unknown.

As detailed in Chapter 3, I attempted to investigate the role of mab21l2 by seeking to identify its binding partners via a yeast-2-hybrid screen. However, I was unable to validate the binding of mab21l2 and any of the identified potential binding partners. Another approach toward defining the role of an unknown protein, especially one thought to be a transcriptional regulator, is to perform RNA-sequencing experiments. Future work on mab21l2 should perform an RNA-seq on wild type and *mab21l2* $^{-/-}$ eyes and compare the two samples to determine what genes and pathways are up- and down-regulated upon loss of mab21l2. Time points of interest may include the onset of lens morphogenesis, at approximately 16hpf (Greiling and Clark, 2009), or the beginning of choroid fissure closure as marked by basement membrane breakdown, at approximately 34 to 36hpf (Bernstein *et al.*, 2018), which coincides with development of the cornea (Zhao *et al.*, 2006).

Mining of the data gathered from this experiment could be used to determine which genes are differentially expressed in wild type versus *mab21l2*$^{-/-}$ samples. A list of genes up- and down-regulated in *mab21l2*$^{-/-}$ could then be analyzed for genes and pathways which seem likely to be or are known to be involved in developmental processes of the eye. While verification of these data would be required, it could provide

evidence as to with which previously researched pathways mab21l2 may be involved- for example, this experiment could support the potential involvement of mab21l2 in TGFβ/BMP signaling, and/or link mab21l2 to other pathways which have not yet been suggested to have a connection to this enigmatic protein. This would provide directions for future work, for example to place mab21l2 more precisely in these pathways, to use inhibitors or activators of these pathways (or mutant/overexpression lines, if available) to attempt to rescue or phenocopy *mab21l2*$^{-/-}$ mutants, and more.

The differentially upregulated genes in *mab21l2* $^{-/-}$ embryos may also provide some surprising results of genes not otherwise known to be involved in development of the eye. Determining if these are true results or artifactual through *in situ* hybridization, qRT-PCR, or other methods would be required before any conclusions could be made, but could provide interesting and unexpected insight into the role of mab21l2 in the formation of the eye.

CONCLUDING REMARKS:

The work presented in this dissertation represents the most thorough characterization to date of ocular defects in a *mab21l2* deficient system. This is particularly useful given the *MAB21L2* mutations associated with human disease identified over the past several years, providing a tractable animal model to further investigate the underpinnings of the observed clinical phenotypes. These results show that *mab21l2* $^{-/-}$ zebrafish display defects in the lens, closure of the choroid fissure, and cornea, the latter of which had not previously been described. In the lens, *mab21l2* is required for lens morphogenesis, lens epithelial cell proliferation and survival, and proper patterning/expression of markers of mature lens cell types. *mab21l2* is also required for choroid fissure closure, and its loss results in elevated cell death in the optic stalk as well as failure to break down the basement membrane at the fissure site. Interestingly, despite the smaller eye in *mab21l2* $^{-/-}$ embryos, the retina is fully patterned and forms mature retinal cell types. The results presented in this dissertation also show that corneal defects are present upon loss of *mab21l2*, including multiple extra layers of cells, swelling, and lack of a properly differentiated corneal stroma. Additionally, this dissertation presents several potential binding partners for mab21l2 which could point to a function in transcriptional regulation and/or regulation of the shape and migration of cells. Lastly, we present evidence showing that the dominant human mutations MAB21L2^{R51C} and MAB21L2^{R51H} serve as gain-of-function mutations which induce colobomas even in the presence of normal levels of wild type mab21l2 protein. Future studies should further investigate the molecular and cell biological underpinnings of the observed phenotypes and defects upon loss of *mab21l2.*

Appendix: Materials and Methods

ZEBRAFISH HUSBANDRY:

Zebrafish were maintained at 28.5°C on a 14hr/10hr light-dark cycle. Embryos were obtained from natural pairwise spawns from heterozygous mutant crosses. Embryos were collected and maintained at 28.5°C in Danieu's medium in the dark. The *mab21l2* $^{-/-}$ line used in this study has line identifier *au10* and is being submitted to ZIRC for maintenance. The *au10* line was created in our lab using an ENU based mutagenesis protocol, previously published (Lee *et al.*, 2012). The *au10* line was propagated by outcrosses to wild type AB animals. All animals were treated in accordance with provisions established by the University of Texas at Austin and University of Pittsburgh School of Medicine Institutional Animal Care and Use Committees.

EMBRYO MICROINJECTION

mRNA for injections was transcribed in vitro using mMessage mMachine transcription kits for capped RNA (Roche) according to manufacturer instructions. After transcription, the RNA reaction was treated with Turbo DNAse (Roche) for 20 minutes. Finished mRNA was purified using a Qiagen RNeasy Plus mini kit.

Embryos were injected at the one-cell stage, into the yolk. 250pg of mRNA was injected into each embryo.

BRDU INCORPORATION ASSAYS:

50-60 dechorionated zebrafish embryos were placed in a small dish of 10mL of 10mM BrdU (Sigma-Aldrich) in Danieu's medium. They were incubated at 28.5°C for

20 minutes (36 and 48hpf samples) or one hour (22SS and 26SS samples). Embryos were immediately sacrificed using Tricaine (Spectrum Chemical) and fixed for analysis.

TISSUE PREPARATION AND CRYOSECTIONING:

Embryos were collected and fixed overnight in 4% PFA in PBS at 4°C. Embryos were then washed 3x with PBS and placed into two successive 25% and 35% sucrose/PBS washes for at least one hour. Embryos were then embedded in Tissue Freezing Medium (Electron Microscopy) and placed at -80°C until solidified, then stored at -20°C. Cryosections were made at 12µm thickness on polylysine coated FrostPlus slides (Fisher). These slides were dried at RT for 1 to 2 days and stored at -20°C.

IMMUNOHISTOCHEMISTRY:

Slides were rehydrated in PBS. Prior to blocking, antigen retrieval of a 30 minute incubation in 0.5% SDS at 37°C was used for laminin α1 staining. An 8 minute incubation in 4N HCl at 37°C was used for antigen retrieval prior to BrdU staining. Blocking followed in 5% normal goat serum solution in PBS for at least one hour. Antibody incubation took place overnight at 4°C in block solution. The following antibodies and dilutions were used: BrdU (Abcam) 1:250, CKS (Millipore Sigma) 1:500, HuC/HuD (Invitrogen) 1:200, laminin α1 (Sigma-Aldrich) 1:100, pax2 (Abcam) 1:500, zn-8 (ZIRC) 1:200, zpr-1 (ZIRC) 1:200. Slides were washed 3x in PBS for 10 minutes each. Incubation with the corresponding Cy3 or Cy5 conjugated secondary antibody (Jackson Immunoresearch, 1:250) and/or phalloidin (Fisher, 1:50) in block followed for 2 to 3 hours. Slides were washed 3x in PBS for 10 minutes each followed by counterstaining with DAPI (Life Technologies) 1:300 or Sytox-orange (Molecular Probes) 1:4000 for 15 minutes. Slides were quickly rinsed 3 times in PBS and blotted

dry, then covered with Vectashield mounting medium (Vector Laboratories) and coverslipped.

TUNEL ASSAY:

TUNEL assay was performed using a TMR Red in situ cell death detection kit (Roche) according to manufacturer instructions, except that all reagents were diluted 1:2 using PBS.

IMAGING:

Confocal section imaging was performed on an Olympus FV1200 confocal microscope using Olympus software. 3-7 1µm optical sections were acquired of each image using 2x Kahlman filtering. Sections were stacked using a maximum-intensity projection in ImageJ (imagej.nih.gov). Whole mount imaging was performed on a Zeiss Axio Zoom.V16 microscope dissecting scope using Z3 Zeiss software. Living embryos were anesthetized with Tricaine (Spectrum Chemical) and immobilized in 3% methylcellulose solution (Fisher) for imaging. For all assays, n>6 individual eyes.

IN SITU HYBRIDIZATION:

In situ hybridization was performed essentially as described (Jowett and Lettice, 1994), using DIG-labeled antisense riboprobes. Probes were synthesized from clones maintained in pGEM-T-Easy (Promega) using Sp6 or T7 polymerase and DIG RNA labeling mix (Roche). Post in situ hybridization, embryos were fixed for 1hr at room temperature, washed 3x with PBS, and imaged in whole mount. n>30 embryos for each hybridization.

CELL COUNTING:

Cells were counted in ImageJ (imagej.nih.gov) using the Cell Counter plugin. For corneal cell counts, the cornea was defined as the outermost cellular surface of the eye visible in each section, until the surface cells were no longer directly adjacent to the retinal/RPE cells. For all assays, n>6 individual eyes, >3 sections per eye.

YEAST-2-HYBRID:

The yeast-2-hybrid described in this dissertation was performed by Hybrigenics company. Briefly, bait used in the screen was wild type zebrafish mab21l2. Preys were members of a fragment-based library representing the proteome of a 20hpf zebrafish. Two separate screens were performed, one using a traditional GAL4-based approach, and one using a LexA-based method. 3-amino trizol was used in the LexA screen to decrease nonspecific binding. 132.6 million potential interactions were screened. 320 positive interactions were identified, representing 84 different preys. Seven of these were identified as highly likely to be experimental artifacts, leaving 77 likely preys, with 15 at high confidence levels. 11 of these were identified and named proteins, while 4 were uncharacterized, unnamed proteins derived from gene prediction.

Results were ranked and assigned confidence levels based on Hybrigenics criteria as described in Formstecher *et al.* (Formstecher *et al.*, 2005). Briefly, some of the factors taken into account were the proportion of overlapping prey fragments that bound to the bait, the frame of the identified prey, whether the prey was sense or antisense, whether or not the prey was identified in both independent screens, and whether the prey was known from previous studies to be likely to bind nonspecifically.

CELL CULTURE:

HEK293t cells were used for expression of yeast-2-hybrid preys for co-immunoprecipitation-based verification of binding. Preys were cloned into pDEST26 6x-His tagged mammalian expression vector (ThermoFisher). mab21l2 bait was tagged with GFP at the N-terminus and expressed from a pCS107 vector. All plasmids for cellular transfection were purified with a Qiagen Midiprep kit. Cells were maintained at 37ºC with 5% carbon dioxide content in 10cm coated dishes. Media used was DMEM (Gibco) with 10% FBS (Gibco). 10^6 cells were plated from frozen stocks. For transfection, cells were seeded at $5x10^5$ per well in 6 well coated plates. Transfection was performed 24hrs after seeding using Roche Xtremegene 9. 180µL of Optimem medium (Gibco), 6µL of Xtremegene, and 2µg of plasmid were combined for 20 minutes at room temperature and added dropwise to wells containing 1mL of fresh DMEM/FBS, then swirled to mix. Cells were maintained in transfection medium for 24 hours, then media was replaced with fresh DMEM/FBS. No antibiotics were used. Cells were harvested via scraping 48 hours after transfection and processed for western blot.

WESTERN BLOTTING:

Cells were lysed in 75µL of Lemeer's lysis buffer on ice for 1-2 hours. Lysate was spun down at 4ºC for 10 minutes at 13.2 RCF, and the supernatant was collected. 15µL of lysate was combined with 5µL of 4x NuPage LDS Sample Buffer (Invitrogen) and heated at 70ºC for 10 minutes. The resulting 20µL of sample was run on a 4% Bis-Tris NuPage mini gel (Invitrogen) using NuPage SDS-MOPS buffer (Invitrogen) at 125 volts for 1.5 hours.

Wet transfer was used to transfer the gel bands onto 0.2µm PVDF membrane (ThermoFisher). Transfer was accomplished under NuPage transfer buffer (Invitrogen) containing 10% methanol. Transfer was run at 35V for 4 hours at room temperature.

The membrane was washed in PBS, then blocked in 5% milk, 1% BSA (ThermoFisher) in PBS for 1.5 hours. 1:1000 primary antibody in block (αGFP, Abcam and/or α6xHIs, Abcam) was incubated on the membrane overnight at 4ºC. Membrane was washed in PBS with 0.1% tween (PBST) 3x for 5 minutes each. 1:2500 goat-α-mouse HRP-conjugated secondary antibody (Jackson Immunoresearch) in block was added to the membrane for 1.5 hours. Membrane was washed 3x in PBST for 5 minutes. 1mL total volume of binary developing fluid from a SuperSignal West Femto kit (ThermoFisher) was mixed and incubated in the dark for 3 minutes before being added to the membrane and incubated in the dark for 3 minutes, then poured off. Membrane was imaged using a ChemiDoc XRS+ (BioRad).

GRAPHING AND STATISTICS:

All graphs were prepared and statistical analyses performed in GraphPad Prism v8.0 (GraphPad Software). For all graphs, the line indicates mean, box encompasses 25th to 75th percentile, and whiskers encompass the entire range of the data. Circles and triangles each represent one counted section of an individual eye. *=$p<0.05$, **=$p<0.01$, ***= $p<0.001$, ****=$p<0.0001$. P values were computed using unpaired t-test with Welch's correction.

Works Cited

Adamson, K. I., Sheridan, E. and Grierson, A. J. (2018) Use of zebrafish models to investigate rare human disease. *J. Med. Genet.*, 55(10), pp. 641–649.

Armour, S. M., Remsberg, J. R., Damle, M., Sidoli, S., Ho, W. Y., Li, Z., Garcia, B. A. and Lazar, M. A. (2017) An HDAC3-PROX1 corepressor module acts on HNF4α to control hepatic triglycerides. *Nat. Commun.*, 8(1), p. 549.

Ashery-Padan, R., Marquardt, T., Zhou, X. and Gruss, P. (2000) Pax6 activity in the lens primordium is required for lens formation and for correct placement of a single retina in the eye. *Genes Dev.*, 14(21), pp. 2701–11.

Atkinson-Leadbeater, K., Hehr, C. L. and Mcfarlane, S. (2014) Fgfr signaling is required as the early eye field forms to promote later patterning and morphogenesis of the eye. *Dev. Dyn.*, 243(5), pp. 663–675.

Auer, T. O., Duroure, K., Cian, A. De, Concordet, J. and Bene, F. Del (2014) Highly efficient CRISPR / Cas9-mediated knock-in in zebrafish by homology-independent DNA repair. *Genome Res.*, 24, pp. 142–153.

Auw-Haedrich, C., Agrawal, M., Gabbert, H. E., Meyer, P., Arnold, N. and Reinhard, T. (2011) Immunohistochemical expression of epithelial cell markers in corneas with congenital aniridia and ocular cicatrizing pemphigoid. *Acta Ophthalmol.*, 89(1), pp. 47–53.

Baldessari, D., Badaloni, A., Longhi, R., Zappavigna, V. and Consalez, G. G. (2004) MAB21L2, a vertebrate member of the Male-abnormal 21 family, modulates BMP signaling and interacts with SMAD1. *BMC Cell Biol.*, 5(1), p. 48.

Barbieri, A. M., Broccoli, V., Bovolenta, P., Alfano, G., Marchitiello, A., Mocchetti, C., Crippa, L., Bulfone, A., Marigo, V., Ballabio, A. and Banfi, S. (2002) Vax2 inactivation in mouse determines alteration of the eye dorsal-ventral axis, misrouting of the optic fibres and eye coloboma. *Development*, 129(3), pp. 805–813.

Bardakjian, T., Weiss, A. and Schneider, A. (2015) *Microphthalmia/Anophthalmia/Coloboma Spectrum*. *GeneReviews®*. Edited by M. Adam, H. Ardinger, and R. Pagon. University of Washington, Seattle.

Bassett, E. A. and Wallace, V. A. (2012) Cell fate determination in the vertebrate retina. *Trends Neurosci.*, 35(9), pp. 565–573.

Behesti, H., Holt, J. K. and Sowden, J. C. (2006) The level of BMP4 signaling is critical for the regulation of distinct T-box gene expression domains and growth along the dorso-ventral axis of the optic cup. *BMC Dev. Biol.*, 6(1), p. 62.

Bernstein, C. S., Anderson, M. T., Gohel, C., Slater, K., Gross, J. M. and Agarwala, S. (2018) The cellular bases of choroid fissure formation and closure. *Dev. Biol.*, 440(2), pp. 137–151.

Bertrand, S., Thisse, B., Tavares, R., Sachs, L., Chaumot, A., Bardet, P.-L., Escrivà, H., Duffraisse, M., Marchand, O., Safi, R., Thisse, C. and Laudet, V. (2007) Unexpected Novel Relational Links Uncovered by Extensive Developmental Profiling of Nuclear Receptor Expression. *PLoS Genet.*, 3(11), p. e188.

Beznosková, P., Cuchalová, L., Wagner, S., Shoemaker, C. J., Gunišová, S., von der Haar, T. and Valášek, L. S. (2013) Translation initiation factors eIF3 and HCR1 control translation termination and stop codon read-through in yeast cells. *PLoS Genet.*, 9(11), p. e1003962.

Bibliowicz, J., Tittle, R. K. and Gross, J. M. (2011) Toward a better understanding of human eye disease insights from the zebrafish, Danio rerio. *Prog. Mol. Biol. Transl. Sci.*, 100, pp. 287–330.

Blech-Hermoni, Y., Stillwagon, S. J. and Ladd, A. N. (2013) Diversity and conservation of CELF1 and CELF2 RNA and protein expression patterns during embryonic development. *Dev. Dyn.*, 242(6), pp. 767–77.

Blixt, A., Mahlapuu, M., Aitola, M., Pelto-Huikko, M., Enerbäck, S. and Carlsson, P. (2000) A forkhead gene, FoxE3, is essential for lens epithelial proliferation and closure of the lens vesicle. *Genes Dev.*, 14(2), pp. 245–54.

Boswell, B. A., Overbeek, P. A. and Musil, L. S. (2008) Essential role of BMPs in FGF-induced secondary lens fiber differentiation. *Dev. Biol.*, 324(2), pp. 202–12.

Boyden, L. M., Choi, M., Choate, K. A., Nelson-Williams, C. J., Farhi, A., Toka, H. R., Tikhonova, I. R., Bjornson, R., Mane, S. M., Colussi, G., Lebel, M., Gordon, R. D., Semmekrot, B. A., Poujol, A., Välimäki, M. J., Ferrari, M. E. De, Sanjad, S. A., Gutkin, M., Karet, F. E., *et al.* (2012) Mutations in Kelch-like 3 and Cullin 3 cause hypertension and electrolyte abnormalities. *Nature*, 482(7383), p. 98.

Cai, Z., Tao, C., Li, H., Ladher, R., Gotoh, N., Feng, G.-S., Wang, F. and Zhang, X. (2013) Deficient FGF signaling causes optic nerve dysgenesis and ocular coloboma. *Development*, 140(13), pp. 2711–2723.

Canning, P., Cooper, C. D. O., Krojer, T., Murray, J. W., Pike, A. C. W., Chaikuad, A., Keates, T., Thangaratnarajah, C., Hojzan, V., Marsden, B. D., Gileadi, O., Knapp, S., von Delft, F., Bullock, A. N. and Bullock, A. N. (2013) Structural Basis for Cul3 Protein Assembly with the BTB-Kelch Family of E3 Ubiquitin Ligases. *J. Biol. Chem.*, 288(11), pp. 7803–7814.

Cavodeassi, F. (2018) Dynamic Tissue Rearrangements during Vertebrate Eye Morphogenesis: Insights from Fish Models. *J. Dev. Biol.*, 6(1), p. 4.

Cederlund, M. L., Vendrell, V., Morrissey, M. E., Yin, J., Gaora, P. Ó., Smyth, V. A., Higgins, D. G. and Kennedy, B. N. (2011) mab21l2 transgenics reveal novel expression patterns of mab21l1 and mab21l2, and conserved promoter regulation without sequence conservation. *Dev. Dyn.*, 240(4), pp. 745–754.

Cheah, F. S. H., Jabs, E. W. and Chong, S. S. (2005) Genomic, cDNA, and embryonic expression analysis of zebrafish transforming growth factor beta 3 (tgfB3). *Dev. Dyn.*, 232(4), pp. 1021–1030.

Chen, S., Lewis, B., Moran, A. and Xie, T. (2012) Cadherin-mediated cell adhesion is critical for the closing of the mouse optic fissure. *PLoS One*, 7(12), p. e51705.

Chen, S., Li, H., Gaudenz, K., Paulson, A., Guo, F., Trimble, R., Peak, A., Seidel, C., Deng, C., Furuta, Y. and Xie, T. (2013) Defective FGF signaling causes coloboma formation and disrupts retinal neurogenesis. *Cell Res.*, 23(2), pp. 254–273.

Chen, W. Y., Mui, M. M., Kao, W. W., Liu, C. Y. and Tseng, S. C. (1994) Conjunctival epithelial cells do not transdifferentiate in organotypic cultures: expression of K12 keratin is restricted to corneal epithelium. *Curr. Eye Res.*, 13(10), pp. 765–78.

Choi, J. J. Y., Ting, C.-T., Trogrlic, L., Milevski, S. V., Familari, M., Martinez, G. and de Iongh, R. U. (2014) A Role for Smoothened during Murine Lens and Cornea Development. *PLoS One*, 9(9), p. e108037.

Chou, W.-C., Prokova, V., Shiraishi, K., Valcourt, U., Moustakas, A., Hadzopoulou-Cladaras, M., Zannis, V. I. and Kardassis, D. (2003) Mechanism of a Transcriptional Cross Talk between Transforming Growth Factor-β–regulated Smad3 and Smad4 Proteins and Orphan Nuclear Receptor Hepatocyte Nuclear Factor-4. *Mol. Biol. Cell*. Edited by C. Henrik-Heldin, 14(3), pp. 1279–1294.

Chow, K. L., Hall, D. H. and Emmons, S. W. (1995) The mab-21 gene of Caenorhabditis elegans encodes a novel protein required for choice of alternate cell fates. *Development*, 121(11), pp. 3615–3626.

Collomb, E., Yang, Y., Foriel, S., Cadau, S., Pearton, D. J. and Dhouailly, D. (2013) The corneal epithelium and lens develop independently from a common pool of precursors. *Dev. Dyn.*, 242(5), pp. 401–413.

Costa, R. H., Van Dyke, T. A., Yan, C., Kuo, F., Darnell, J. E. and Jr (1990) Similarities in transthyretin gene expression and differences in transcription factors: liver and yolk sac compared to choroid plexus. *Proc. Natl. Acad. Sci. U. S. A.*, 87(17), pp. 6589–93.

Cui, W., Tomarev, S. I., Piatigorsky, J., Chepelinsky, A. B. and Duncan, M. K. (2004) Mafs, Prox1, and Pax6 Can Regulate Chicken β B1-Crystallin Gene Expression. *J. Biol. Chem.*, 279(12), pp. 11088–11095.

Cvekl, A., Kashanchi, F., Sax, C. M., Brady, J. N. and Piatigorsky, J. (1995) Transcriptional regulation of the mouse alpha A-crystallin gene: activation dependent on a cyclic AMP-responsive element (DE1/CRE) and a Pax-6-binding site. *Mol. Cell. Biol.*, 15(2), pp. 653–60.

Cvekl, A. and Wang, W.-L. (2009) Retinoic acid signaling in mammalian eye

development. *Exp. Eye Res.*, 89(3), pp. 280–91.

Cvekl, A. and Zhang, X. (2017a) Signaling and Gene Regulatory Networks in Mammalian Lens Development. *Trends Genet.*, 33(10), pp. 677–702.

Cvekl, A. and Zhang, X. (2017b) Signaling and Gene Regulatory Networks in Mammalian Lens Development. *Trends Genet.*, 33(10), pp. 677–702.

Dahm, R., Schonthaler, H. B., Soehn, A. S., van Marle, J. and Vrensen, G. F. J. M. (2007) Development and adult morphology of the eye lens in the zebrafish. *Exp. Eye Res.*, 85(1), pp. 74–89.

Deml, B., Kariminejad, A., Borujerdi, R., Muheisen, S., Reis, L. and Semina, E. (2015) Mutations in MAB21L2 Result in Ocular Coloboma, Microcornea and Cataracts. *PLoS Genet.*, 11(2), p. e1005002.

Deml, B., Kariminejad, A., Borujerdi, R. H. R., Muheisen, S., Reis, L. M. and Semina, E. V. (2015) Mutations in MAB21L2 Result in Ocular Coloboma, Microcornea and Cataracts. *PLoS Genet.*, 11(2), pp. 1–26.

Dooley, K. and Zon, L. I. (2000) Zebrafish: a model system for the study of human disease. *Curr. Opin. Genet. Dev.*, 10(3), pp. 252–256.

Dudley, A. T. and Robertson, E. J. (1997) Overlapping expression domains of bone morphogenetic protein family members potentially account for limited tissue defects inBMP7 deficient embryos. *Dev. Dyn.*, 208(3), pp. 349–362.

Dutton, K. A., Pauliny, A., Lopes, S. S., Elworthy, S., Carney, T. J., Rauch, J., Geisler, R., Haffter, P. and Kelsh, R. N. (2001) Zebrafish colourless encodes sox10 and specifies non-ectomesenchymal neural crest fates. *Development*, 128(21).

Easter, Jr., S. S. and Nicola, G. N. (1996) The Development of Vision in the Zebrafish (Danio rerio). *Dev. Biol.*, 180(2), pp. 646–663.

Formstecher, E., Aresta, S., Collura, V., Hamburger, A., Meil, A., Trehin, A., Reverdy, C., Betin, V., Maire, S., Brun, C., Jacq, B., Arpin, M., Bellaiche, Y., Bellusci, S., Benaroch, P., Bornens, M., Chanet, R., Chavrier, P., Delattre, O., *et al.* (2005) Protein interaction mapping: A Drosophila case study. *Genome Res.*, 15(3), pp. 376–384.

Fuhrmann, S. (2010) Eye morphogenesis and patterning of the optic vesicle. *Curr. Top. Dev. Biol.*, 93, pp. 61–84.

Furuta, Y. and Hogan, B. L. (1998) BMP4 is essential for lens induction in the mouse embryo. *Genes Dev.*, 12(23), pp. 3764–75.

Gagnon, K. T., Biswas, S., Zhang, X., Brown, B. A., Wollenzien, P., Mattos, C. and Maxwell, E. S. (2012) Structurally conserved Nop56/58 N-terminal domain facilitates archaeal box C/D ribonucleoprotein-guided methyltransferase activity. *J. Biol. Chem.*, 287(23), pp. 19418–28.

Gath, N. and Gross, J. M. (2019) Zebrafish mab21l2 mutants possess severe defects in optic cup morphogenesis, lens and cornea development . *Dev. Dyn.*, 248(9), pp. 514-529.

Gawden-Bone, C., Zhou, Z., King, E., Prescott, A., Watts, C. and Lucocq, J. (2010) Dendritic cell podosomes are protrusive and invade the extracellular matrix using metalloproteinase MMP-14. *J. Cell Sci.* Company of Biologists, 123(Pt 9), pp. 1427–37.

Geeraets, R. (1976) An electron microscopic study of the closure of the optic fissure in the golden hamster. *Am. J. Anat.*, 145(4), pp. 411–31.

Gestri, G., Bazin-Lopez, N., Scholes, C. and Wilson, S. W. (2018) Cell Behaviors during Closure of the Choroid Fissure in the Developing Eye. *Front. Cell. Neurosci.*, 12, p. 42.

Gestri, G., Link, B. A. and Neuhauss, S. C. F. (2012) The visual system of zebrafish and its use to model human ocular Diseases. *Dev. Neurobiol.*, 72(3), pp. 302–327.

Goel, M., Picciani, R. G., Lee, R. K. and Bhattacharya, S. K. (2010) Aqueous humor dynamics: a review. *Open Ophthalmol. J.*, 4, pp. 52–9.

Gomez, G. A., Veldman, M. B., Zhao, Y., Burgess, S. and Lin, S. (2009) Discovery and Characterization of Novel Vascular and Hematopoietic Genes Downstream of Etsrp in Zebrafish. *PLoS One*, 4(3), p. e4994.

Gordon-Thomson, C., de Iongh, R. U., Hales, A. M., Chamberlain, C. G. and McAvoy, J. W. (1998) Differential cataractogenic potency of TGF-beta1, -beta2, and -beta3 and their expression in the postnatal rat eye. *Invest. Ophthalmol. Vis. Sci.*, 39(8), pp. 1399–409.

Gordon, H. B., Lusk, S., Carney, K. R., Wirick, E. O., Murray, B. F. and Kwan, K. M. (2018) Hedgehog signaling regulates cell motility and optic fissure and stalk formation during vertebrate eye morphogenesis. *Development*, 145(22).

Gray, M. P., Smith, R. S., Soules, K. A., John, S. W. M. and Link, B. A. (2009) The aqueous humor outflow pathway of zebrafish. *Invest. Ophthalmol. Vis. Sci.*, 50(4), pp. 1515–21.

Gregory-Evans, C. Y., Williams, M. J., Halford, S. and Gregory-Evans, K. (2004) Ocular coloboma: a reassessment in the age of molecular neuroscience. *J. Med. Genet.*, 41(12), pp. 881–91.

Greiling, T. M. S., Aose, M. and Clark, J. I. (2010) Cell fate and differentiation of the developing ocular lens. *Invest. Ophthalmol. Vis. Sci.*, 51(3), pp. 1540–6.

Greiling, T. M. S. and Clark, J. I. (2009) Early lens development in the zebrafish: A three-dimensional time-lapse analysis. *Dev. Dyn.*, 238(9), pp. 2254–2265.

Grocott, T., Johnson, S., Bailey, A. P. and Streit, A. (2011) Neural crest cells organize the

eye via TGF-β and canonical Wnt signalling. *Nat. Commun.*, 2, p. 265.

Gu, W., Monteiro, R., Zuo, J., Simões, F. C., Martella, A., Andrieu-Soler, C., Grosveld, F., Sauka-Spengler, T. and Patient, R. (2015) A Novel TGFβ Modulator that Uncouples R-Smad/I-Smad-Mediated Negative Feedback from R-Smad/Ligand-Driven Positive Feedback. *PLoS Biol.*, 13(2), pp. 1–22.

Gunhaga, L. (2011) The lens: a classical model of embryonic induction providing new insights into cell determination in early development. *Philos. Trans. R. Soc. Lond. B. Biol. Sci.*, 366(1568), pp. 1193–203.

Halbleib, J. M. and Nelson, W. J. (2006) Cadherins in development: cell adhesion, sorting, and tissue morphogenesis. *Genes Dev.*, 20(23), pp. 3199–3214.

Hartsock, A., Lee, C., Arnold, V. and Gross, J. M. (2014) In vivo analysis of hyaloid vasculature morphogenesis in zebrafish: A role for the lens in maturation and maintenance of the hyaloid. *Dev. Biol.*, 394(2), pp. 327–39.

Hartsock, A. and Nelson, W. J. (2008) Adherens and tight junctions: structure, function and connections to the actin cytoskeleton. *Biochim. Biophys. Acta*, 1778(3), pp. 660–9.

Haustein, J. (1983) On the ultrastructure of the developing and adult mouse corneal stroma. *Anat. Embryol. (Berl).*, 168(2), pp. 291–305.

Hay, E. D. (1980) Development of the Vertebrate Cornea. *Int. Rev. Cytol.*, 63, pp. 263–322.

Hayashi, S., Osawa, T. and Tohyama, K. (2002) Comparative observations on corneas, with special reference to Bowman's layer and Descemet's membrane in mammals and amphibians. *J. Morphol.*, 254(3), pp. 247–258.

Henriksson, J. T., McDermott, A. M. and Bergmanson, J. P. G. (2009) Dimensions and Morphology of the Cornea in Three Strains of Mice. *Invest. Ophthalmol. Vis. Sci.*, 50(8), p. 3648.

Hero, I. (1989) The optic fissure in the normal and microphthalmic mouse. *Exp. Eye Res.*, 49(2), pp. 229–239.

Hero, I. (1990) Optic fissure closure in the normal cinnamon mouse. An ultrastructural study. *Invest. Ophthalmol. Vis. Sci.*, 31(1), pp. 197–216.

Hero, I., Farjah, M. and Scholtz, C. L. (1991) The prenatal development of the optic fissure in colobomatous microphthalmia. *Invest. Ophthalmol. Vis. Sci.*, 32(9), pp. 2622–35.

Ho, S. H., So, G. M. K. and Chow, K. L. (2001) Postembryonic expression of Caenorhabditis elegans mab-21 and its requirement in sensory ray differentiation. *Dev. Dyn.*, 221(4), pp. 422–430.

Horii, T. and Hatada, I. (2016) Challenges to increasing targeting efficiency in genome

engineering. *J. Reprod. Dev.*, 62(1), pp. 7–9.

Horn, D., Prescott, T., Houge, G., Brække, K., Rosendahl, K., Nishimura, G., FitzPatrick, D. R. and Spranger, J. (2015) A Novel Oculo-Skeletal syndrome with intellectual disability caused by a particular MAB21L2 mutation. *Eur. J. Med. Genet.*, 58(8), pp. 387–391.

Huang, J., Liu, Y., Filas, B., Gunhaga, L. and Beebe, D. C. (2015) Negative and positive auto-regulation of BMP expression in early eye development. *Dev. Biol.*, 407(2), pp. 256–264.

Inge-Vechtomov, S., Zhouravleva, G. and Philippe, M. (2003) Eukaryotic release factors (eRFs) history. *Biol. Cell*, 95(3–4), pp. 195–209.

James, A., Lee, C., Williams, A. M., Angileri, K., Lathrop, K. L. and Gross, J. M. (2016) The hyaloid vasculature facilitates basement membrane breakdown during choroid fissure closure in the zebrafish eye. *Dev. Biol.*, 419(2), pp. 262–272.

Johnston, M. C., Noden, D. M., Hazelton, R. D., Coulombre, J. L. and Coulombre, A. J. (1979) Origins of avian ocular and periocular tissues. *Exp. Eye Res.*, 29(1), pp. 27–43.

Kardassis, D., Pardali, K. and Zannis, V. I. (2000) SMAD Proteins Transactivate the Human ApoCIII Promoter by Interacting Physically and Functionally with Hepatocyte Nuclear Factor 4. *J. Biol. Chem.* American Society for Biochemistry and Molecular Biology, 275(52), pp. 41405–41414.

Kennedy, B. N., Stearns, G. W., Smyth, V. A., Ramamurthy, V., van Eeden, F., Ankoudinova, I., Raible, D., Hurley, J. B. and Brockerhoff, S. E. (2004) Zebrafish rx3 and mab21l2 are required during eye morphogenesis. *Dev. Biol.*, 270(2), pp. 336–49.

Kenyon, K., Starck, T., Cockerham, G. and Hersh, P. (2008) Corneal dysgeneses, dystrophies, and degenerations. in Albert, D. et al. (eds) *Albert Jakobiec's Princ. Pract. Ophthalmol.* 3rd edn. WB Saunders, p. 498.

Kerr, C. L., Huang, J., Williams, T. and West-Mays, J. A. (2012) Activation of the hedgehog signaling pathway in the developing lens stimulates ectopic FoxE3 expression and disruption in fiber cell differentiation. *Invest. Ophthalmol. Vis. Sci.* Association for Research in Vision and Ophthalmology, 53(7), pp. 3316–30.

Kim, J.-Y., Kim, K.-B., Eom, G. H., Choe, N., Kee, H. J., Son, H.-J., Oh, S.-T., Kim, D.-W., Pak, J. H., Baek, H. J., Kook, Hoon, Hahn, Y., Kook, Hyun, Chakravarti, D. and Seo, S.-B. (2012) KDM3B Is the H3K9 Demethylase Involved in Transcriptional Activation of lmo2 in Leukemia. *Mol. Cell. Biol.*, 32(14), p. 2917.

Komor, A. C., Kim, Y. B., Packer, M. S., Zuris, J. A. and Liu, D. R. (2016) Programmable editing of a target base in genomic DNA without double-stranded DNA cleavage. *Nature*, 533(7603), pp. 420–4.

Koudijs, M. J., den Broeder, M. J., Groot, E. and van Eeden, F. J. (2008) Genetic analysis of the two zebrafish patched homologues identifies novel roles for the hedgehog signaling pathway. *BMC Dev. Biol.*, 8(1), p. 15.

Kreslova, J., Machon, O., Ruzickova, J., Lachova, J., Wawrousek, E. F., Kemler, R., Krauss, S., Piatigorsky, J. and Kozmik, Z. (2007) Abnormal lens morphogenesis and ectopic lens formation in the absence of β-catenin function. *Genesis*, 45(4), pp. 157–168.

Kuchta, K., Knizewski, L., Wyrwicz, L. S., Rychlewski, L. and Ginalski, K. (2009) Comprehensive classification of nucleotidyltransferase fold proteins: identification of novel families and their representatives in human. *Nucleic Acids Res.*, 37(22), pp. 7701–14.

Kudoh, T. and Dawid, I. B. (2001) Zebrafish mab21l2 is specifically expressed in the presumptive eye and tectum from early somitogenesis onwards. *Mech. Dev.*, 109(1), pp. 95–98.

Kwak, J., Park, O. K., Jung, Y. J., Hwang, B. J., Kwon, S.-H. and Kee, Y. (2013) Live image profiling of neural crest lineages in zebrafish transgenic lines. *Mol. Cells*, 35(3), pp. 255–260.

Kwan, K. M., Otsuna, H., Kidokoro, H., Carney, K. R., Saijoh, Y. and Chien, C.-B. (2012) A complex choreography of cell movements shapes the vertebrate eye. *Development*, 139(2), pp. 359–72.

Lee, J., Willer, J. R., Willer, G. B., Smith, K., Gregg, R. G. and Gross, J. M. (2008) Zebrafish blowout provides genetic evidence for Patched1-mediated negative regulation of Hedgehog signaling within the proximal optic vesicle of the vertebrate eye. *Dev. Biol.*, 319(1), pp. 10–22.

Lee, J., Cox, B. D., Daly, C. M. S., Lee, C., Nuckels, R. J., Tittle, R. K., Uribe, R. A. and Gross, J. M. (2012) An ENU mutagenesis screen in zebrafish for visual system mutants identifies a novel splice-acceptor site mutation in patched2 that results in Colobomas. *Invest. Ophthalmol. Vis. Sci.*, 53(13), pp. 8214–21.

Lee, J. and Gross, J. M. (2007) Laminin beta1 and gamma1 containing laminins are essential for basement membrane integrity in the zebrafish eye. *Invest. Ophthalmol. Vis. Sci.*, 48(6), pp. 2483–90.

Lee, J., Lee, B. K. and Gross, J. M. (2013) Bcl6a function is required during optic cup formation to prevent p53-dependent apoptosis and colobomata. *Hum. Mol. Genet.*, 22(17), pp. 3568–3582.

Li, J., Ning, G. and Duncan, S. A. (2000) Mammalian hepatocyte differentiation requires the transcription factor HNF-4alpha. *Genes Dev.*, 14(4), pp. 464–74.

Li, T. and Lu, L. (2005) Epidermal Growth Factor-induced Proliferation Requires Down-regulation of Pax6 in Corneal Epithelial Cells. *J. Biol. Chem.*, 280(13), pp.

12988–12995.

Li, Z., Joseph, N. M. and Easter, S. S. (2000) The morphogenesis of the zebrafish eye, including a fate map of the optic vesicle. *Dev. Dyn.*, 218(1), pp. 175–188.

Linder, S. (2007) The matrix corroded: podosomes and invadopodia in extracellular matrix degradation. *Trends Cell Biol.*, 17(3), pp. 107–117.

Link, B. A., Gray, M. P., Smith, R. S. and John, S. W. M. (2004) Intraocular Pressure in Zebrafish: Comparison of Inbred Strains and Identification of a Reduced Melanin Mutant with Raised IOP. *Invest. Ophthalmol. Vis. Sci.*, 45(12), p. 4415.

Liu, C., Widen, S. A., Williamson, K. A., Ratnapriya, R., Gerth-Kahlert, C., Rainger, J., Alur, R. P., Strachan, E., Manjunath, S. H., Balakrishnan, A., Floyd, J. A., Li, T., Waskiewicz, A., Brooks, B. P., Lehmann, O. J., FitzPatrick, D. R., Swaroop, A. and Swaroop, A. (2016) A secreted WNT-ligand-binding domain of FZD5 generated by a frameshift mutation causes autosomal dominant coloboma. *Hum. Mol. Genet.*, 25(7), pp. 1382–1391.

Lupo, G., Gestri, G., O'Brien, M., Denton, R. M., Chandraratna, R. A. S., Ley, S. V, Harris, W. A. and Wilson, S. W. (2011) Retinoic acid receptor signaling regulates choroid fissure closure through independent mechanisms in the ventral optic cup and periocular mesenchyme. *Proc. Natl. Acad. Sci. U. S. A.*, 108(21), pp. 8698–703.

Lwigale, P. Y. and Bronner-Fraser, M. (2009) Semaphorin3A/neuropilin-1 signaling acts as a molecular switch regulating neural crest migration during cornea development. *Dev. Biol.*, 336(2), pp. 257–265.

Macedo-Souza, L. I., Kok, F., Santos, S., Amorim, S. C., Starling, A., Nishimura, A., Lezirovitz, K., Lino, A. M. M. and Zatz, M. (2005) Spastic paraplegia, optic atrophy, and neuropathy is linked to chromosome 11q13. *Ann. Neurol.*, 57(5), pp. 730–737.

Maeda, A., Moriguchi, T., Hamada, M., Kusakabe, M., Fujioka, Y., Nakano, T., Yoh, K., Lim, K.-C., Engel, J. D. and Takahashi, S. (2009) Transcription factor GATA-3 is essential for lens development. *Dev. Dyn.*, 238(9), p. 2280.

Mann, I. C. (1921) On the Development of the Fissural and Associated Regions in the Eye of the Chick, with some Observations on the Mammal. *J. Anat.*, 55(Pt 2-3), pp. 113–8.

Marcora, E., Gowan, K. and Lee, J. E. (2003) Stimulation of NeuroD activity by huntingtin and huntingtin-associated proteins HAP1 and MLK2. *Proc. Natl. Acad. Sci. U. S. A.*, 100(16), pp. 9578–83.

Mariani, M., Baldessari, D., Francisconi, S., Viggiano, L., Rocchi, M., Zappavigna, V., Malgaretti, N. and Consalez, G. G. (1999) Two Murine and Human Homologs of Mab-21, a Cell Fate Determination Gene Involved in Caenorhabditis Elegans

Neural Development. *Hum. Mol. Genet.*, 8(13), pp. 2397–2406.

Masai, I., Lele, Z., Yamaguchi, M., Komori, A., Nakata, A., Nishiwaki, Y., Wada, H., Tanaka, H., Nojima, Y., Hammerschmidt, M., Wilson, S. W. and Okamoto, H. (2003) N-cadherin mediates retinal lamination, maintenance of forebrain compartments and patterning of retinal neurites. *Development*, 130(11), pp. 2479–94.

Matt, N., Ghyselinck, N. B., Pellerin, I. and Dupé, V. (2008) Impairing retinoic acid signalling in the neural crest cells is sufficient to alter entire eye morphogenesis. *Dev. Biol.*, 320(1), pp. 140–148.

McMahon, C., Gestri, G., Wilson, S. W. and Link, B. A. (2009) Lmx1b is essential for survival of periocular mesenchymal cells and influences Fgf-mediated retinal patterning in zebrafish. *Dev. Biol.*, 332(2), pp. 287–298.

Melo, U. S., Macedo-Souza, L. I., Figueiredo, T., Muotri, A. R., Gleeson, J. G., Coux, G., Armas, P., Calcaterra, N. B., Kitajima, J. P., Amorim, S., Olávio, T. R., Griesi-Oliveira, K., Coatti, G. C., Rocha, C. R. R., Martins-Pinheiro, M., Menck, C. F. M., Zaki, M. S., Kok, F., Zatz, M., *et al.* (2015) Overexpression of KLC2 due to a homozygous deletion in the non-coding region causes SPOAN syndrome. *Hum. Mol. Genet.*, 24(24), pp. 6877–85.

Meyers, J. R. (2018) Zebrafish: Development of a Vertebrate Model Organism. *Curr. Protoc. Essent. Lab. Tech.*, 16(1), p. e19.

Morcillo, J., Martínez-Morales, J. R., Trousse, F., Fermin, Y., Sowden, J. C. and Bovolenta, P. (2006) Proper patterning of the optic fissure requires the sequential activity of BMP7 and SHH. *Development*, 133(16), pp. 3179–3190.

Morita, K., Chow, K. L. and Ueno, N. (1999) Regulation of body length and male tail ray pattern formation of Caenorhabditis elegans by a member of TGF-beta family. *Development*, 126(6), pp. 1337–1347.

Mui, S. H., Kim, J. W., Lemke, G. and Bertuzzi, S. (2005) Vax genes ventralize the embryonic eye. *Genes Dev.*, 19(10), pp. 1249–59.

Nagano, T., Yoneda, T., Hatanaka, Y., Kubota, C., Murakami, F. and Sato, M. (2002) Filamin A-interacting protein (FILIP) regulates cortical cell migration out of the ventricular zone. *Nat. Cell Biol.*, 4(7), pp. 495–501.

Nagase, T., Ishikawa, K., Kikuno, R., Hirosawa, M., Nomura, N. and Ohara, O. (1999) Prediction of the coding sequences of unidentified human genes. XV. The complete sequences of 100 new cDNA clones from brain which code for large proteins in vitro. *DNA Res.*, 6(5), pp. 337–45.

Nakamura, K. M., Diehl, N. N. and Mohney, B. G. (2011) Incidence, ocular findings, and systemic associations of ocular coloboma: a population-based study. *Arch. Ophthalmol.*, 129(1), pp. 69–74.

Nickla, D. L. and Wallman, J. (2010) The multifunctional choroid. *Prog. Retin. Eye Res.*, 29(2), pp. 144–68.

Nishiguchi, S., Wood, H., Kondoh, H., Lovell-Badge, R. and Episkopou, V. (1998) Sox1 directly regulates the γ-crystallin genes and is essential for lens development in mice. *Genes Dev.*, 12(6), p. 776.

Nornes, H. O., Dressler, G. R., Knapik, E. W., Deutsch, U. and Gruss, P. (1990) Spatially and temporally restricted expression of Pax2 during murine neurogenesis. *Development*, 109(4), pp. 797–809.

Ohta, A., Schumacher, F.-R., Mehellou, Y., Johnson, C., Knebel, A., Macartney, T. J., Wood, N. T., Alessi, D. R. and Kurz, T. (2013) The CUL3-KLHL3 E3 ligase complex mutated in Gordon's hypertension syndrome interacts with and ubiquitylates WNK isoforms: disease-causing mutations in KLHL3 and WNK4 disrupt interaction. *Biochem. J.*, 451(1), pp. 111–22.

de Oliveira Mann, C. C., Kiefersauer, R., Witte, G. and Hopfner, K. P. (2016) Structural and biochemical characterization of the cell fate determining nucleotidyltransferase fold protein MAB21L1. *Sci. Rep.*, 6(June), pp. 1–14.

Onwochei, B. C., Simon, J. W., Bateman, J. B., Couture, K. C. and Mir, E. (2000) Ocular Colobomata. *Surv. Ophthalmol.*, 45(3), pp. 175–194.

Pagon, R. A. (1981) Ocular coloboma. *Surv. Ophthalmol.*, 25(4), pp. 223–36.

Papizan, J. B., Garry, G. A., Brezprozvannaya, S., McAnally, J. R., Bassel-Duby, R., Liu, N. and Olson, E. N. (2017) Deficiency in Kelch protein Klhl31 causes congenital myopathy in mice. *J. Clin. Invest.*, 127(10), pp. 3730–3740.

Parain, K., Mazurier, N., Bronchain, O., Borday, C., Cabochette, P., Chesneau, A., Colozza, G., Yakoubi, W. El, Hamdache, J., Locker, M., Gilchrist, M. J., Pollet, N. and Perron, M. (2012) A large scale screen for neural stem cell markers in Xenopus retina. *Dev. Neurobiol.*, 72(4), pp. 491–506.

Parmigiani, C. and McAvoy, J. (1984) Localisation of laminin and fibronectin during rat lens morphogenesis. *Differentiation*, 28(1), pp. 53–61.

Patel, A. and Sowden, J. C. (2017) Genes and pathways in optic fissure closure. *Semin. Cell Dev. Biol.*

Popowicz, G. M., Schleicher, M., Noegel, A. A. and Holak, T. A. (2006) Filamins: promiscuous organizers of the cytoskeleton. *Trends Biochem. Sci.*, 31(7), pp. 411–419.

Prigge, J. R. and Schmidt, E. E. (2007) HAP1 can sequester a subset of TBP in cytoplasmic inclusions via specific interaction with the conserved TBP(CORE). *BMC Mol. Biol.*, 8, p. 76.

Rainger, J., Pehlivan, D., Johansson, S., Bengani, H., Sanchez-Pulido, L., Williamson, K.

A., Ture, M., Barker, H., Rosendahl, K., Spranger, J., Horn, D., Meynert, A., Floyd, J. A. B., Prescott, T., Anderson, C. A., Rainger, J. K., Karaca, E., Gonzaga-Jauregui, C., Jhangiani, S., *et al.* (2014) Monoallelic and biallelic mutations in MAB21L2 cause a spectrum of major eye malformations. *Am. J. Hum. Genet.*, 94(6), pp. 915–923.

Rajagopal, R., Dattilo, L. K., Kaartinen, V., Deng, C.-X., Umans, L., Zwijsen, A., Roberts, A. B., Bottinger, E. P. and Beebe, D. C. (2008) Functions of the Type 1 BMP Receptor Acvr1 (Alk2) in Lens Development: Cell Proliferation, Terminal Differentiation, and Survival. *Investig. Opthalmology Vis. Sci.*, 49(11), p. 4953.

Rajagopal, R., Huang, J., Dattilo, L. K., Kaartinen, V., Mishina, Y., Deng, C.-X., Umans, L., Zwijsen, A., Roberts, A. B. and Beebe, D. C. (2009) The type I BMP receptors, Bmpr1a and Acvr1, activate multiple signaling pathways to regulate lens formation. *Dev. Biol.*, 335(2), pp. 305–316.

Raymond, P. A., Barthel, L. K., Bernardos, R. L. and Perkowski, J. J. (2006) Molecular characterization of retinal stem cells and their niches in adult zebrafish. *BMC Dev. Biol.*, 6, p. 36.

Recher, G., Jouralet, J., Brombin, A., Heuzé, A., Mugniery, E., Hermel, J.-M., Desnoulez, S., Savy, T., Herbomel, P., Bourrat, F., Peyriéras, N., Jamen, F. and Joly, J.-S. (2013) Zebrafish midbrain slow-amplifying progenitors exhibit high levels of transcripts for nucleotide and ribosome biogenesis. *Development*, 140(24), pp. 4860–9.

Reza, H. M. and Yasuda, K. (2004) Roles of maf family proteins in lens development. *Dev. Dyn.*, 229(3), pp. 440–448.

Robinson, M. L. and Overbeek, P. A. (1996) Differential Expression of aA- and aB-Crystallin During Murine Ocular Development. *Invest. Ophthalmol.*, 37(11), pp. 2276–2284.

Schimmenti, L. A., de la Cruz, J., Lewis, R. A., Karkera, J. D., Manligas, G. S., Roessler, E. and Muenke, M. (2003) Novel mutation in sonic hedgehog in non-syndromic colobomatous microphthalmia. *Am. J. Med. Genet.*, 116A(3), pp. 215–221.

Schmitt, E. A. and Dowling, J. E. (1994) Early-eye morphogenesis in the zebrafish,Brachydanio rerio. *J. Comp. Neurol.*, 344(4), pp. 532–542.

Schwarz, M., Cecconi, F., Bernier, G., Andrejewski, N., Kammandel, B., Wagner, M. and Gruss, P. (2000) Spatial specification of mammalian eye territories by reciprocal transcriptional repression of Pax2 and Pax6. *Development*, 127, pp. 4325–4334.

See, A. W.-M. and Clagett-Dame, M. (2009) The temporal requirement for vitamin A in the developing eye: Mechanism of action in optic fissure closure and new roles for the vitamin in regulating cell proliferation and adhesion in the embryonic retina. *Dev. Biol.*, 325(1), pp. 94–105.

Semina, E. V., Reiter, R. S. and Murray, J. C. (1997) Isolation of a New Homeobox Gene Belonging to the Pitx/Rieg Family: Expression During Lens Development and Mapping to the Aphakia Region on Mouse Chromosome 19. *Hum. Mol. Genet.*, 6(12), pp. 2109–2116.

Seth, A., Ye, J., Yu, N., Guez, F., Bedford, D. C., Neale, G. A., Cordi, S., Brindle, P. K., Lemaigre, F. P., Kaestner, K. H. and Sosa-Pineda, B. (2014) Prox1 ablation in hepatic progenitors causes defective hepatocyte specification and increases biliary cell commitment. *Development*, 141(3), pp. 538–47.

Sghari, S. and Gunhaga, L. (2018) Temporal Requirement of Mab21l2 During Eye Development in Chick Reveals Stage-Dependent Functions for Retinogenesis. *Invest. Ophthalmol. Vis. Sci.*, 59(10), p. 3869.

Shalom-Feuerstein, R., Serror, L., De La Forest Divonne, S., Petit, I., Aberdam, E., Camargo, L., Damour, O., Vigouroux, C., Solomon, A., Gaggioli, C., Itskovitz-Eldor, J., Ahmad, S. and Aberdam, D. (2012) Pluripotent Stem Cell Model Reveals Essential Roles for miR-450b-5p and miR-184 in Embryonic Corneal Lineage Specification. *Stem Cells*, 30(5), pp. 898–909.

Shibata, S., Zhang, J., Puthumana, J., Stone, K. L. and Lifton, R. P. (2013) Kelch-like 3 and Cullin 3 regulate electrolyte homeostasis via ubiquitination and degradation of WNK4. *Proc. Natl. Acad. Sci. U. S. A.*, 110(19), pp. 7838–43.

Siddam, A. D., Gautier-Courteille, C., Perez-Campos, L., Anand, D., Kakrana, A., Dang, C. A., Legagneux, V., Méreau, A., Viet, J., Gross, J. M., Paillard, L. and Lachke, S. A. (2018) The RNA-binding protein Celf1 post-transcriptionally regulates p27Kip1 and Dnase2b to control fiber cell nuclear degradation in lens development. *PLoS Genet.*, 14(3), p. e1007278.

Silla, Z. T. V., Naidoo, J., Kidson, S. H. and Sommer, P. (2014) Signals from the lens and Foxc1 regulate the expression of key genes during the onset of corneal endothelial development. *Exp. Cell Res.*, 322(2), pp. 381–388.

Sladek, F. M., Zhong, W., Lai, E. and Darnell, J. E. (1990) Liver-enriched transcription factor HNF-4 is a novel member of the steroid hormone receptor superfamily. *Genes Dev.*, 4(12 B), pp. 2353–2365.

Smith, A. N., Miller, L.-A. D., Song, N., Taketo, M. M. and Lang, R. A. (2005) The duality of β-catenin function: A requirement in lens morphogenesis and signaling suppression of lens fate in periocular ectoderm. *Dev. Biol.*, 285(2), pp. 477–489.

Smyth, N., Vatansever, H. S., Murray, P., Meyer, M., Frie, C., Paulsson, M. and Edgar, D. (1999) Absence of basement membranes after targeting the LAMC1 gene results in embryonic lethality due to failure of endoderm differentiation. *J. Cell Biol.*, 144(1), pp. 151–60.

Song, I.-K. and Joo, C.-K. (2004) Morphological and Functional Changes in the Rat Cornea with an Ethanol-Mediated Epithelial Flap. *Invest. Ophthalmol. Vis. Sci.*,

45(2), p. 423.

Song, N., Schwab, K. R., Patterson, L. T., Yamaguchi, T., Lin, X., Potter, S. S. and Lang, R. A. (2007) pygopus 2 has a crucial, Wnt pathway-independent function in lens induction. *Development*, 134(10), pp. 1873–1885.

Soules, K. A. and Link, B. A. (2005) Morphogenesis of the anterior segment in the zebrafish eye. *BMC Dev. Biol.*, 5(1), p. 12.

Spokony, R. F., Aoki, Y., Saint-Germain, N., Magner-Fink, E. and Saint-Jeannet, J.-P. (2002) The transcription factor Sox9 is required for cranial neural crest development in Xenopus. *Development*, 129, pp. 421–432.

Stossel, T. P., Condeelis, J., Cooley, L., Hartwig, J. H., Noegel, A., Schleicher, M. and Shapiro, S. S. (2001) Filamins as integrators of cell mechanics and signalling. *Nat. Rev. Mol. Cell Biol.*, 2(2), pp. 138–145.

Sugar, H. S. (1978) Oculodentodigital dysplasia syndrome with angle-closure glaucoma. *Am. J. Ophthalmol.*, 86(1), pp. 36–8.

Sun, L., Wu, J., Du, F., Chen, X. and Chen, Z. J. (2013) Cyclic GMP-AMP synthase is a cytosolic DNA sensor that activates the type I interferon pathway. *Science*, 339(6121), pp. 786–91.

Thisse, B. and Thisse, C. (2004) *Fast Release Clones: A High Throughput Expression Analysis*. *ZFIN Direct Data Submiss.*

Tollervey, D., Lehtonen, H., Jansen, R., Kern, H. and Hurt, E. C. (1993) Temperature-sensitive mutations demonstrate roles for yeast fibrillarin in pre-rRNA processing, pre-rRNA methylation, and ribosome assembly. *Cell*, 72(3), pp. 443–457.

Torres, M., Gomez-Pardo, E. and Gruss, P. (1996) Pax2 contributes to inner ear patterning and optic nerve trajectory. *Development*, 122(11).

Toyama, R., Kobayashi, M., Tomita, T. and Dawid, I. . (1998) Expression of LIM-domain binding protein (ldb) genes during zebrafish embryogenesis. *Mech. Dev.*, 71(1–2), pp. 197–200.

Tsang, S., Guo, Y., Chan, T., Huang, Y., Chow, K. L. (2018) Generation and characterization of pathogenic Mab21l2(R51C) mouse model. *genesis,* 56 (11-12), pp. e23261.

Tsang, W. H., Shek, K. F., Lee, T. Y. and Chow, K. L. (2009) An evolutionarily conserved nested gene pair — Mab21 and Lrba/Nbea in metazoan. *Genomics*, 94(3), pp. 177–187.

Tsuji, N., Kita, K., Ozaki, K., Narama, I. and Matsuura, T. (2012) Organogenesis of mild ocular coloboma in FLS mice: Failure of basement membrane disintegration at optic fissure margins. *Exp. Eye Res.*, 94(1), pp. 174–178.

Twyffels, L., Gueydan, C. and Kruys, V. (2014) Transportin-1 and Transportin-2: Protein

nuclear import and beyond. *FEBS Lett.*, 588(10), pp. 1857–1868.

van Spronsen, M., Mikhaylova, M., Lipka, J., Schlager, M. A., van den Heuvel, D. J., Kuijpers, M., Wulf, P. S., Keijzer, N., Demmers, J., Kapitein, L. C., Jaarsma, D., Gerritsen, H. C., Akhmanova, A. and Hoogenraad, C. C. (2013) TRAK/Milton Motor-Adaptor Proteins Steer Mitochondrial Trafficking to Axons and Dendrites. *Neuron*, 77(3), pp. 485–502.

Viringipurampeer, I. A., Ferreira, T., DeMaria, S., Yoon, J. J., Shan, X., Moosajee, M., Gregory-Evans, K., Ngai, J. and Gregory-Evans, C. Y. (2012) Pax2 regulates a fadd-dependent molecular switch that drives tissue fusion during eye development. *Hum. Mol. Genet.*, 21(10), pp. 2357–69.

Wall, G. (1942) *The vertebrate eye and its adaptive radiation*. New York, New York: Hafner Publishing Company.

Wawersik, S., Purcell, P., Rauchman, M., Dudley, A. T., Robertson, E. J. and Maas, R. (1999) BMP7 Acts in Murine Lens Placode Development. *Dev. Biol.*, 207(1), pp. 176–188.

Wigle, J. T., Chowdhury, K., Gruss, P. and Oliver, G. (1999) Prox1 function is crucial for mouse lens-fibre elongation. *Nat. Genet.*, 21(3), pp. 318–322.

Williams, A. M. (2016) *Determining the molecular underpinnings of extracellular matrix breakdown during choroid fissure closure*. University of Texas, Austin.

Williamson, K. A. and FitzPatrick, D. R. (2014) The genetic architecture of microphthalmia, anophthalmia and coloboma. *Eur. J. Med. Genet.*, 57(8), pp. 369–380.

Wong, R. L. Y., Chan, K. K. L. and Chow, K. L. (1999) Developmental expression of Mab21l2 during mouse embryogenesis. *Mech. Dev.*, 87(1–2), pp. 185–188.

Wu, L. L. and Zhou, X.-F. (2009) Huntingtin associated protein 1 and its functions. *Cell Adh. Migr.*, 3(1), pp. 71–6.

Wu, Y. L. and Gong, Z. (2004) A novel zebrafish kelchlike gene klhl and its human ortholog KLHL display conserved expression patterns in skeletal and cardiac muscles. *Gene*. Elsevier, 338(1), pp. 75–83.

Xiao, H., Bai, X.-H., Kapus, A., Lu, W.-Y., Mak, A. S. and Liu, M. (2010) The protein kinase C cascade regulates recruitment of matrix metalloprotease 9 to podosomes and its release and activation. *Mol. Cell. Biol.*, 30(23), pp. 5545–61.

Yamada, R., Mizutani-Koseki, Y., Hasegawa, T., Osumi, N., Koseki, H. and Takahashi, N. (2003) Cell-autonomous involvement of Mab21l1 is essential for lens placode development. *Development*, 130(9), pp. 1759–70.

Yamada, R., Mizutani-Koseki, Y., Koseki, H. and Takahashi, N. (2004) Requirement for Mab21l2 during development of murine retina and ventral body wall. *Dev. Biol.*,

274(2), pp. 295–307.

Yamaguchi, M., Shima, N., Kimoto, M., Ebihara, N., Murakami, A. and Yamagami, S. (2015) Markers for Distinguishing Cultured Human Corneal Endothelial Cells from Corneal Stromal Myofibroblasts. *Curr. Eye Res.*, 40(12), pp. 1211–1217.

Yang, Y. and Cvekl, A. (2005) Tissue-specific regulation of the mouse alphaA-crystallin gene in lens via recruitment of Pax6 and c-Maf to its promoter. *J. Mol. Biol.*, 351(3), pp. 453–69.

Yoshihara, M., Ohmiya, H., Hara, S., Kawasaki, S., FANTOM consortium, F., Hayashizaki, Y., Itoh, M., Kawaji, H., Tsujikawa, M. and Nishida, K. (2015) Discovery of molecular markers to discriminate corneal endothelial cells in the human body. *PLoS One*, 10(3), p. e0117581.

Zhang, Y., Qin, W., Lu, X., Xu, J., Huang, H., Bai, H., Li, S. and Lin, S. (2017) Programmable base editing of zebrafish genome using a modified CRISPR-Cas9 system. *Nat. Commun.*, 8(1), p. 118.

Zhao, L., Saitsu, H., Sun, X., Shiota, K. and Ishibashi, M. (2010) Sonic hedgehog is involved in formation of the ventral optic cup by limiting Bmp4 expression to the dorsal domain. *Mech. Dev.*, 127(1–2), pp. 62–72.

Zhao, X. C., Yee, R. W., Norcom, E., Burgess, H., Avanesov, A. S., Barrish, J. P. and Malicki, J. (2006) The Zebrafish Cornea: Structure and Development. *Invest. Ophthalmol. Vis. Sci.*, 47(10), p. 4341.

Zu, Y., Tong, X., Wang, Z., Liu, D., Pan, R., Li, Z., Hu, Y., Luo, Z., Huang, P., Wu, Q., Zhu, Z., Zhang, B. and Lin, S. (2013) TALEN-mediated precise genome modification by homologous recombination in zebrafish. *Nat. Methods*, 10(4), pp. 329–331.